Morre lentamente quem não troca de idéias,
não troca de discurso, evita as próprias contradições.
Morre lentamente quem vira escravo do hábito,
repetindo todos os dias o mesmo trajeto e as mesmas compras no supermercado.
Quem não troca de marca, não arrisca vestir uma cor nova,
não dá papo para quem não conhece.

– Martha Medeiros.

University of Alberta

Analysis and Improvement of Achievable Data Rates in Multi-Way Relay Channels

by

Moslem Noori

A thesis submitted to the Faculty of Graduate Studies and Research
in partial fulfillment of the requirements for the degree of

Doctor of Philosophy
in
Communications

Department of Electrical and Computer Engineering

©Moslem Noori
Spring 2013
Edmonton, Alberta

Dedicated to My Beloved Parents

Abstract

Increasing demand for bandwidth-hungry applications, along with the bandwidth scarcity, has generated a certain momentum toward designing bandwidth-efficient techniques. Recently, multi-way relay channels (MWRCs) have been proposed to improve the spectral efficiency in wireless systems. The main focus of this dissertation is studying the achievable rates of MWRCs as well as proposing methods to improve it.

In the first part of our work, we focus on the users' bit mapping and propose a new mapping for phase-shift keying modulation which increases the achievable rate and decreases the bit error rate of a pairwise MWRC. Interestingly, our proposed mapping outperforms the well-known Gray mapping in terms of both metrics on an additive white Gaussian noise (AWGN) channel.

Then, the achievable rates of a pairwise MWRC, with a simple memoryless relay, where the communication happens over a fading channel with AWGN is studied. For this setup, we determine what relaying strategy suits best based on the system's signal-to-noise ratio.

Later, we extend our rate analysis to the case where the relay is more complex and has memory. First, a symmetric MWRC with AWGN is considered. For this setup, the capacity gap of different relaying strategies are derived and then they are compared with that of one-way relaying. Second, we consider a pairwise MWRC where the links are asymmetric. We show that the system's achievable rate is dependent on the users' transmission pairing in this case. An optimal pairing to maximize the achievable rate is also found.

In the last part of our contributions, erasure MWRCs are the subject of interest. For such channels, we derive an upper bound on the system's achievable rate and also propose low-latency data sharing schemes based on fountain coding. Further, we define a measure, called end-to-end erasure rate, which is used to compare the performance of our proposed schemes with the rate upper bound and the achievable rate of one-way relaying.

Summarily speaking, in the MWRCs' setups studied in this dissertation, multi-way relaying is beneficial when the number of users and the error (erasure) rate are not large. Otherwise, one-way relaying may provide higher data rates.

Acknowledgements

When you approach the end of your journey and look back, you remember many people on the road who helped you throughout the journey. Their support, friendship and encouragement have been constant and touching.

First of all, I owe many thanks to my supervisor, Professor Masoud Ardakani. Fulfilling this research project undoubtedly was impossible without his care, guidance and encouragement. I have not only benefited from Masoud's professionalism in academic issues, but also in the other aspects of life.

I also wish to acknowledge the members of the evaluation committee: Professor Ali Ghrayeb, Professor John Doucette, Professor Chintha Tellambura and Professor Yindi Jing. In addition, I like to thank Pinder Bains for organizing the thesis defence session.

In addition to my supervisor, other people have helped me to proceed in my work through. Hereby, I like to thank Dr. Hossein Bagheri, Dr. Raman Yazdani, Dr. Payam Dehghani, Mahdi Ramezani, Kaveh Mahdavani and Gayan Amarasuriya for all of their valuable discussions and ideas.

I desire to cordially acknowledge my dear friends in Edmonton for their invaluable friendship, sympathy and help. They have made every moment of my life joyful and hopeful to progress. Specially, I would like to sincerely appreciate Hamid Moghadas, Hadi Moosavi, Mehdi Omidghane and Sadegh Amiri.

And my most heartfelt thanks go to my family which I always feel their wholehearted and endless support, even here, far away from them. Without my parents' support, trust and encouragement, none of my accomplishments were achievable.

Unfortunately, I am not able to adequately express my appreciation for all adorable people, who helped me to reach this point, through the words and in this limited space. This formal acknowledgment was just what my mind could think, but my heart forever thanks you all!

Table of Contents

List of Tables

List of Figures

List of Symbols

List of Abbreviations

Chapter 1

Introduction

Bandwidth and energy are the two most precious resources in communication systems. The exploding demand for high-speed data communications, e.g. multimedia-rich data applications, has exposed a serious challenge into the telecommunications and information theory communities across the globe. On one hand, bandwidth-hungry applications constantly take bite on the currently available frequency range. On the other hand, expansion of the communications networks has led to an increasing energy consumption and CO_2 emission by information communications technology (ICT) industries.

The importance of achieving energy-efficient communications has two folds: i) Environmental causes: It has been reported that ICT-related industries have three percent of the world-wide energy consumption causing two percent of the global carbon emission [3]. Although the share of ICT in energy consumption looks small, it is expected to rapidly increase specially in developing counties resulting in higher carbon emission. ii) Operational cost: Extension of the communications networks and providing higher data rates have caused the energy cost to hold a significantly high share of the operating expenses for communications service providers. To sustain affordable services for their customers and increase their revenue, service providers are also interested in developing energy-efficient methods by researchers.

To overcome the energy consumption issue, there have been efforts in communications society toward reaching *green communications*. In green communications, we look for new communication paradigms to lower the energy consumption in ICT systems. Figure 1.1 presents a relation between the consumed energy and the data rate over the time. As seen in this figure, it is forecasted that while data rate and power consumption proportionally have been increasing in the past years, using new green technologies, we can save on the power consumption and still increase the data rate.
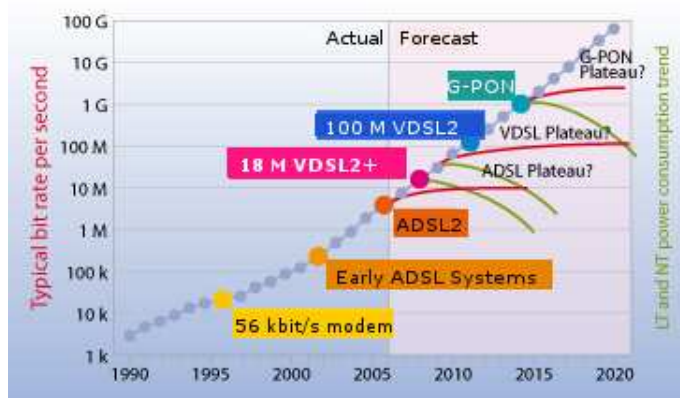
Figure 1.1: Relation between bit rate and power consumption over time (figure is from [1]).

The importance of bandwidth lays on its direct connection with the data rate in a communication system. In early days of digital communications, Shannon showed that the data rate is directly proportional to the system's available bandwidth. Thus, it is always desirable for a wireless operator to have as much bandwidth as possible for being able to provide high data rate service to its costumers. However, the bandwidth has a limited operational range and cannot be freely dedicated to the operators. To better indicate the bandwidth scarcity, we bring the attention of the reader to Figure 1.2 showing the frequency allocation in US. For the map of frequency allocation in Canada, the interested reader is referred to [4]. As seen in this figure, for each communication application, a fixed frequency chunk has been assigned and packed into the crowded spectrum map. For each application, the system should be designed in a way that the application requirements, e.g. data rate, are met without exceeding its assigned frequency band.

Nowadays, wireless operators are faced with a challenging dilemma. While emerging popular broadband services, like mobile TV or social networking, have found their way through the consumers' market, the operators' available spectrum has not been much extended by governing organizations. Thus, to cope with the increasing data rate demand, the operators are eager to find ways in order to acquire more bandwidth or use the available spectrum more effectively.

One solution for the operators is to acquire the bandwidth of the less popular services through spectrum auctions. A well-known example of these auctions is *Auction 73* for the 700 MHz, previously used for analog TV broadcast [5]. The auction was organized by the Federal Communications Commission (FCC) in 2008 and major wireless operators in US took part in the auction. Auction 73 raised around 20 billion dollars in total. Considering the increasing data rate demand, it is not surprising to know that FCC is planning to

Figure 1.2: Frequency allocation for communications services in US (figure is from [2]).

hold another auction in 2014 to sell another part of the analog TV broadcast spectrum [6]. Although operators are able to resolve some of their bandwidth issues through auctions, it costs the operators a significant money to bid on the spectrum and also makes the bandwidth even pricier!

1.1 Techniques to Provide more Bandwidth Access

Following the above discussion on the bandwidth scarcity and increasing demand for broadband data services, researchers are well-motivated by industry to develop methods for communication over frequency bands which are not currently utilized due to technical issues as well as using the current available bandwidth in a more smart fashion. In the following, we briefly discuss the state of the art on the developed techniques to achieve these goals.

1.1.1 SHF and EHF Communications

As seen in Figure 1.2, many different frequency chunks have been assigned to mobile services across the spectrum map. Current mobile systems (2G, 3G and 4G systems) use frequency bands in the ultra-high frequency (UHF) band, i.e. 300 MHz to 3 GHz. However, there are still many unused sections in the super high frequency (SHF), i.e. 3 GHz to 30 GHz, and extremely high frequency (EHF), i.e. 30 GHz to 300 GHz, bands which are licensed for mobile applications.

The most important feature of SHF and EHF frequency sections is their significantly large bandwidth. While the frequency chunks in the UHF band are in the order of tens of MHz, SHF and EHF can provide bandwidth in the order of hundreds of MHz and even GHz. Such large bandwidths can easily support broadband data applications. However, there is a major barrier to use the SHF and EHF frequency bands for data communications. As we go higher in the frequency, the signal strength attenuates much faster over the distance. This makes SHF and EHF bands mainly applicable to very-short range communication applications. This limits the possible applications of SHF and EHF bands. However, academic and industry researchers plan to employ SHF and EHF bands along with femtocell design [7] to achieve significantly high data rates in cellular systems.

1.1.2 Dynamic Spectrum Access

Spectrum measurements over different municipal areas have shown that while for each application a fixed frequency portion is assigned, most of the time the channel is indeed not in use. For instance, a spectrum measurement between August 31 and September 1, 2004

4

in New York City revealed that only 13 percent of the dedicated spectrum were utilized [8, 9]. This means that fixed spectrum assignment could lead into 87 percent of spectrum waste. Measurements over other locations across the globe give the same outcome on the inefficient use of frequency bands.

To improve the spectral-efficiency in the system and fill the time when spectrum sits idle, some ideas were suggested promoting dynamic channel assignment for users [10, 11]. The idea has been developed since then and novel spectrum sharing and dynamic spectrum access schemes have been developed unleashing innovative new products and services [12, 13]. For instance, a thorough study on the dynamic spectrum access was conducted by defence advanced research project agency (DARPA) whose main goal was developing techniques for dynamic spectrum access in military applications. Later, based on the idea of dynamic spectrum access, *Cognitive Radio Systems* (CRSs) were proposed which have gained a significant attention in communications society [14–16]. The basic idea behind CRSs is to prioritize users based on their quality of service requirements and allow them to access the spectrum according to their priorities. Bringing CRSs into reality is still an ongoing research field facing its own challenges such as developing spectrum sensing techniques, new physical layer design, and multiple-access schemes.

1.1.3 Efficient Use of Acquired Bandwidth

After acquiring a frequency bandwidth, regardless of the fact whether the bandwidth access is static or dynamic, it is desirable to use the bandwidth as effectively as possible. Design of bandwidth-efficient methods have been considered since early days of digital communications. One important measure in this regard is *spectral efficiency* indicating the information rate (reliably) transmitted over a given bandwidth.

Over that past few decades, various techniques have been developed to improve spectral efficiency. One recent development is the idea of *network coding* [17]. The fundamental notion of network coding is to allow data mixing at intermediate nodes of the network instead of only blindly forwarding it. In some situations, it has been shown that network coding can actually achieve the ultimate data throughput of the network [18] which was not feasible through conventional data forwarding schemes.

Since the proposal of network coding, the communications research community has applied the concept of network coding into different applications including relay networks. A good example of the network coding's application in relay networks is called *two-way relay channels* (TWRCs) [19–21]. In a TWRC, two users (fully) share their data through a relay

without having direct links. It is shown that TWRCs are able to significantly increase the data rate compared to the conventional one-way relaying (OWR). In fact, TWRCs exploit the interference, instead of avoiding it, in order to elevate the system throughput.

Later, Gunduz *et al.* extended the setup of TWRCs to more than two users and suggested *multi-way relay channels* (MWRCs) [22]. In a multi-way relay channel, several users want to (fully) share data with the help of one or more relays. Instead of treating the data of each user individually, in an MWRC, relay applies the concept of network coding to deal with the users' data in a more smart fashion. Unlike OWR where we have separate sets of data source and destination, each user serves as both data source and destination in an MWRC.

MWRCs are still in their early stage of development. Due to their potential importance in improving the spectral efficiency, design of rate-efficient MWRCs is considered in this dissertation. A summary of our work as well as the organization of the presented contributions in this thesis are provided in the next section.

1.2   Summary of Contributions and Thesis Organization

In this thesis, we first describe the concept of MWRCs in more detail. Then, we proceed with presenting our contributions that are mostly focused on proposing rate-efficient schemes to enable data communications for different setups of MWRCs. We also suggest some ideas for future research directions.

Chapter 2 focuses on the preliminaries of MWRCs. We present a literature review on the development of MWRCs and summarize the state of the art in the field. Then, we describe MWRCs in more detail and provide a brief review on different multi-way relaying (MWR) techniques employed in MWRCs: i) amplify-and-forward (AF), ii) decode-and-forward (DF), iii) compress-and-forward (CF) and iv) functional-decode-forward (FDF). For each relaying scheme, its achievable rate is also presented.

One of the first challenges in an MWRC is signal demodulation at the relay. An important example of these challenges is the existence of ambiguous point(s) in the received constellation at the relay. The ambiguous point represents the superposition of two or more different transmitted symbols by users. Thus, the relay is not able to correctly demodulate the received signal. Our first concern is to make sure that the received constellation at the relay is ambiguity-free by choosing proper mapping at the user side. Then, we will discuss design of a set of mappings to decrease the system bit error rate (BER) and also increase the achievable data rate. The result of our symbol mapping design for TWRCs and pairwise

MWRCs with phase-shift keying modulation (PSK) is discussed in Chapter 3.

We present an analysis for the achievable rate of memoryless TWRCs in Chapter 4. Memoryless relaying is important in low-complexity networks, e.g. sensor networks, and delay-intolerant systems. We compare the achievable rate of AF and demodulate-and-forward (DMF) which can be considered as DF for memoryless systems. Our results show that unlike memoryless one-way relaying, increasing users' signal-to-noise ratio (SNR) benefits AF more than DMF. Another interesting observation is that while with DMF a higher data rate is provided for the user whose channel condition is better, with AF the situation is the reverse. That is, the user with worse channel condition can receive at a higher data rate. Further, we find that for a TWRC with asymmetric users' channels, AF can take advantage of power back-off at the users, without degrading the data rate, to save energy while power back-off is not beneficial for DMF. Please note that the results are applicable to the pairwise MWRCs as well.

Another research problem that we address in this thesis is related to the achievable rates of MWRCs with symmetric channels and additive white Gaussian noise (AWGN). More specifically, considering an MWRC with N users, we prove that similar to CF, FDF guarantees a gap less than $\frac{1}{2(N-1)}$ bit from the capacity upper bound while DF and AF are unable to ensure this rate gap. For DF and AF, we identify situations where they also have a rate gap less than $\frac{1}{2(N-1)}$ bit. Then, we compare the performance of the aformentioned MWR techniques with OWR. We show that although MWR has higher relaying complexity, surprisingly, it can be outperformed by OWR depending on N and the system's SNR. Summarily speaking, for large N and small users' transmit power, OWR usually provides higher rates than MWR.

In addition, we consider the situation where the links between the users and the relay are not symmetric and have different SNRs. For instance, in a fading environment, different users most likely have channels with different gains resulting in different received SNRs. In Chapter 6, we first study the achievable common rate of an MWRC, considering the possible difference between the condition of the users' channels. Our common rate analysis reveals that for pairwise MWRCs, the achievable common data rate depends on the order of users' transmission pairing (scheduling). This motivates us to find the optimal users' transmissions pairing maximizing the achievable common rate of the system.

In Chapter 7, we consider an erasure multi-way relay channel (EMWRC) in which several users share their data through a relay over erasure links. Assuming no feedback channel between the users and the relay, we first identify the challenges for designing a

data sharing scheme over an EMWRC. Then, to overcome these challenges, we propose practical low-latency and low-complexity data sharing schemes based on fountain coding. Later, we introduce the notion of end-to-end erasure rate (EEER) and analytically derive it for the proposed schemes. Using EEER and computer simulations, the achievable rate and fountain coding overhead of our proposed schemes are compared with the ones of OWR. This comparison implies that when the number of users and the channel erasure rates are not large, our proposed schemes outperform OWR over EMWRCs.

The conclusion of this dissertation along with the future research directions are presented in Chapter 8. Furthermore, the proofs of the theorems presented in this dissertation are brought in the appendix to improve the readability.

Chapter 2

Background

In this chapter, we first provide the history of the development of MWRCs. Then, we present a general system model for MWRCs and then explain existing relaying strategies for them. The achievable rates of these relaying strategies are also presented.

2.1 Development of MWRCs

Conventionally, relays are used to assist the data communication in only one direction. That is, a group of users, serving as data sources, send their data to another group of users, called data destinations, with the help of one or more relays. In this setup, there is a data flow in one direction from data sources to the data destinations. This scheme is often called one-way relaying (OWR). The relaying paradigm eventually changed with the introduction of two-way relaying (TWR).

Before proceeding with the literature review on TWR and then multi-way relaying (MWR), we first provide an intuition on how the spectral efficiency of a simple relay network can be enhanced. In Figure 2.1, users A and B want to exchange their data, called x_A and x_B respectively, through a relay, denoted by $\mathcal{R}$. Different relaying approaches can be employed by the relay to accomplish the task. Figure 2.1(a) depicts OWR where the users share their data in four time slots. First, x_A is sent to B in two time slots and then x_B is delivered to A in two other time slots. This approach can be enhanced by employing the concept of network coding [17] (Figure 2.1(b)) in which $\mathcal{R}$ does some operations on the data instead of simply forwarding them. First, users transmit their data to the relay in two time slots. Then, the relay XORs x_A and x_B and broadcasts $x_A \oplus x_B$ to both users. Now, having its own data, each user derives the other user's data from the transmitted XORed signal. In this scheme, data exchange between the users is accomplished after three time slots and its spectral efficiency is $\frac{4}{3}$ times better than OWR. This is a simple form of TWR

where both users are data sources and data destinations. The spectral efficiency in this example can be further improved by employing the network coding at the physical layer. This scenario is shown in Figure 2.1(c). In this case, instead of combining the users' data at the relay, the wireless media is exploited to perform the data combining. For this purpose, both users transmit simultaneously and their data is in fact XORed at the physical layer. After receiving the XORed data, relay broadcasts it to the users. Using network coding at the physical layer, the data exchange between the users is done in only two time slots and its spectral efficiency is two times better than OWR. Note that this solution consumes the minimum number of time slots for data exchange between the users.

(a) Conventional one-way relaying

(b) Two-way relaying with network coding

(c) Two-way relaying with physical-layer network coding
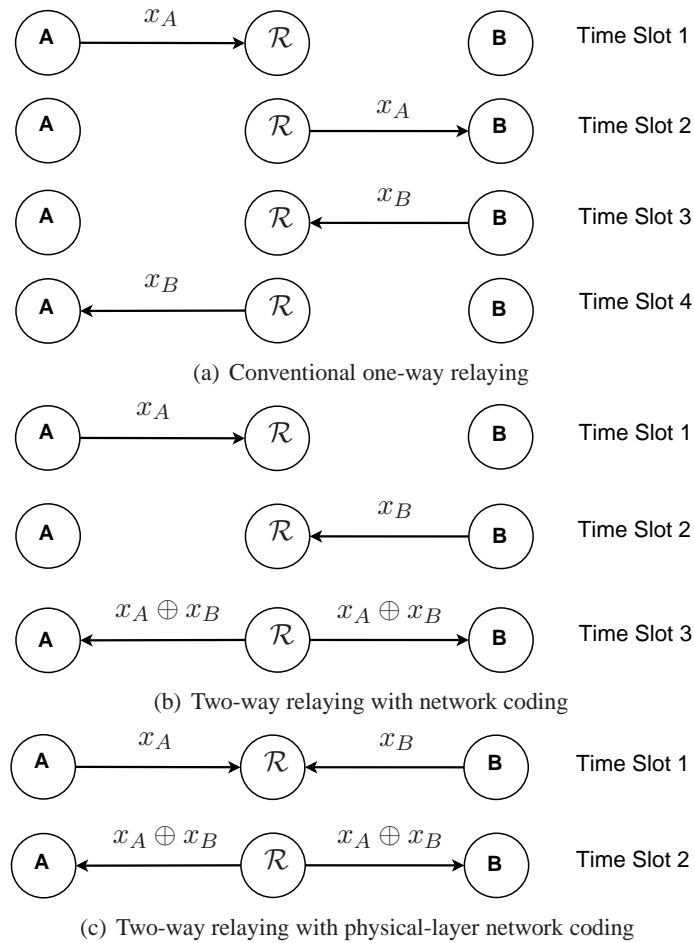
Figure 2.1: Different Relaying Approaches.

Employing TWR to improve the spectral efficiency in a relay network first appeared in [19, 20]. In these contributions, authors first consider a two-way relay communication between two users and exploit network coding and the physical-layer broadcast property of the wireless channels to improve data throughput. The result is a significant enhancement

over conventional OWR. They further propose a *physical piggybacking* to extend the concept to the networks with more than two users, however, the communication between the users still happen in the form of TWR.

TWR has been usually studied under a standard framework called two-way relay channel (TWRC). Basically, a TWRC is similar to the scenario depicted in Figure 2.1 where two users exchange their data with the help of a relay. There exist extensive studies on TWRCs considering different aspects of them [21, 23–27]. Further, multi-pair two-way relaying is considered in some recent works where several pairs of users exchange their data based on the concept of TWR [28].

A more general scheme, called multi-way relay channel (MWRC), was later proposed. In an MWRC, several users exchange their data via the relay. This setup is the extension of TWRCs to more than two users. MWRCs were first studied by Gunduz *et al.* in [22] where they consider a relay network with several clusters of users. The users within each cluster want to fully exchange their data with each other with the help of a relay. For this setup, the authors find the upper bound on the achievable common rate as well as the achievable rates of different relaying strategies when the links between the users and the relay are symmetric with AWGN. Later, the achievable rates of MWRCs have been studied for different scenarios, e.g. binary symmetric [29], symmetric Gaussian [30], and finite field channels [31].

Use of MWRCs is counted as a promising approach to enable multicasting in wireless networks. Some applications of MWRCs are in the device-to-device communications [32], file sharing between several wireless devices, or conference calls in a cellular network.

2.2   Data Sharing Model in an MWRC

In an MWRC, $N \geq 2$ users communicate their data without having direct user-to-user links. We name users by $u_1, u_2, \ldots, u_N$ and their information message by $m_1, m_2, \ldots, m_N$. To overcome the effect of the noise, u_i applies channel coding on m_i which results in the coded message x_i. To enable data communication between users, a relay $\mathcal{R}$ is employed. Here, each user aims to decode all other users data as well as to transmit its data to all other users.

In this MWRC, data communication consists of uplink and downlink phases. In the uplink phase, users transmit their coded data over a multiple access (MAC) channel. Each user has a limited power P, thus, for all i, $E[x_i^2] \leq P$. Assuming a zero-mean Gaussian

noise with unit variance for relay, n_r, the received signal at $\mathcal{R}$ is

$$y_r = \sum_{i=1}^{N} x_i + n_r. \tag{2.1}$$

Please note that (2.1) is also valid for fading MWRCs when perfect power control [33] at the users is applied. The system model for MWRCs with fading and imperfect (or no) power control is discussed later.

Depending on the relaying strategy, $\mathcal{R}$ forms its message, x_r, based on y_r. Then, x_r is broadcast to all users during the downlink phase. The data transmission in the downlink is in fact a broadcast (BC) channel where each user has side information, i.e. its own information. The received signal by u_i in the downlink phase is

$$y_i = x_r + n_i \tag{2.2}$$

where n_i is u_i's receiver Gaussian noise with zero mean and unit variance. Here, relay has also a limited power P_r, thus, $E[x_r^2] \leq P_r$. Figure 6.1(a) and 6.1(b) depict the uplink and downlink phases in an MWRC. Here, we presented a simple symmetric model for MWRCs to ease the discussion. However, in Chapter 6, we consider an asymmetric MWRC with different channel gains for the users.

(a) Uplink phase.
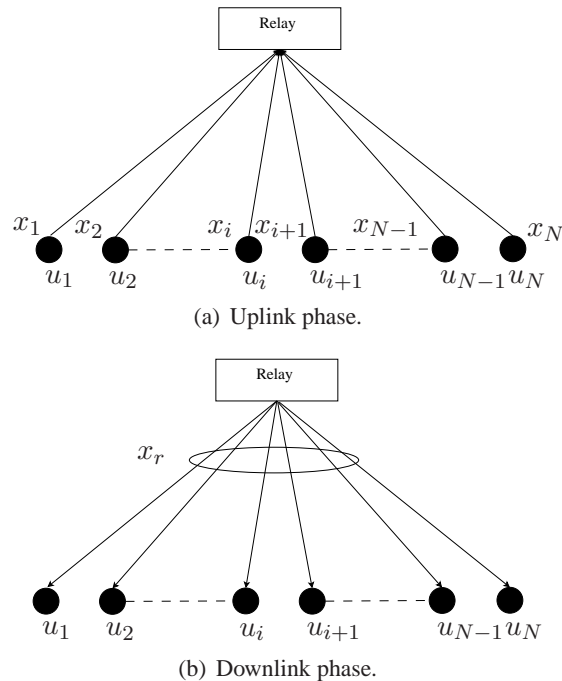
(b) Downlink phase.

Figure 2.2: Demonstration of the uplink and downlink phases.

In this dissertation, we mainly focus on the common rate capacity of MWRCs. The

common rate capacity is the data rate at which all users can transmit and receive data reliably. According to this definition, if we denote the uplink rate for u_i by R_i^u and the downlink data rate by R_i^d, then, the common rate capacity, R^c, is

$$R^c = \sup\{\min\{R_1^u, R_2^u, \ldots, R_N^u, R_1^d, R_2^d, \ldots, R_N^d\}\}. \tag{2.3}$$

For more details on common rate definition and its applications in MWRCs, the reader is encouraged to see [22] and [34]. Please note that even for a symmetric MWRC with AWGN, R^c is yet to be known. However, an upper bound on R^c can be derived using the cut-set theorem [35]:

Theorem 2.1 *The upper bound on the achievable common data rate of the assumed MWRC, R_{UB}^c, is*

$$R_{\mathrm{UB}}^c = \min \left\{ \frac{\log\left(1 + (N-1)P\right)}{2(N-1)}, \frac{\log\left(1 + P_r\right)}{2(N-1)} \right\} \tag{2.4}$$

Proof: Please see [22].

2.3 Relaying Strategies in MWRCs

As mentioned, after receiving the users' transmitted signal in the uplink, the relay forms its message based on the relaying strategy and forwards it to the users in the downlink. Different relaying strategies provide different levels of the performance in the system. In the following, we describe the relaying strategies used in MWRCs in detail and also present their achievable common data rate when the links are symmetric AWGN channels. A detailed comparison between the achievable rates of the following relaying schemes is provided in Chapter 5.

2.3.1 Amplify-and-Forward

Amplify-and-forward (AF) is the simplest relaying strategy in terms of the relaying complexity. AF was first proposed for OWR and is easily adopted in MWRCs. With AF, all users simultaneously transmit their data over the channel in the uplink phase. After receiving the users' signals, the relay then simply amplifies the received signal and broadcasts it back to all users. The amplification is done such that the transmit power of the relay does not exceed P_r. Thus, $x_{\mathrm{r}} = \alpha(\sum_{i=1}^{N} x_i + n_{\mathrm{r}})$ where

$$\alpha = \sqrt{\frac{P_r}{NP+1}}. \tag{2.5}$$

After receiving the relay's broadcast signal, each user then subtracts its own message from the broadcast message and then decodes the data of all other users. After subtracting its own signal, the received signal at u_i is modeled as

$$y_i = \alpha(\sum_{j \neq i} x_j + n_{\mathrm{r}}) + n_i = \alpha \sum_{j \neq i} x_j + (\alpha n_{\mathrm{r}} + n_i). \tag{2.6}$$

The signal model in (2.6) is similar to the signal model for an AWGN multiple-access channel with $N-1$ users where the noise is $\alpha n_{\mathrm{r}} + n_i$. Thus, it is easy to show that the achievable common data rate of AF, R_{AF}^c, is as follows.

Lemma 2.1 *In an N-user MWRC with AWGN channels,*

$$R_{\mathrm{AF}}^c = \frac{1}{2(N-1)} \log \left(1 + \frac{(N-1)PP_r}{1 + NP + P_r} \right) \tag{2.7}$$

is the maximum common data rate that AF can achieve.

2.3.2 Decode-and-Forward

Decode-and-forward (DF) is another relaying strategy commonly used in relay networks. In DF, all users simultaneously transmit their coded packets to the relay in the uplink phase. After receiving users' signals', $\mathcal{R}$ decodes the data of all users. To broadcast in the downlink phase, relay employs a broadcast scheme based on Slepian-Wolf coding [36] where $m_1, m_2, \ldots, m_N$ are treated as source messages and m_i is considered as the correlated side information at u_i [22]. After receiving x_{r}, each user then decodes the data of the rest of the users.

Lemma 2.2 *The maximum achievable common rate for a DF MWRC with AWGN links is*

$$R_{\mathrm{DF}}^c = \min \left\{ \frac{\log(1+NP)}{2N}, \frac{\log(1+P_r)}{2(N-1)} \right\}. \tag{2.8}$$

Proof: See [22].

In (2.8), the first term inside the braces reflects the uplink achievable rate and the second term is related to the downlink achievable rate.

2.3.3 Compress-and-Forward

Compress-and-forward (CF) was proposed many years ago in the early stages of relay channels by Cover and El Gamal in [37]. Recently, its application for TWR and MWR has been

studied [22,38]. In CF, relay quantizes its received signal in the uplink and then compresses it. Naming the quantized version of y_r by $\hat{y}_r$, we have

$$\hat{y}_r = \sum_{i=1}^{N} x_i + n_r + n_q \tag{2.9}$$

where n_q is the quantization error. Then, without attempting to decode users' messages, relay applies a source coding scheme on $\hat{y}_r$ and forms x_r. The source coding scheme can be lossless, e.g. Slepian-Wolf [39], or can be lossy like Wyner-Ziv [40]. Then, the relay broadcasts x_r to the users and they decode the other users' data through the noisy version of the compressed relay's observation. The interested reader is referred to [41] for more information on the application of CF in relay networks. For the achievable rate of CF in MWRCs, the following lemma is proved.

Lemma 2.3 *The maximum achievable common rate by CF for the described MWRC is*

$$R_{\text{CF}}^c = \frac{1}{2(N-1)} \log\left(1 + \frac{(N-1)PP_r}{1 + (N-1)P + P_r}\right) \tag{2.10}$$

Proof: Please see [22].

It can be shown that for an MWRCs with symmetric channels and AWGN, CF achieves the common rate capacity to within $\frac{1}{2(N-1)}$ bit.

2.3.4 Functional-Decode-Forward

Ong *et al.* propose a relaying strategy for MWRCs, called functional-decode-forward (FDF) [29, 34]. FDF is based on the use of nested lattice codes [42] at the users to encode their messages. Lattice-based relaying was initially considered for TWRCs resulting in significant performance improvement [27,43]. Nam *et al.* show that nested lattice codes indeed achieve to within $\frac{1}{2}$ bit of the TWRCs' capacity even when the users' channels are asymmetric. Lattice-based relaying can also be used for data transmission from several sources to a destination in a cooperative network and is often called compute-and-forward [44].

For an MWRC with FDF, the uplink and downlink phases are divided into $N-1$ MAC and BC slots respectively [34]. Users encode their data with a special class of lattice codes and in each MAC slot, a pair of users transmits their coded packets to the relay. Denoting the relay's received signal at lth uplink slot by $y_{r,l}$, we have

$$y_{r,l} = x_l + x_{l+1} + n_r \tag{2.11}$$

for $l = 1, 2, \ldots, N-1$. Due to the special structure of nested lattice codes, $\mathcal{R}$ is able to directly decode the sum of the users' data instead of decoding them separately. Thus, the

relays message at lth downlink slot is $x_{\mathrm{r},l} = x_l \oplus x_{l+1}$. After $N-1$ downlink time slots in which $\mathcal{R}$ sends its messages, each user has received $N-1$ independent linear combinations of the other users' data. Hence, it can decode the data of all of them. Please note that each user on average transmits in only $\frac{2}{N}$ of the uplink phase, hence, it can upscale its transmit power to $\frac{NP}{2}$ without violating the users' average power constraint. Please note that in the MWRCs with FDF, users transmit to the relay in pairs. In other words, only two users transmit their data to the relay at each uplink slot. We refer to this approach by *pairwise MWRCs*.

The following theorem is proved [34] for the achievable rate of FDF.

Lemma 2.4 *The maximum achievable common rate of FDF over an MWRC with AWGN links between the users and the relay is*

$$R_{\mathrm{FDF}}^c = \min \left\{ \frac{\log\left(\frac{1}{2} + \frac{NP}{2}\right)}{2(N-1)}, \frac{\log\left(1 + P_r\right)}{2(N-1)} \right\}. \tag{2.12}$$

Proof: Please see [34].

Similar to DF, the first and second terms between the brackets in (2.12) present the uplink and downlink achievable rates by FDF respectively.

Later, we consider a simpler version of FDF, called demodulate-and-forward (DMF), used for memoryless relaying. In DMF, the relay simply demodulates the modulo-sum of the users' transmitted symbols and broadcasts it to the users. The scheme is explained with more details in Chapter 4.

Chapter 3

Bit Mapping Design for FDF MWRCs with PSK Modulation

In a system employing physical-layer network coding, the superimposed constellation at the relay may have ambiguity where one received signal is associated with more than one possible combination of users' data. In this chapter, we find the necessary and sufficient condition on a user bit mapping which removes this ambiguity for phase shift keying (PSK) modulation. Further, we introduce the concept of semi-Gray mapping which improves the system BER performance and achievable rate.

3.1 Introduction

As mentioned in the previous chapter, in an FDF MWRC, the relay directly decodes the modulo-sum of the users' transmitted messages. Before proceeding to the decoding, the relay needs to first demodulate the sum of the users' transmitted symbols. Note that due to simultaneous users' transmissions, relay receives the superimposed version of the users' transmitted constellation.

For a fixed modulation scheme at the users, the performance of the decoding at the relay depends on the users' symbol mapping. The first performance issue which needs consideration is the ability of demodulating the modulo-sum of the users' data without ambiguity. For conventional modulation schemes and assuming perfect power control and synchronization at the user side, the generated constellation at the relay usually has at least one point associated with more than one combination of the users' constellation points. This in turn causes a demodulation ambiguity at the relay which should be resolved. When power control and synchronization at the users are imperfect, instead of ambiguity points, constellation points at very small distance from one another will be formed at the relay.

This will significantly increase the bit error rate (BER) of the system. Thus, resolving the ambiguity in the ideal case would immediately benefit any practical case too.

The signal ambiguity at the relay can be handled by using a non-binary demodulation at the relay proposed in [24] when users apply pulse amplitude modulation (PAM) or quadrature amplitude modulation (QAM). While a binary system needs simple XOR operation, non-binary schemes are not as simple. Hence, it is a matter of interest to design binary demodulation schemes without ambiguity. For this purpose, the authors propose a new PAM scheme in [45] which modifies the spacing between PAM constellation points. Although this method can remove the ambiguity, the non-uniform spacing of PAM points results in a smaller noise margin and higher BER at the relay. It should be added that the proposed demodulation schemes in [24] and [45] do not include phase modulation, e.g. PSK.

In this work, we focus on designing simple modulation/demodulation scheme for FDF TWRCs (and similarly pairwise MWRCs) when PSK modulation is used for data communication. To this end, we resolve the ambiguity through careful mapping of the symbols by finding the necessary and sufficient condition of the mapping for an ambiguity-free demodulation at the relay. A user mapping holding this condition is called a *legitimate* mapping.

Since our solution is not based on modifying the spacing between constellation points, the BER is not compromised. In fact, we find a set of legitimate mappings that even improve the BER. For this, we use a symbol labeling at the users that results in a superimposed constellation at the relay whose minimum-distance points are Gray-labeled. Thus, the labeling of minimum-distance points differs in only one bit [1]. In this case, the superimposed constellation is said to be *semi-Gray* mapped. Notice that the user constellation may not be Gray-labeled. Our simulation results confirm that the semi-Gray scheme outperforms binary reflected Gray mapping (BRGM) which is shown to be the optimal mapping for conventional systems over AWGN channels in high SNR regime [47]. Further, under bit-interleaved coded modulation (BICM), our proposed semi-Gray mapping achieves higher rates than BRGM. Convergence to the achievable rate of coded modulation (CM) also occurs at much lower SNRs.

This chapter is organized as follows: Section 3.2 describes the system model and defines the considered problem. The properties of the received superimposed constellation at the relay are identified in Section 3.3. Our proposed symbol mapping and some analytical

---

[1]The bit error rate of a constellation in the high SNR region can be written in the form of $k_1 k_2 \mathcal{Q}(d_{\min}/2\sigma)$ [46]. Here, $d_{\min}$ is the minimum distance of the constellation and σ^2 is the noise variance. Also, k_1 represents the average number of constellation points at distance $d_{\min}$ and k_2 is the average number of mapping bits that the points in distance $d_{\min}$ differ. The minimum value of k_2 is 1 which is achieved by our proposed labeling.

performance analysis are presented in Section 3.4. Section 3.5 evaluates the performance of our proposed set of mappings through simulations. The work of this chapter is concluded in Section 3.6.

3.2 Preliminaries

3.2.1 System Model

Here, we consider a FDF TWRC with a relay $\mathcal{R}$ and two users u_1 and u_2 communicating over AWGN channels. The system model can be readily extended to pairwise FDF in MWRCs. Users apply power control and are synchronized at the symbol and phase level [48], however, our symbol mapping study is still helpful when these assumptions do not hold perfectly. Users and the relay apply M-PSK modulation, $M \geq 4$ and $M = 2^k$, where k is a positive integer.

Without loss of generality, it is assumed that the users' constellation has one point on (1,0) which is assigned to the all zero symbol. We name the constellation points, starting counter clockwise from the point on (1,0), by $C_0, C_1, \ldots, C_{M-1}$. We assume similar symbol mappings for both users. We like to have binary operation at the relay such that users send their data symbols to the relay in time slot 1 while in time slot 2, relay broadcasts the bit-wise XOR of the users' transmitted symbols. Denoting the users transmitted symbol by S_{u_1} and S_{u_2}, the relay wants to send $S_r = S_{u_1} \oplus S_{u_2}$ back to the users. Having S_r and their own data, each user can extract the other user data by a simple bit-wise XOR.

3.2.2 Statement of the Problem

The received constellation at the relay, $\mathcal{C}_r$, is the superimposition of the two users constellations. Although the size of $\mathcal{C}_r$ is larger than M, only M XOR sequences are associated with it. Thus, the relay can still use a constellation with M points to transmit S_r to the users. Figure 3.1 shows $\mathcal{C}_r$ when 8-PSK is used and the synchronization and power control are accurate. Notice that in Figure 3.1, there is a constellation point at (0,0) associated with eight different pairs of (S_{u_1}, S_{u_2}). If the XOR value of these pairs differ from each other, an ambiguity will occur, i.e., the relay cannot decide which of the possible XOR values is correct.

If the synchronization or power control is not perfect, there may not be any ambiguity in $\mathcal{C}_r$, but small minimum Euclidean distance is an issue. Figure 3.2 shows one such case with a small power control error. If the XORs of the opposite points in the constellation are not

19

equal, the points formed around $(0, 0)$ will have different mappings causing a small $d_{\min}$ and therefore a high error probability. Thus, a mapping which removes the ambiguity under perfect power control is helpful in the case of imperfect power control by ensuring that the closest points in $\mathcal{C}_{\mathrm{r}}$ (points around $(0, 0)$ in Fig. 3.2) have the same labeling. As a consequence, the minimum distance among the points with non-identical labels is improved. In the rest of this chapter, we assume perfect synchronization and power control.
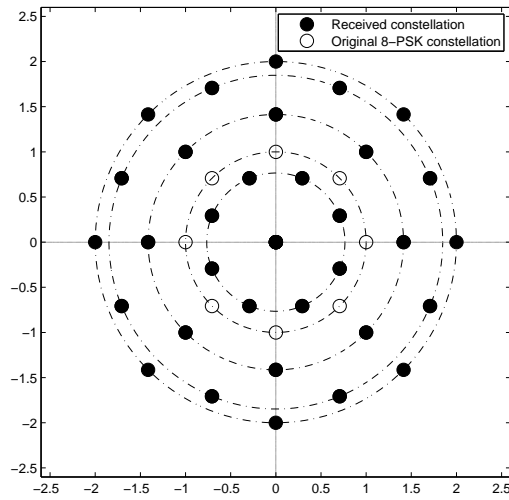
Figure 3.1: Transmitted and received constellations for an 8-PSK system.
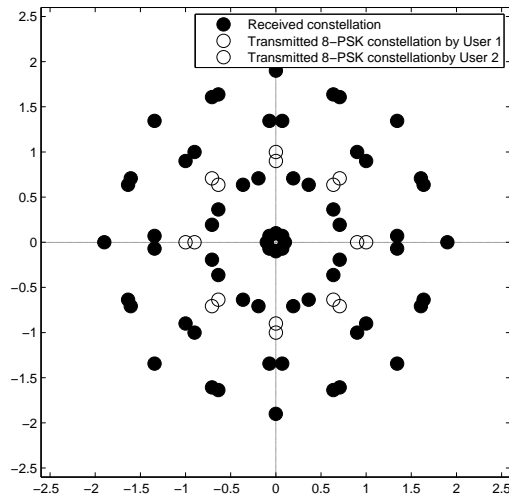
Figure 3.2: Transmitted and received constellations for an 8-PSK system when power control is not accurate.

20

3.2.3 Definitions

Later, we use the known BRGM and set-partitioning mappings for performance studies. Hence, we review them.

A BRGM of order M is derived by $M-1$ recursive reflections of the binary mapping, $(0,1)$. In the recursive reflection to construct the mapping of order i from $i-1$, first we reflect the mapping of order $i-1$. Then, we add 0 to the left of each mapping in the first half of the resulted sequence and put 1 at the left of the mappings in the second half. BRGM has a unique property where neighboring labels are different in only one bit. Examples of BRGM for 8-PSK and 16-PSK are presented in Table 3.1 and 3.2 respectively.

Another important mapping proposed for applications in coded modulation (CM) systems is the set-partitioning mapping proposed by Ungerboeck in [49]. The purpose of this mapping is partitioning the constellation points into subsets with increasing minimum distance. The importance of set-partitioning labeling is that under sequential decoding it results in the maximum achievable rate. Please notice that set-partitioning mapping for an M-PSK constellation results in natural mapping for the constellation points from 0 to $M-1$. Table 3.1 and 3.2 give examples for set-partitioning mappings for 8-PSK and 16-PSK.

3.3 Properties of the Relay's Received Constellation ($\mathcal{C}_\mathrm{r}$)

Now, we briefly describe the structure of $\mathcal{C}_\mathrm{r}$ for any arbitrary PSK modulation under perfect power control and synchronization and then find its minimum Euclidean distance.

Lemma 3.1 $\mathcal{C}_\mathrm{r}$ *has* $\frac{M^2}{2}+1$ *points. One of these points is located at (0,0) and the rest are located on* $\frac{M}{2}$ *co-centered circles with different radii.*

Proof: See Appendix. ■

We denote the $\frac{M}{2}$ groups (circles) stated in Lemma 3.1 by $g_1, g_2, \ldots, g_{\frac{M}{2}}$ starting from the closest group to the center. All points in $\mathcal{C}_\mathrm{r}$ are associated with a unique combination of users pair of symbols except the center point which represents the combination of any two opposite points on the M-PSK constellation. Since the mappings of these points are different, their XOR cannot be all zero symbol. In fact, depending on the users' mapping, the center point can take any possible $M-1$ XOR values, namely $A_1, A_2, \ldots, A_{M-1}$, other than all zero symbol, A_0.

Theorem 3.1 gives d_{min} of $\mathcal{C}_\mathrm{r}$, but we state the following lemma first.

Lemma 3.2 *The distance between a point in g_i and its neighbor from g_{i+1} is independent of i and equal to*

$$d_n = \sqrt{2\left[1 - \cos\left(\frac{2\pi}{M}\right)\right]} = 2\sin\left(\frac{\pi}{M}\right). \tag{3.1}$$

Proof: Assume $P_1 = C_j + C_{M/2+j-i-1}$ represents an arbitrary point in g_i. The closest point to P_1 on g_{i+1}, called P_2, is in the form of $P_2 = C_j + C_{M/2+j-i-2}$. Thus, if we denote the distance between two points by $d(\cdot, \cdot)$, then $d(P_1, P_2) = d(C_{M/2+j-i-1}, C_{M/2+j-i-2})$. This is the distance between two neighboring points on the M-PSK constellation which is equal to d_n in (3.1). ∎

Theorem 3.1 *The minimum Euclidean distance of $\mathcal{C}_r$ is*

$$d_{\min} = 2\left[1 - \cos\left(\frac{2\pi}{M}\right)\right] \tag{3.2}$$

and $d_{\min}$ happens between two neighboring points on g_1 and also between two neighboring points which one of them is located on $g_{\frac{M}{2}-2}$ and the other on $g_{\frac{M}{2}}$.

Proof: See Appendix. ∎

3.4 Symbol Mapping Strategy for PSK

3.4.1 Legitimate Mappings

Since the only ambiguity point in $\mathcal{C}_r$ is the (0,0) point, for an M-PSK mapping not to cause any ambiguity, the XORs of its opposite points must all be equal. We refer to such a mapping as a legitimate mapping.

It has been shown in [47] that BRGM is the optimal mapping for PSK in terms of BER. We show that it is also a legitimate mapping. It is easy to show that for a 4-PSK (QPSK) constellation, BRGM is a legitimate mapping. Now, BRGM for any $M \geq 8$, S, is constructed from BRGM for $\frac{M}{4}$, S', as follows, where $0 \leq i < \frac{M}{4}$-PSK

$$S_i = (00S_i'), \quad S_{\frac{M}{4}+i} = (01S_i'), \quad S_{\frac{M}{2}+i} = (11S_i'), \quad S_{\frac{3M}{4}+i} = (10S_i'). \tag{3.3}$$

Now, for any $0 \leq j < \frac{M}{2}$, $S_j \oplus S_{\frac{M}{2}+j} = (110\ldots0)$. Thus, BRGM is legitimate.

Set-partitioning is also a legitimate mapping because in the set-partitioning mapping, the mapping of every two opposite points differ in their last bit. Hence, the XOR of any two opposite constellation points gives $(10\ldots0)$.

To this point, we discussed what mappings do not cause ambiguity in the system. Comparing the performance of different legitimate mappings is addressed in the following. In

fact, we find out that BRGM, although a legitimate mapping, is not a desired mapping in terms of the BER and achievable rate. As a consequence, it is important to look for other legitimate mappings that improve these performance metrics.

3.4.2 Semi-Gray Mapping for $\mathcal{C}_r$

It is shown in [50] that BRGM is optimal for PSK, PAM and QAM modulation and gives the lowest average probability of error. Also, Caire *et. al* [51] show that BRGM is BER-optimal when BICM is used and they conjecture that it maximizes the capacity.

Even if users apply BRGM, it does not mean that the superimposed constellation at the relay is Gray-labeled or has its desired properties. This hints that a careful mapping must be performed at the user side, which in turn motivates us to introduce the concept of *semi-Gray* mapping. $\mathcal{C}_r$ is semi-Gray mapped if any two points of it with distance $d_{\min}$ differ in only one bit. While in BRGM any point differs in maximum one bit from its closest neighbors, here, the focus is only on pairs with the minimum distance $d_{\min}$. Please notice that we use the semi-Gray mapping term for both user and relay interchangeably. By semi-Gray mapping for users, we mean a legitimate mapping at the users which results in a semi-Gray mapped constellation at the relay.

Theorem 3.2 *A legitimate mapping at the users results in a semi-Gray mapping at the relay if and only if for any $i = 0, 1, \ldots, M - 1$, S_i and S_{i+2} differ in only one bit. Here, if $i + 2 > M - 1$, we consider S_{i+2-M} instead of S_{i+2}.*

Proof: See Appendix. ∎

Corollary 3.1 *The superimposition of two PSK constellations with BRGM is not semi-Gray.*

Proof: In BRGM, for any i, S_i and S_{i+2} differs in two bits. ∎

Corollary 3.2 *Except for QPSK, set-partitioning mapping is not semi-Gray.*

Proof: Since set-partitioning mapping for PSK results in natural mapping, clearly, not all S_i and S_{i+2} differ in one bit. ∎

We like to find a legitimate mapping for M-PSK such that it results in a semi-Gray mapping at the relay. To this aim, we use a technique similar to the approach used for generating BRGM [50]. Assume that $G_0, G_1, \ldots, G_{\frac{M}{2}-1}$ denotes BRGM for $\frac{M}{2}$-PSK modulation. To build the desired mapping, we assign $0G_0, 0G_1, \ldots, 0G_{\frac{M}{2}-1}$ to the even constellation

points and $1G_0, 1G_1, \ldots, 1G_{\frac{M}{2}-1}$ to the odd constellation points. Now, it is easy to show that the XORs of every two opposite constellation points are equal. Also, according to Theorem 3.2, the mapping is semi-Gray. We call this mapping *reflected semi-Gray* mapping.

In addition to the above example, one can find other legitimate mappings resulting in semi-Gray mapping. In Section 4.4, we compare the performance of some of these mappings.

Remark 3.1 *our discussion can be extended to other modulation schemes depending on the constellation shape. For instance, Figure 3.3(a) and Figure 3.3(b) show two different constellations for 8-QAM [52]. It can be shown that while one can find a semi-Gray mapping for the constellation in Figure 3.3(b), there is no semi-Gray mapping for Figure 3.3(a). Both constellations, however, have legitimate mappings, because they cause ambiguity only at (0,0).*

(a) Lattice 8-QAM   (b) Aligned 8-QAM
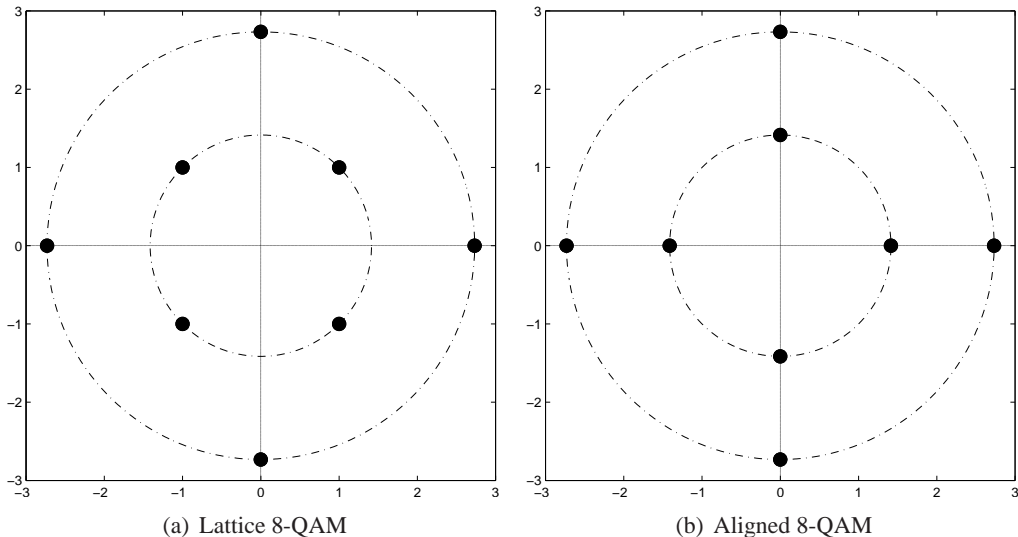
Figure 3.3: Two different constellations for 8-QAM.

3.4.3 Achievable Uplink Rate Analysis

The symbol mapping at the users can also affect the achievable rate of the system in the uplink, i.e. users to relay transmission. To this end, we find the achievable rates of our proposed mappings under CM and BICM in the uplink. Then, we use the derived rates to compare the performance of different symbol mappings. It is assumed that a user sends each of the PSK constellation points with equal probability.

24

It is worthy to mention that the FDF rates presented in Chapter 2 are for the ideal case where the relay uses Gaussian modulation. In a practical system, due to the infeasibility of the Gaussian modulation, the achievable rates are smaller when common modulations are used. Note that CM and BICM can be built based on the (nested) lattice codes [53].

Assume $x_\mathrm{r} \in \{A_0, A_1, \ldots, A_{M-1}\}$ is the bitwise XOR of the users data. Notice that x_r is the desired information to be decoded at the relay. Also, y_r represents the received signal at the relay. Thus, the transmission from the users to the relay can be viewed as a virtual single-input single-output channel whose input is x_r and its output is y_r. Then, the achievable rate of this channel is

$$R = I(x_\mathrm{r}; y_\mathrm{r}) = E_{x_\mathrm{r}, y_\mathrm{r}} \left[\log_2 \frac{p(y_\mathrm{r}|x_\mathrm{r})}{p(y_\mathrm{r})} \right]. \tag{3.4}$$

Notice that for a point z from $\mathcal{C}_\mathrm{r}$ with mapping x_r, the relay receives the correct symbol if it detects any of the constellation points with mapping x_r which may not necessarily be z. Thus,

$$p(y_\mathrm{r}|x_\mathrm{r}) = \sum_{z \in \mathcal{C}_\mathrm{r}^{x_\mathrm{r}}} \frac{p(y_\mathrm{r}|z)p(z)}{p(x_\mathrm{r})}, \quad p(y_\mathrm{r}) = \sum_{z \in \mathcal{C}_\mathrm{r}} p(y_\mathrm{r}|z)p(z) \tag{3.5}$$

where $\mathcal{C}_\mathrm{r}^{x_\mathrm{r}}$ denotes the points of $\mathcal{C}_\mathrm{r}$ with mapping x_r. Now, considering $p(x_\mathrm{r}) = 1/M, \forall x_\mathrm{r} \in \{A_0, A_a, \ldots, A_{M-1}\}$, (3.4) can be rewritten as

$$R = \log_2 M - E_{x_\mathrm{r}, y_\mathrm{r}} \left[\log_2 \frac{\sum\limits_{z \in \mathcal{C}_\mathrm{r}} p(y_\mathrm{r}|z)p(z)}{\sum\limits_{z \in \mathcal{C}_\mathrm{r}^{x_\mathrm{r}}} p(y_\mathrm{r}|z)p(z)} \right]. \tag{3.6}$$

Similarly, when BICM is applied, if b denotes a binary random variable for the users data bits, we have

$$R = I(x_\mathrm{r}; y_\mathrm{r}) = \log_2 M - \sum_{i=1}^{\log_2 M} E_{b, y_\mathrm{r}} \left[\log_2 \frac{\sum\limits_{z \in \mathcal{C}_\mathrm{r}} p(y_\mathrm{r}|z)p(z)}{\sum\limits_{z \in \mathcal{C}_{R_b}^i} p(y_\mathrm{r}|z)p(z)} \right] \tag{3.7}$$

where $\mathcal{C}_{R_b}^i$ represents the constellation points in $\mathcal{C}_\mathrm{r}$ whose ith bit of mapping is b. For the simplicity of presentation, we skip deriving the analytical form of the probability distrivutions and derive the capacity for the proposed schemes through computer simulation.

3.5   Simulation Results

In this section, we compare the performance of different mappings in terms of their BER and achievable rate. Please note that the BER and achievable rates are calculated at the

relay. While many user mappings result in semi-Gray mapping at the relay, we consider two of them. The first mapping is reflected semi-Gray mapping and the second one is an arbitrary semi-Gray mapping, both presented in Table 3.1 and Table 3.2. We compare the BER performance of these two semi-Gray mappings with BRGM. Also, for achievable rates' comparison, we compare the performance of semi-Gray mapping with BRGM and set-partitioning mapping under BICM and CM. The simulations are performed for 8-PSK and 16-PSK.

BRGM	(000)(100)(101)(111)(110)(010)(011)(001)
Reflected semi-Gray	(000)(100)(001)(101)(011)(111)(010)(110)
Arbitrary semi-Gray	(000)(111)(001)(110)(101)(010)(100)(011)
Set-partitioning	(000)(001)(010)(011)(100)(101)(110)(111)

Table 3.1: Different mappings for 8-PSK.

BRGM	(0000)(0001)(0011)(0010)(0110)(0111)(0101)(0100)
	(1100)(1101)(1111)(1110)(1010)(1011)(1001)(1000)
Reflected semi-Gray	(0000)(1000)(0100)(1100)(0101)(1101)(0111)(1111)
	(0110)(1110)(0010)(1010)(0011)(1011)(0001)(1001)
Arbitrary semi-Gray	(0000)(1111)(1000)(0111)(1100)(0110)(0100)(1110)
	(0101)(1010)(1101)(0010)(1001)(0011)(0001)(1011)
Set-partitioning	(0000)(0001)(0010)(0011)(0100)(0101)(0110)(0111)
	(1000)(1001)(1010)(1011)(1100)(1101)(1110)(1111)

Table 3.2: Different mappings for 16-PSK.

Figure 3.4 shows the BER of BRGM, reflected semi-Gray and the arbitrary semi-Gray mappings in terms of the user transmitted SNR. We consider both cases of perfect and imperfect power control at the users. Here, both semi-Gray mappings outperform BRGM in higher SNRs and have the same BER performance in high SNR region. However, in low SNRs, we can see that while BRGM and reflected semi-Gray mappings have almost the same performance, the arbitrary semi-Gray mapping has a higher BER. This comes from the mapping of the $\mathcal{C}_r$ points with the second smallest distance after $d_{\min}$, called d_s. With BRGM, points with distance d_s are all Gray-mapped (i.e., differ in only one bit) at the relay, while for the chosen arbitrary semi-Gray mapping, none of these points are Gray-mapped. On the other hand, using the reflected semi-Gray mapping, half of the points with distance d_s are Gray mapped. Hence, it has a lower BER compared to the arbitrary semi-Gray

mapping and a slightly higher BER compared to BRGM.
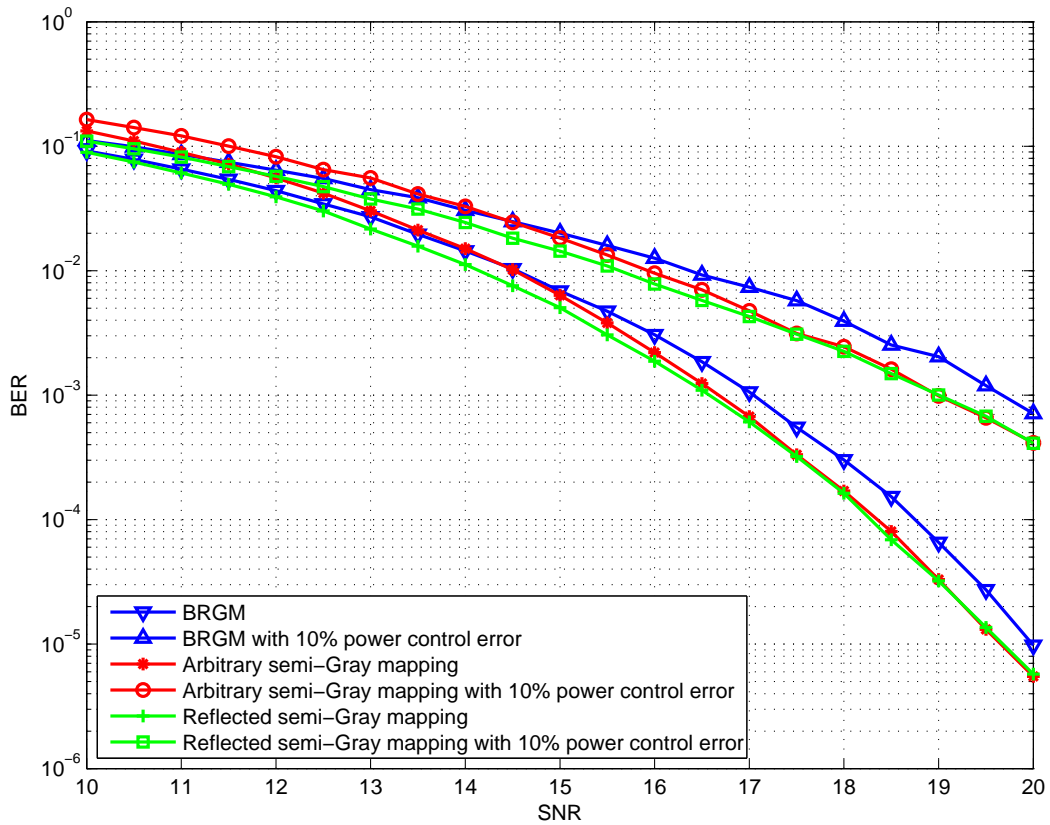
Figure 3.4: BER performance of the relay when users apply 8-PSK modulation.

Figure 3.5 represents the BER performance of three different mappings for 16-PSK modulation. Similar to the previous case, here, we have BRGM, reflected semi-Gray mapping and the arbitrary semi-Gray mapping. Again, we see a performance improvement by both reflected semi-Gray and arbitrary semi-Gray mappings in high SNRs compared to BRGM. Since the superimposed constellation for 16-PSK is more sensitive to power control error than 8-PSK, in this figure we use a smaller deviation in the power control compared to Figure 3.4.

Figures 3.6 and 3.7 depict the comparison between the achievable rates of BRGM, semi-Gray and set-partitioning mappings under BICM and CM. As we can see, in higher SNRs, reflected semi-Gray outperforms other mappings and decreases the gap between BICM and CM.
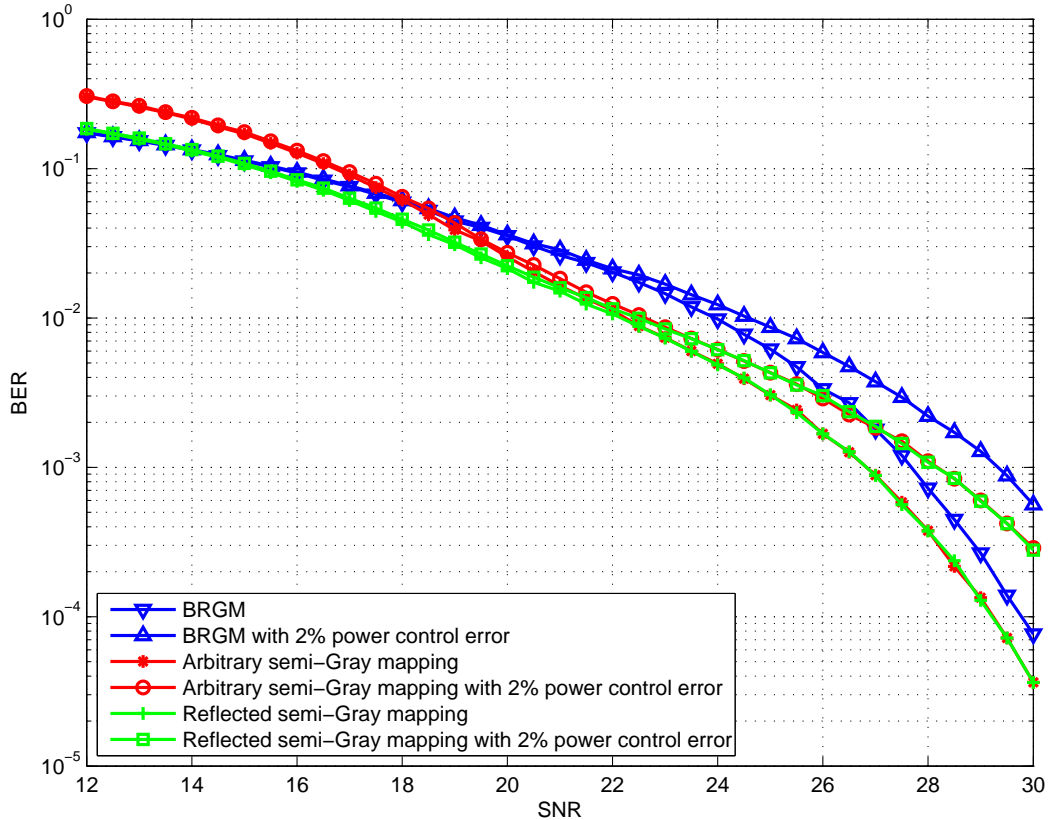
Figure 3.5: BER performance of the relay when users apply 16-PSK modulation.

3.6 Conclusion

In this chapter, we studied the symbol mapping for applying simple bitwise XOR detection at the relay when PSK modulation is used. First, we characterized the received constellation at the relay. Then, we found a set of mappings for the users, called legitimate mappings, which prevent decoding ambiguity at the relay. Further, we introduced the concept of semi-Gray mapping at the relay where the constellation points with distance $d_{\min}$ are Gray-mapped. The necessary and sufficient condition for a legitimate mapping at the users which generates a semi-Gray mapping at the relay was also found. Our simulations showed that a semi-Gray mapping can generally improve the BER and achievable rate in high SNRs, but the performance of different semi-Gray mappings varies in low SNRs. Finding the optimal semi-Gray mapping is an open problem for future work. Since communication systems typically operate in small error rate regions, this optimal mapping should guarantee the lowest BER in medium to high SNR regime.
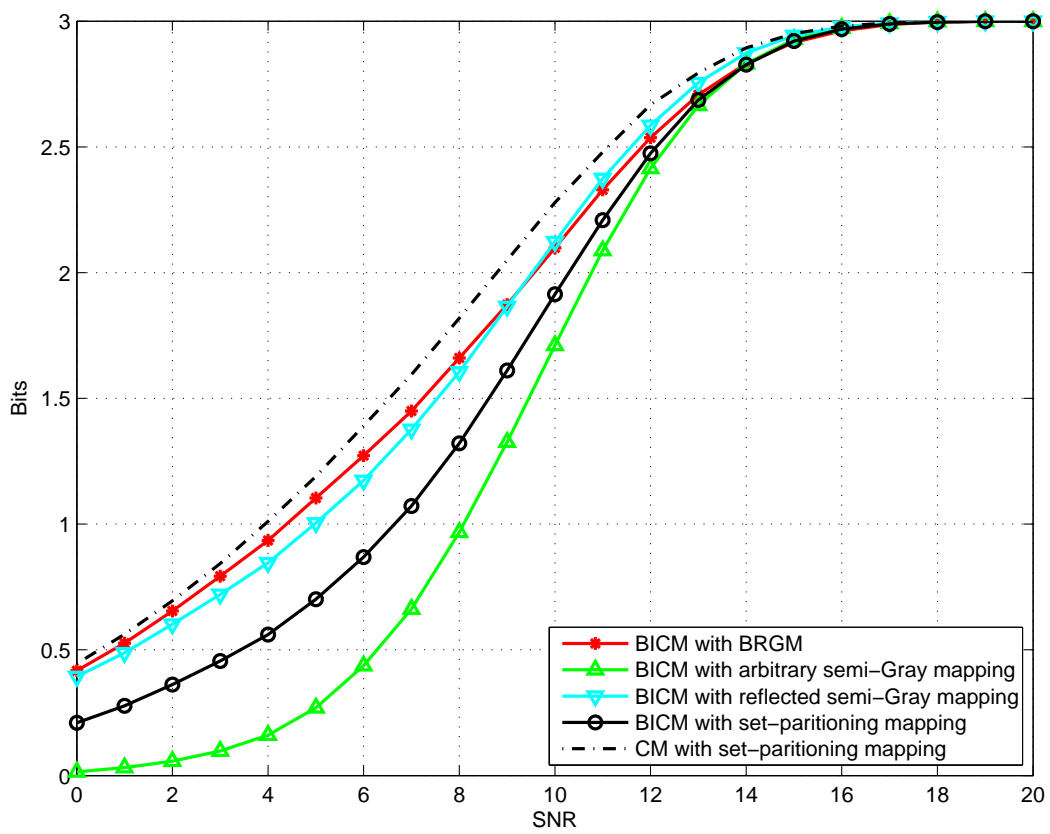
Figure 3.6: Achievable rates of 8-PSK modulation.
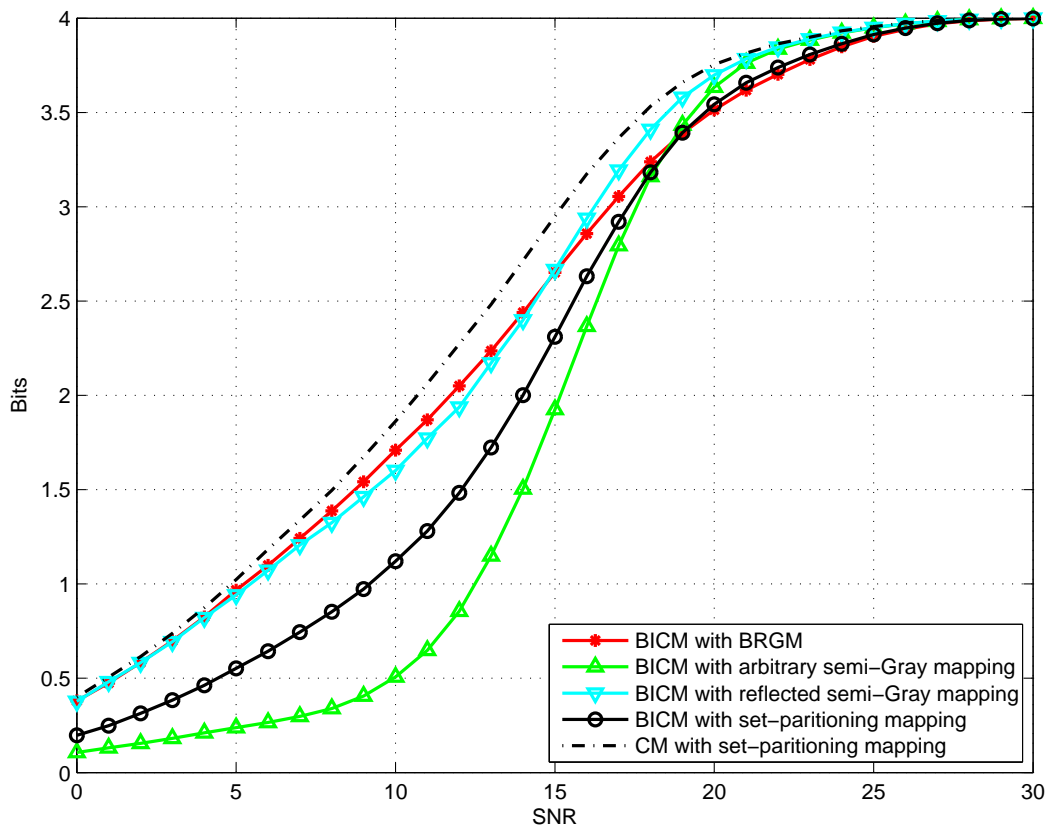
Figure 3.7: Achievable rates of 16-PSK modulation.

Chapter 4

Achievable Rates of Memoryless TWRCs

In this chapter, we study AF and DMF, in terms of their achievable data exchange rate, for a memoryless TWRC. Our results show that unlike memoryless one-way relaying, increasing users' SNR benefits AF more than DMF. Another interesting observation is that while with DMF a higher data rate is provided for the user whose channel condition is better, with AF the situation is the reverse. Further, we find that for a TWRC with asymmetric users' channels, AF can take advantage of power back-off at the users, without degrading the data rate, to save energy.

4.1   Introduction

In a memoryless relaying scenario, the relay performs only simple operations on its current received signal. Such systems are found in delay-intolerant or sensor network applications [48]. Since AF relay just amplifies its received signal, it can be readily used in memoryless MWRCs. To use DF in a memoryless MWRC, demodulate-and-forward (DMF) [24, 54] is proposed. In DMF, the relay first demodulates its current received signal and then forwards it to the users. The main focus of this chapter is studying the achievable data rate of AF and DMF for practical memoryless TWRCs. While we discuss TWRCs, the arguments are valid for pairwise MWRCs as well.

In this chapter, it is assumed that users want to exchange data through a memoryless relay over a fading environment with AWGN. For simplicity of the analysis, similar to [48] and [54], we assume that BPSK is used for DMF. However, our rate analysis approach can be easily extended to other modulations schemes.

Based on the considered TWRC setup, we find the achievable data reception rate for

each user, which is defined as the rate that the user can receive data from the other user. Then, we determine the users' data exchange rate which is the minimum of the two users reception rates. Note that the data exchange rate represents the common rate at which both users can share data.

Our study reveals that for memoryless relaying over a Rayleigh fading environment, AF generally achieves better performance. More specifically, by increasing the users' SNR, AF achieves higher data exchange rates than DMF for a fixed relay SNR. This is opposite to the behavior seen in memoryless one-way relaying [55]. Also, we show that, surprisingly, the user with worse channel condition has a higher data reception rate than the other user when AF is used.

A practical application of our rate analysis is for TWRCs with asymmetric users' channels. When users have asymmetric fading characteristics, we observe that DMF provides almost equal reception rate for both users while users have different reception rates in AF. Now, if a symmetric data exchange rate is intended, AF can be more power-efficient by decreasing the transmission power of the user with better channel condition without degrading the data rate. This is a valuable observation for energy-limited systems like sensor networks.

Here is the organization of the chapter. Section 4.2 presents the system model and describe AF and DMF in more detail. Then, the rate analysis for AF and DMF is presented in Section 4.3. Numerical examples are provided in Section 4.4. Finally, Section 4.5 concludes the chapter.

4.2 System Model

Here, we denote users by u_1 and u_2 and the relay by $\mathcal{R}$. In the first time slot, called multiple access (MAC) phase, u_1 and u_2 simultaneously transmit their coded data bits, x_1 and x_2, with power P_1 and P_2 respectively. We assume that each user transmits 0 or 1 with equal probability. Also, there is no direct link between the users. Then, R broadcasts the amplified version of the received signal (for AF) or the XOR of the messages (for DMF) in the broadcast (BC) phase with power P_r. Please note that the relay does not attempt to decode the users data. Knowing its own data, each user then subtracts its data from the relay broadcast message and retrieves the other users transmitted bit and proceed with data decoding.

The communication between the users and the relay takes place over a fading channel

with Gaussian noise. The channel gains from u_1 to $\mathcal{R}$ and from u_2 to $\mathcal{R}$ are $0 \leq h_1$ and $0 \leq h_2$ respectively. Further, the channels are assumed to be reciprocal. As we discuss later, in AF, each user has to know its own channel gain, but this assumption is not necessary for DMF. Also, the relay knows both h_1 and h_2. Without loss of generality, we assume $h_1 P_1 \leq h_2 P_2$.

To evaluate the data exchange rate in a memoryless system, we need to take the effect of the modulation into account. Although the Gaussian modulation gives the highest rate, it is not feasible in practice. Using BPSK is appropriate for memoryless relaying [48,54] and we accommodate it here for the relay and users.

4.2.1 Signal Modeling in the MAC Phase

When the users transmit their data to the relay, channel superimposes their transmitted signal. Thus, the arrived signal at $\mathcal{R}$ in the MAC phase is

$$y_{\mathrm{r}} = h_1 \sqrt{P_1} x_1 + h_2 \sqrt{P_2} x_2 + n_{\mathrm{r}} \tag{4.1}$$

where n_{r} is the Gaussian noise with variance σ_{r}^2. Although the MAC phase is similar for both AF and DMF, their BC phases are different. In the following, we present the BC model for AF and DMF separately.

4.2.2 Signal Modeling for AF in the BC Phase

To keep the output power limited to P_r, $\mathcal{R}$ amplifies the received signal by

$$\alpha = \sqrt{\frac{P_r}{h_1^2 P_1 + h_2^2 P_2 + \sigma_{\mathrm{r}}^2}}. \tag{4.2}$$

and then transmits

$$x_{\mathrm{r}} = \alpha y_{\mathrm{r}} = \alpha(h_1 \sqrt{P_1} x_1 + h_2 \sqrt{P_2} x_2 + n_{\mathrm{r}}). \tag{4.3}$$

Now, if u_1 and u_2 know their own channel gains as well as α, they can subtract their own signal from the broadcast signal. Thus, the final received signal by u_1 and u_2, called y_1 and y_2 respectively, are

$$y_1 = \alpha h_1 h_2 \sqrt{P_2} x_2 + \alpha h_1 n_{\mathrm{r}} + n_1, \tag{4.4}$$

$$y_2 = \alpha h_1 h_2 \sqrt{P_1} x_1 + \alpha h_2 n_{\mathrm{r}} + n_2 \tag{4.5}$$

where n_1 and n_2 are the Gaussian noise at u_1 and u_2 with variance σ_1^2 and σ_2^2 respectively.

4.2.3 Signal Modeling for DMF in the BC Phase

In DMF, $\mathcal{R}$ receives y_r and then demodulates it. The demodulated bit at $\mathcal{R}$ can be modeled as $x_r = x_1 \oplus x_2 \oplus z_r$ where z_r represents the effect of the detection error. Then, x_r is modulated by $\mathcal{R}$ with BPSK modulation and broadcast to the users. The received signals by u_1 and u_2 are

$$y_1 = h_1\sqrt{P_r}x_r + n_1, \tag{4.6}$$

$$y_2 = h_2\sqrt{P_r}x_r + n_2. \tag{4.7}$$

Finding the error probability for z_r is necessary to characterize this binary channel. While u_1 and u_2 use binary constellation for data transmission, $\mathcal{R}$ receives a constellation with four points $\{-h_2\sqrt{P_2} - h_1\sqrt{P_1}, -h_2\sqrt{P_2} + h_1\sqrt{P_1}, h_2\sqrt{P_2} - h_1\sqrt{P_1}, h_2\sqrt{P_2} + h_1\sqrt{P_1}\}$. Assuming that -1 is assigned to 0 and +1 to 1, receiving $-h_2\sqrt{P_2} - h_1\sqrt{P_1}$ or $h_2\sqrt{P_2} + h_1\sqrt{P_1}$ means that both users have sent either 0 or 1. Thus, their XOR is 0 and R sends -1. Similarly, R sends +1 when it receives $-h_2\sqrt{P_2} + h_1\sqrt{P_1}$ or $h_2\sqrt{P_2} - h_1\sqrt{P_1}$ (Figure 4.1).
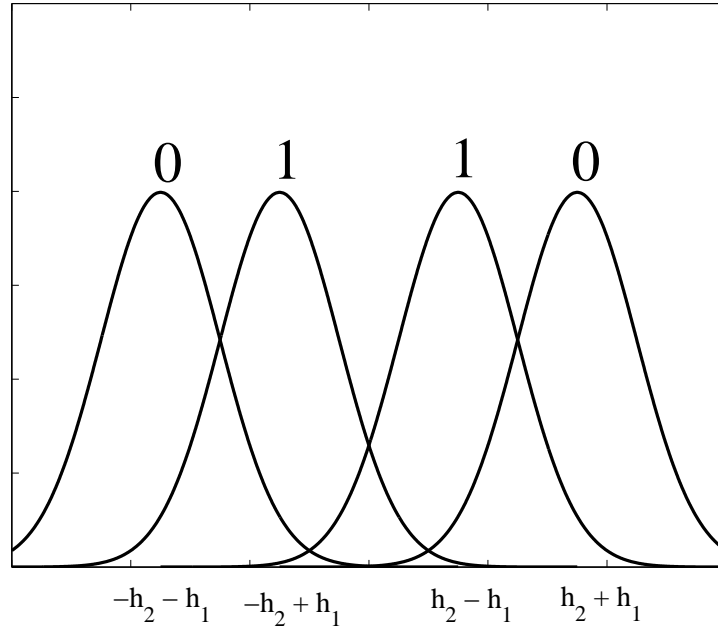
Figure 4.1: The received signal at the relay when $P_1 = P_2 = 1$.

Now, knowing the channel gains at the relay, the conditional probability of wrongly detecting $x_1 \oplus x_2 = 1$, when $x_1 \oplus x_2 = 0$, is

$$p_r^{0 \to 1} = \mathcal{Q}\left(\frac{h_1\sqrt{P_1}}{\sigma_r}\right) - \mathcal{Q}\left(\frac{2h_2\sqrt{P_2} + h_1\sqrt{P_1}}{\sigma_r}\right) \tag{4.8}$$

where $\mathcal{Q}(\cdot)$ is the Gaussian Q-function. Similarly, the conditional probability of detecting $x_1 \oplus x_2 = 0$ when it is indeed 1 is

$$p_r^{1 \to 0} = \mathcal{Q}\left(\frac{h_1\sqrt{P_1}}{\sigma_r}\right) + \mathcal{Q}\left(\frac{2h_2\sqrt{P_2} - h_1\sqrt{P_1}}{\sigma_r}\right). \tag{4.9}$$

4.3   Analysis of the Data Exchange Rate

In this section, we analytically find the data exchange rate of AF and DMF schemes using the system model described in Section 4.2.

4.3.1   Analysis of the AF Data Exchange Rate

Assume X_1 and X_2 are random variables representing input bits at u_1 and u_2. Also, random variables Y_1 and Y_2 stand for the received signal sequence at u_1 and u_2. For a given h_1 and h_2, the achievable reception rate of u_1 is

$$R_{\mathrm{AF}}^1(h_1, h_2) = H(Y_1) - H(Y_1|X_2). \tag{4.10}$$

Given X_2, the only source of ambiguity about Y_1 is the noise term $\alpha h_1 n_r + n_1$, which is a Gaussian noise with variance $\alpha^2 h_1^2 \sigma_r^2 + \sigma_1^2$ because n_1 and n_r are independent. Hence,

$$H(Y_1|X_2) = \frac{1}{2}\log_2(2\pi e \alpha^2 h_1^2 \sigma_r^2 + 2\pi e \sigma_1^2). \tag{4.11}$$

On the other hand, the entropy of Y_1 is

$$H(Y_1) = -\int_{-\infty}^{\infty} f_{Y_1}(y)\log_2 f_{Y_1}(y)\,dy \tag{4.12}$$

where $f_{Y_1}(y)$ is the probability distribution function (pdf) of Y_1. Now, to find all terms in (4.10), we need to derive $f_{Y_1}(y)$. Due to the independency of n_1 and n_r, it can be shown that

$$f_{Y_1}(y) = \frac{1}{2\sqrt{2\pi(\alpha^2 h_1^2 \sigma_r^2 + \sigma_1^2)}}\left(e^{-\frac{(y+\alpha\sqrt{P_2}h_1h_2)^2}{2(\alpha^2 h_1^2 \sigma_r^2 + \sigma_1^2)}} + e^{-\frac{(y-\alpha\sqrt{P_2}h_1h_2)^2}{2(\alpha^2 h_1^2 \sigma_r^2 + \sigma_1^2)}}\right) \tag{4.13}$$

Replacing (4.13) in (4.12), $H(Y_1)$ can be found. In a fading environment, the average reception rate is derived by integration over the distribution of h_1 and h_2 as follows

$$R_{\mathrm{AF}}^1 = \int\int R_{\mathrm{AF}}^1(h_1, h_2)f_{h_1,h_2}(x, y)\,dxdy \tag{4.14}$$

where $f_{h_1,h_2}(x, y)$ is the joint distribution of h_1 and h_2. When h_1 and h_2 are deterministic, $R_{\mathrm{AF}}^1 = R_{\mathrm{AF}}^1(h_1, h_2)$. Similarly, R_{AF}^2 is found. Now, the exchange rate is

$$R_{\mathrm{AF}}^c = \min\{R_{\mathrm{AF}}^1, R_{\mathrm{AF}}^2\}. \tag{4.15}$$

Remark 4.1 *In (4.13), $\alpha^2 h_i^2 \sigma_r^2 + \sigma_i^2$ is a measure of the noise at u_i for $i = 1, 2$. On the other hand, a user with a larger signal to noise ratio receives the data with a higher rate. If $\sigma_1 = \sigma_2$ and $P_1 = P_2$, since $h_1 < h_2$*

$$\alpha^2 h_1^2 \sigma_r^2 + \sigma_1^2 < \alpha^2 h_2^2 \sigma_r^2 + \sigma_2^2. \tag{4.16}$$

Thus, u_1 has a higher reception data rate. It means that the data exchange rate is limited by the reception rate of u_2 which has a better channel condition.

4.3.2   Analysis of the DMF Exchange Rate

Notice that here, Y_1 is an estimation of $X_1 \oplus X_2$. In fact, we can assume that $X_1 \oplus X_2$ is transmitted over the channel. Since u_1 knows its own data, the only ambiguity in $X_1 \oplus X_2$ is related to X_2. Hence, assuming that h_1 and h_2 are given and considering that X_2 is binary, the reception rate of u_1 is

$$R_{\mathrm{DMF^1}}(h_1, h_2) = \frac{1}{2} \sum_{X_2=0,1} \int_{-\infty}^{\infty} f_{Y_1|X_2}(y|x) \log_2 \frac{f_{Y_1|X_2}(y|x)}{f_{Y_1}(y)} \, dy \tag{4.17}$$

where $f_{Y_1|X_2}(y|x)$ is the conditional distribution of Y_1 given X_2. Now, one can show that

$$f_{Y_1,X_2}(y|x_2=0) = \frac{1-p_r^{0\to1}}{\sqrt{2\pi\sigma_1^2}} e^{-\frac{(y+\sqrt{P_r}h_1)^2}{2\sigma_1^2}} + \frac{p_r^{0\to1}}{\sqrt{2\pi\sigma_1^2}} e^{-\frac{(y-\sqrt{P_r}h_1)^2}{2\sigma_1^2}} \tag{4.18}$$

and

$$f_{Y_1,X_2}(y|x_2=1) = \frac{p_r^{1\to0}}{\sqrt{2\pi\sigma_1^2}} e^{-\frac{(y+\sqrt{P_r}h_1)^2}{2\sigma_1^2}} + \frac{1-p_r^{1\to0}}{\sqrt{2\pi\sigma_1^2}} e^{-\frac{(y-\sqrt{P_r}h_1)^2}{2\sigma_1^2}}. \tag{4.19}$$

Notice that $f_{Y_1}(y)$ is easily found from (4.18) and (4.19). Similarly, for the data transfer from u_1 to u_2, the conditional reception rate is

$$R_{\mathrm{DMF^2}}(h_1, h_2) = \frac{1}{2} \sum_{X_1=0,1} \int_{-\infty}^{\infty} f_{Y_2|X_1}(y|x) \log_2 \frac{f_{Y_2|X_1}(y|x)}{f_{Y_2}(y)} \, dy. \tag{4.20}$$

where $f_{Y_2|X_1}(y|x)$ can be found similar to (4.18) and (4.19). If h_1 and h_2 follow a random fading distribution (e.g. Rayleigh distribution), then, averaging over h_1 and h_2 can be done in the same way as (4.14) to obtain the unconditional reception rates, $R_{\mathrm{DMF^1}}$ and $R_{\mathrm{DMF^2}}$. Finally, $R^{\mathrm{DMF}} = \min\{R_{\mathrm{DMF^1}}, R_{\mathrm{DMF^2}}\}$.

Remark 4.2 *Since the broadcast signal from the relay is identical for both users, unlike AF, the signal to noise ratio at the users is proportional to their channel gains. In other words, if $\sigma_1 = \sigma_2$, the user with smaller channel gain, here u_1, receives data with smaller reception rate and dictates the exchange data rate.*

4.4 Simulation Results

Here, we compare the users' achievable reception and exchange rates of AF and DMF. The fading on the users' channels are independent and have a Rayleigh distribution as follows

$$f_{h_i}(x) = \frac{x}{\gamma_i^2} e^{-\frac{x^2}{2\gamma_i^2}} \quad i = 1, 2 \tag{4.21}$$

where $E[h_i^2] = \gamma_i^2$ is the power gain of the fading. Also, $P_1 = P_2 = 1$ and $P_r = 3$ except stated otherwise.

Figure 4.2 shows the rates when $\sigma_1 = \sigma_2 = 0.5$, $\gamma_1^2 = 0.75$ and $\gamma_2^2 = 1$, i.e. we have asymmetric users' channels. As seen, DMF has a better performance in high relay SNRs but AF gives higher rates in low and medium SNRs. The behavior of the users in terms of the reception rate is as mentioned in Remark 4.1 and 4.2. It means that for AF, u_1 (user with smaller channel gain) achieves higher reception rates while u_2 (user with larger channel gain) has higher reception rates when DMF is used.

There is an interesting point about the curves in Figure 4.2. Even with unequal channel conditions, users have almost equal achievable reception rates at low to medium SNRs when DMF is used. This is due to the bottleneck on the rate caused by the demodulation decision at the relay. It means that the demodulation error at the relay limits the rate, not the downlink fading channel from the relay to the users. Hence, users' exchange rate is almost equal to their individual reception rates.

On the other hand, for AF, the user with better channel, u_2, has a lower reception rate than u_1. Using this fact, u_2 can back off its output power without affecting the data exchange rate. This point is significantly helpful in scenarios where users have limited power resources, e.g. in sensor networks. The power adjustment for AF is studied more thoroughly in Figure 4.3. In this figure, $\gamma_2^2 = 1$ and $1/\sigma_r^2 = 10$ dB. Then, by changing γ_1^2, the users' channels become asymmetric and we find the value of P_2 sustaining the same data exchange rate over the asymmetric channels as if $P_2 = 1$. For instance when $1/\sigma_1^2 = 1/\sigma_2^2 = 20$ dB and $\gamma_1^2 = 0.1$, u_2 can save its transmission power by almost 80 percents.

The rate curves for $\gamma_1^2 = 0.5$ and $\gamma_2^2 = 1$ are presented in Figure 4.4. For AF, the data reception rate of both users decreases compared to Figure 4.2. For DMF, changing γ_1 decreases the reception rate of u_1, but the reception rate of u_2 is not noticeably affected in high SNRs. This is because of the small noise power at the relay which keeps the error rate low despite smaller γ_1.

The curves for the achievable reception rates are presented in Figure 4.5 when $\sigma_1 = \sigma_2 = 0.1$. For DMF, despite high SNR at the users, the users' reception rates are limited by
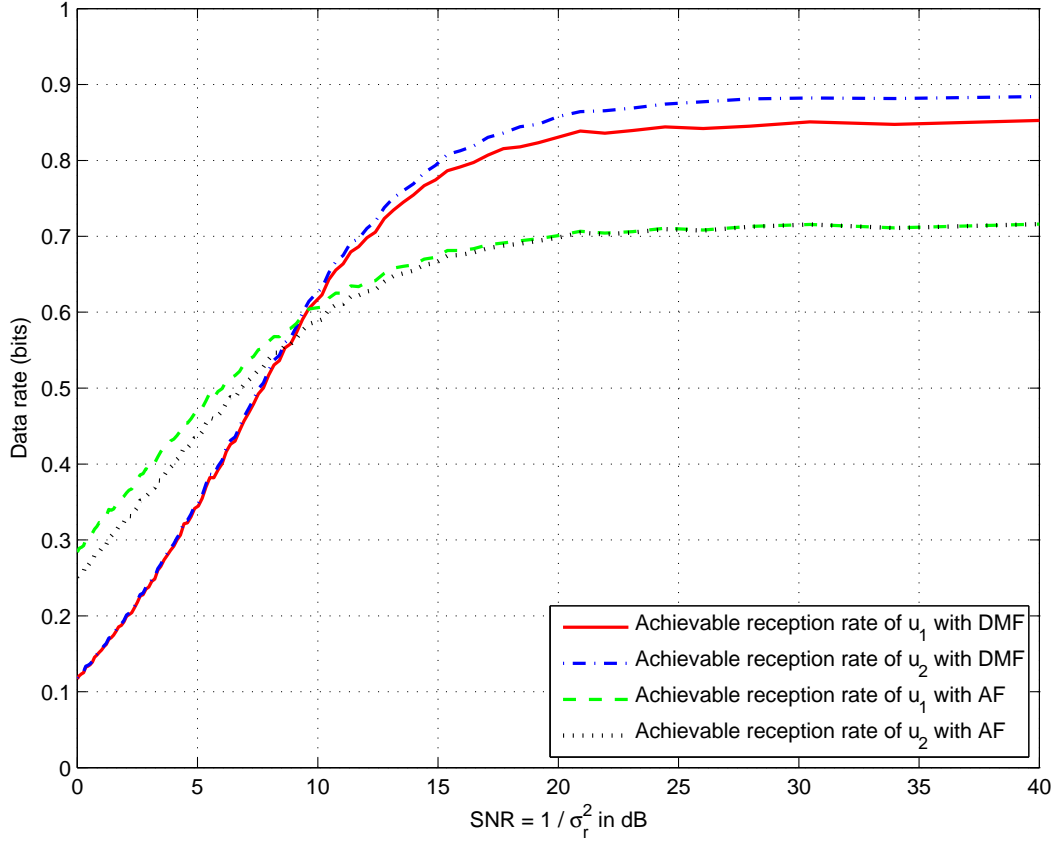
Figure 4.2: Users' achievable reception rates when $\sigma_1 = \sigma_2 = 0.5$ and $\gamma_1^2 = 0.75$ and $\gamma_2^2 = 1$.

the relay decision. As a consequence, both users have almost equal rates. However, for AF, users have different reception rates and power adjustment at u_2 is advantageous. Furthermore, comparing Figure 4.2 and 4.5 shows that AF has a significantly better performance over DMF in a wide range of relay SNRs when users SNR increases. This behavior is different from the memoryless one-way relaying [55] where DMF shows a superior performance over AF when users' SNR increases. To better investigate the effect of increasing users' SNR on the data exchange rate, Figure 4.6 is presented. This figure depicts the comparison between the data exchange rates of AF and DMF for a fixed σ_r. As seen, by increasing the users SNR, AF starts outperforming DMF and the gap between their performance increases by increasing the users SNR.
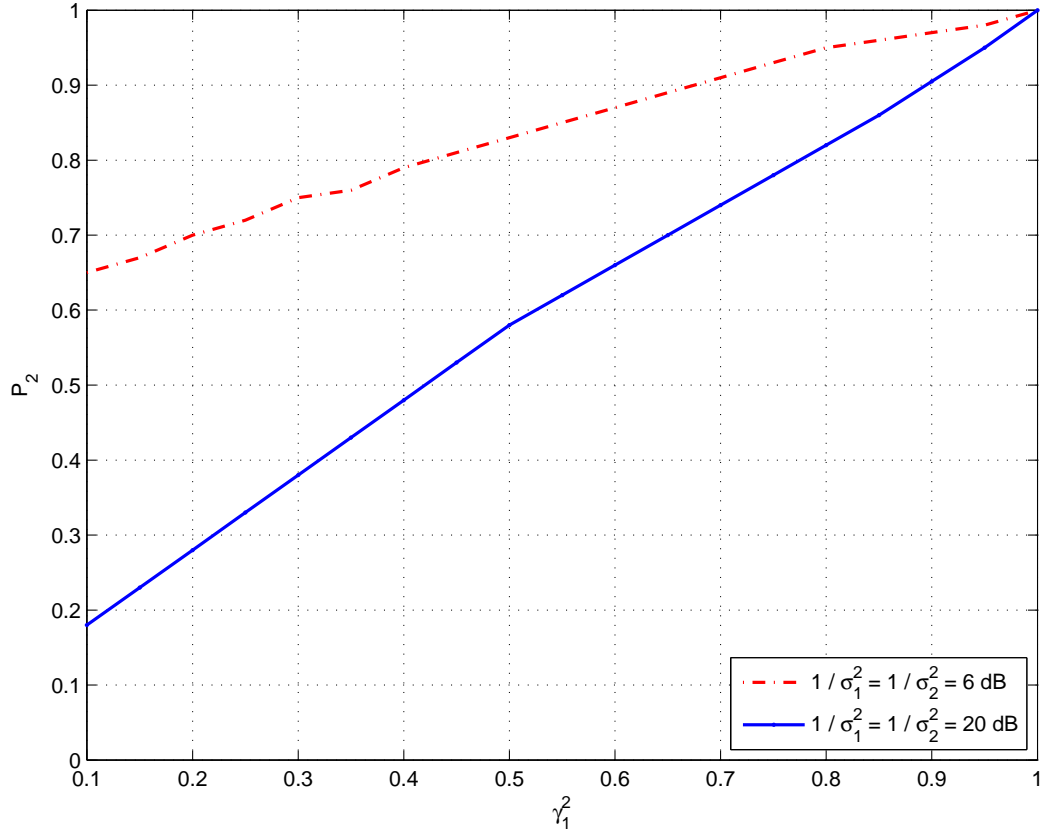
Figure 4.3: Power adjustment of u_2 when the users' channels are asymmetric.

4.5   Conclusion

We studied the data exchange rate between the users in a memoryless TWRC. For this purpose, we assumed that the users transmit their data using BPSK modulation over a fading channel with AWGN. Our study showed that AF outperforms DMF in a wide range of practical SNRs for a Rayleigh fading environment. In fact, unlike memoryless one-way relaying, the advantage of AF over DMF becomes even more by increasing the SNR at the user side. In addition, our analysis revealed that when AF is used, power back-off at the users can significantly save energy without affecting the achievable data exchange rate. The importance of this observation is more notable for energy-limited systems like sensor networks.
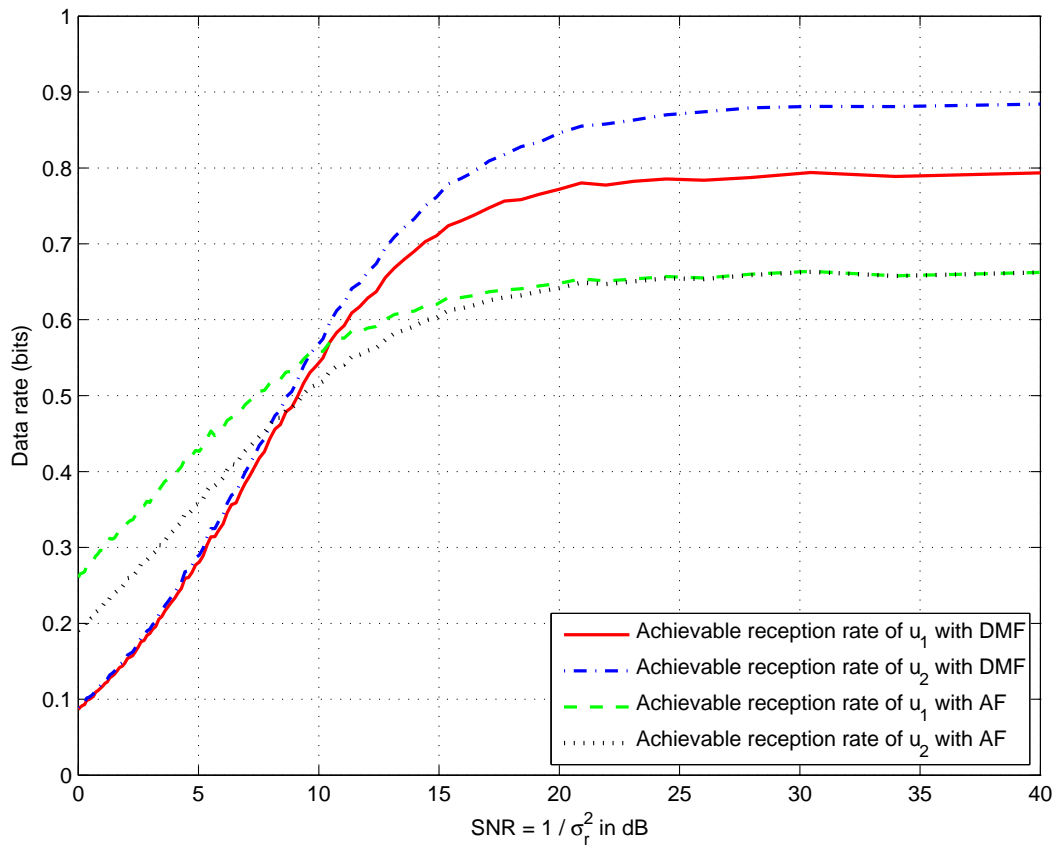
Figure 4.4: Users achievable reception rates when $\sigma_1 = \sigma_2 = 0.5$ and $\gamma_1 = 0.5$ and $\gamma_2 = 1$.
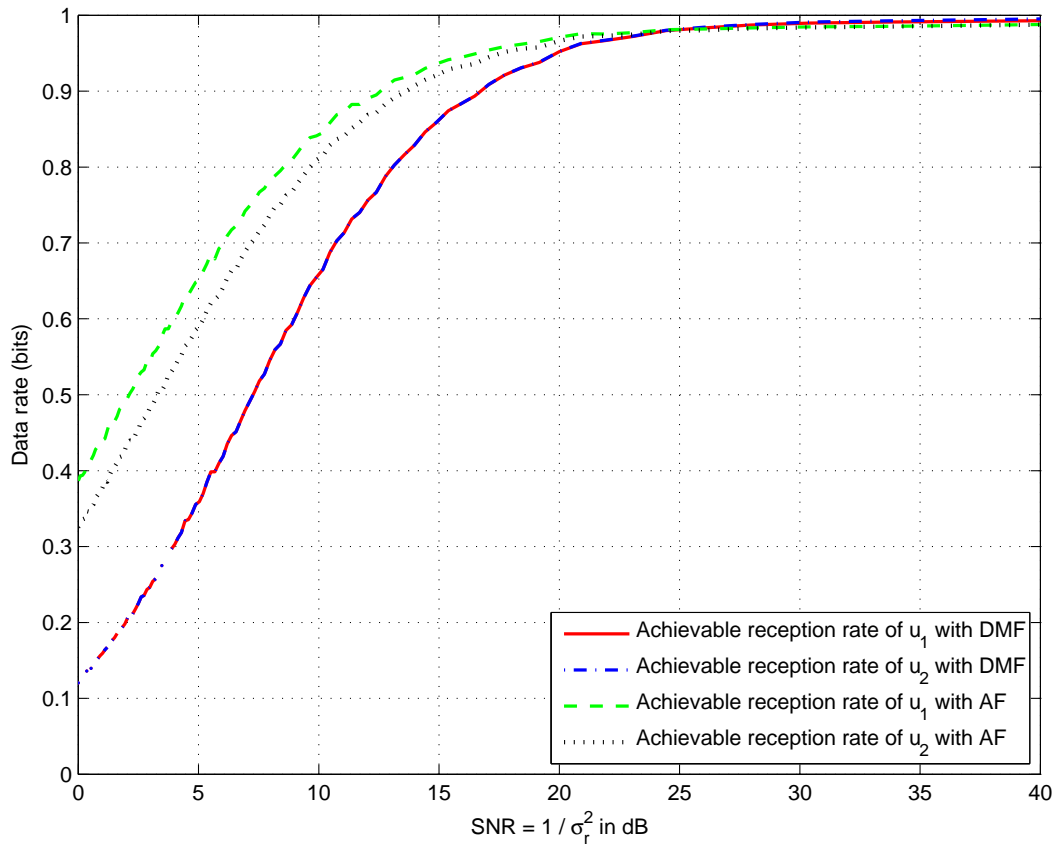
Figure 4.5: Users' achievable reception rates when $\sigma_1 = \sigma_2 = 0.1$ and $\gamma_1^2 = 0.75$ and $\gamma_2^2 = 1$.

41
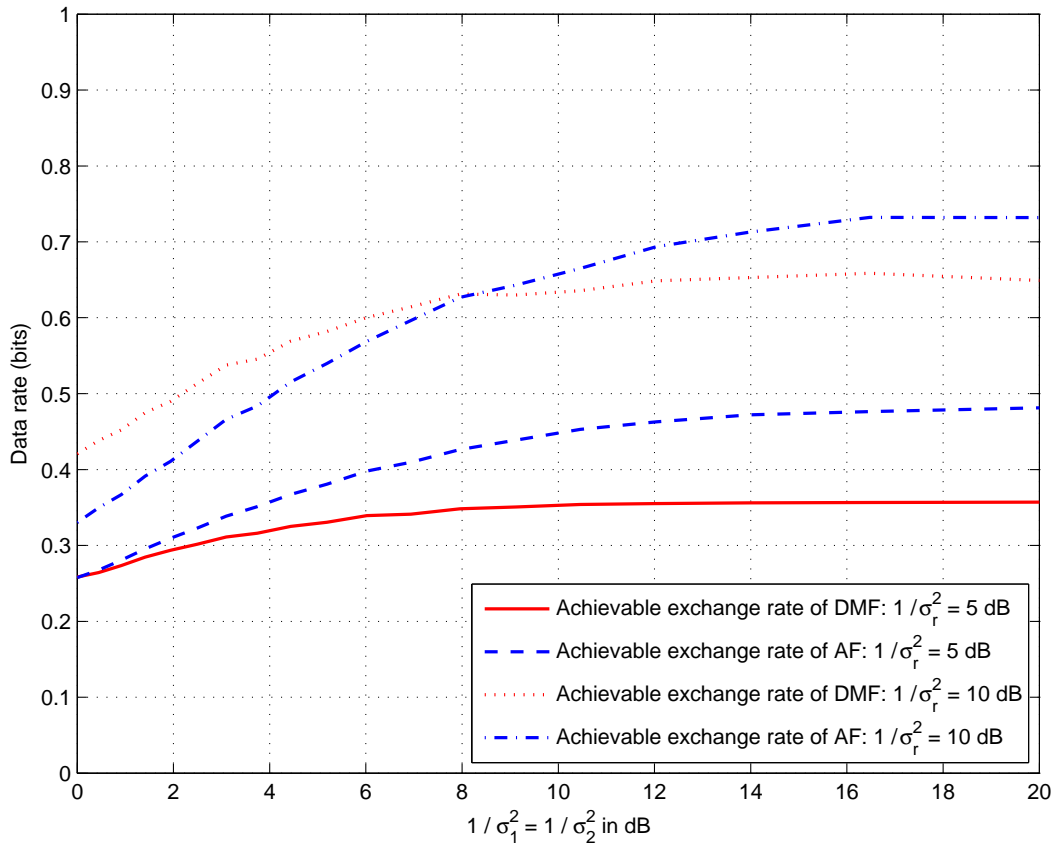
Figure 4.6: Effect of the users' SNR over the achievable exchange rates of AF and DMF.

Chapter 5

Achievable Rates of Symmetric MWRCs with AWGN

In this chapter, we compare OWR and MWR in terms of their achievable rates. First, we prove that for MWR, lattice-based relaying ensures a gap less than $\frac{1}{2(K-1)}$ bit from the capacity upper bound while MWR based on decode-and-forward (DF) or amplify-and-forward (AF) is unable to guarantees this rate gap. For DF and AF, we identify situations where they also have a rate gap less than $\frac{1}{2(K-1)}$ bit. Later, we show that although MWR has higher relaying complexity, surprisingly, it can be outperformed by OWR depending on K and the system SNR. Summarily speaking, for large K and small users' transmit power, OWR usually provides higher rates than MWR.

5.1   Introduction

The performance of MWRCs in terms of their achievable rate has been widely studied. In [22], it is shown that for an MWRC, CF can achieve to within $\frac{1}{2(N-1)}$ bit of the capacity where N is the number of users. Also, for TWRCs with FDF, it is shown that the capacity gap is less than $\frac{1}{2}$ bit [56] while FDF achieves the capacity for binary MWRCs [29]. Ong *et al.* show that under some conditions, FDF achieves the capacity of MWRCs with AWGN [34]. Furthermore, they briefly discuss the capacity gap of FDF when all users and the relay have equal power.

In this chapter, a detailed performance comparison between MWR and OWR is provided. More specifically, we focus on the achievable rate of symmetric MWRCs with AWGN under both relaying schemes. Note that the system model for our analysis in this chapter is similar to the model described in Chapter 2. For MWR, we prove that similar to CF, FDF assures a gap less than $\frac{1}{2(N-1)}$ bit from the capacity. For AF and DF, we first show

that they may have a larger than $\frac{1}{2(N-1)}$ bit capacity gap and then we find the SNR regions where a gap smaller than $\frac{1}{2(N-1)}$ bit is guaranteed. In the next step, we study the achievable rate of the system using OWR. For this purpose, we consider OWR with AF and DF and show that for the considered MWRC setup, DF always outperforms AF when OWR is used. Then, the achievable rate of MWR with CF and FDF (guaranteeing a less than $\frac{1}{2(N-1)}$-bit gap) is compared with the rate of DF OWR. Surprisingly, in spite of a higher relaying complexity, MWR is not always superior to OWR and we find the SNR regions where OWR indeed outperforms MWR. According to our study, by decreasing SNR or increasing N, we may see OWR surpassing MWR.

The chapter is organized as follows: The capacity gap analysis for MWR is discussed in Section 5.2 and Section 5.3 focuses on the rate study for OWR. Rate comparison between MWR and OWR is presented in Section 5.4 and Section 5.5 concludes this chapter.

5.2 Rate Analysis for MWR

In this section, we summarize our results on the capacity gap analysis for different relaying strategies. The capacity gap of the relaying schemes is the measure of their performance compared to maximum possible data rate of the system. Since the exact capacity of MWRCs is yet to be known, here, we use the capacity upper bound to derive the capacity gap of the relaying schemes. In the following, we consider FDF, DF, and AF for the capacity gap study. The capacity gap for the aforementioned schemes is studied for a MWRC where the links are AWGN channels. Note that the capacity gap of CF has been studied previously [22].

5.2.1 Capacity Gap of FDF

Using the achievable rates of FDF presented in Chapter 2, we can prove the following theorem on the capacity gap of FDF.

Theorem 5.1 *The gap between the achievable rate of FDF and the capacity of an N-user symmetric Gaussian MWRC is less than $\frac{1}{2(N-1)}$ bit.*

Proof: See Appendix.

For numerical illustrations, the achievable rate of FDF and the capacity upper bound for several cases are depicted in figures 5.1, 5.2 and 5.3. In Figure 5.1, users' SNR effect on the capacity gap is studied while the effect of the relay SNR and N are presented in Figure

5.2 and Figure 5.3 respectively. As seen, the achievable rate of FDF always sits above the $\frac{1}{2(N-1)}$-bit gap. Further, when downlink limits the rate, FDF achieves the capacity.
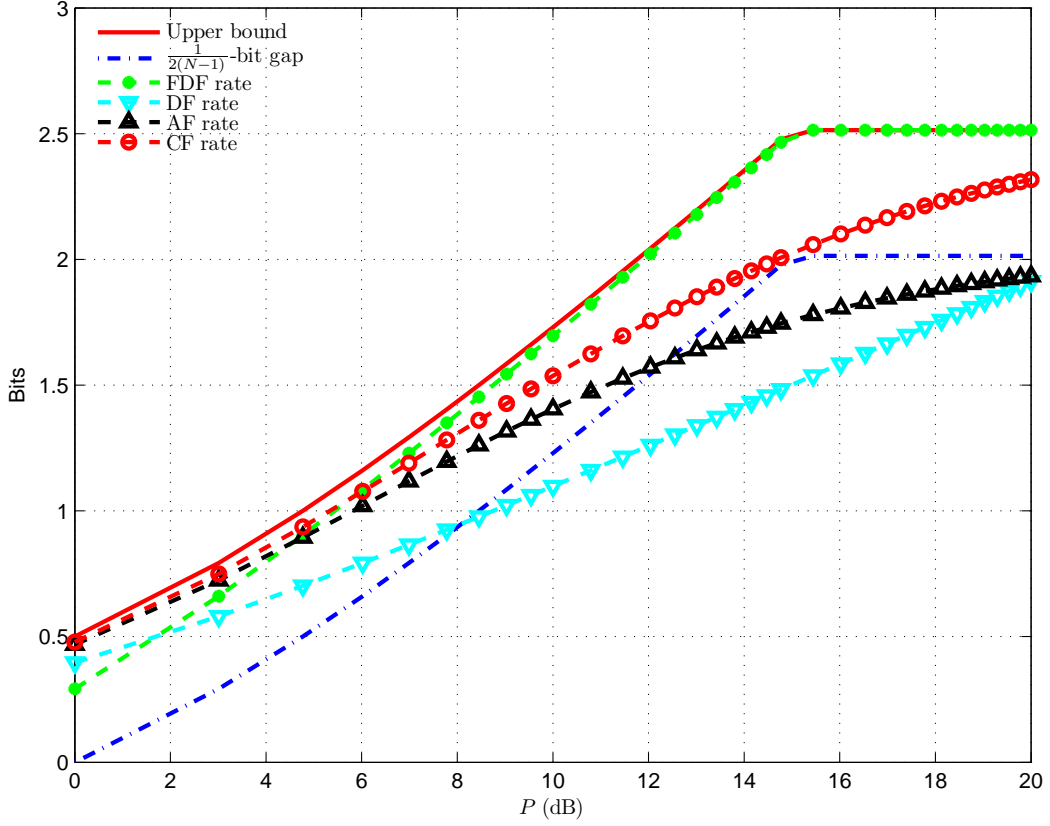
Figure 5.1: Achievable rates of relaying schemes when $N = 3$ and $P_r = 15$ dB.

5.2.2 Capacity Gap of DF

Our analysis reveals that depending on SNR and N, DF may not be able to guarantee a $\frac{1}{2(N-1)}$-bit gap to R^c_{UB}. The following theorem summarizes the result.

Theorem 5.2 *The gap between R^c_{DF} and R^c_{UB} is less than $\frac{1}{2(N-1)}$ bit if either $P_r < \min\{2(1+NP)^{\frac{N-1}{N}}-1, (N-1)P\}$ or $(N-1)P < P_r$ and $(N-1)P < 2(1+NP)^{\frac{N-1}{N}}-1$.*

Proof: Please see Appendix.

As the numerical results in figures 5.1, 5.2 and 5.3 indicate, in some SNR regions and depending on the number of users, the capacity gap might be larger than $\frac{1}{2(N-1)}$ bit for DF.

5.2.3 Capacity Gap of AF

For AF, we state the following theorem on the capacity gap.
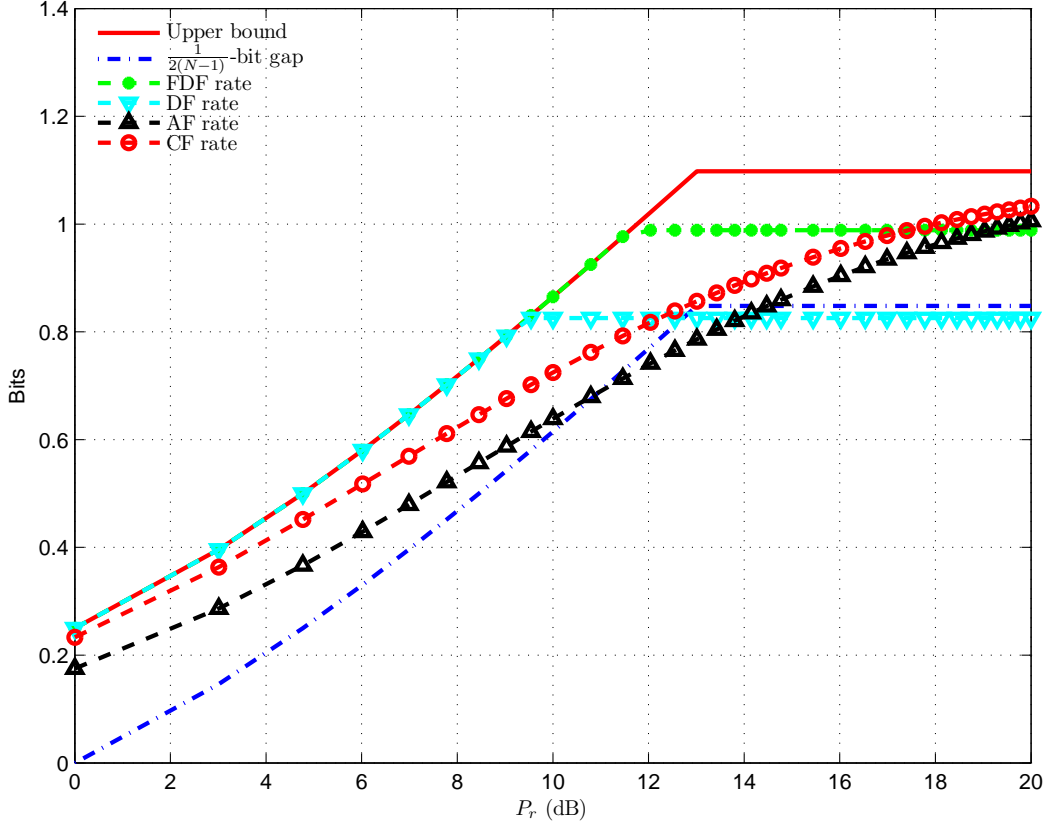
Figure 5.2: Achievable rates of relaying schemes when $N = 3$ and $P = 10$ dB.

Lemma 5.1 *In an N-user symmetric Gaussian MWRC,*

$$R_{AF}^c = \frac{1}{2(N-1)} \log\left(1 + \frac{(N-1)PP_r}{1 + NP + P_r}\right) \tag{5.1}$$

is the maximum common rate that AF can achieve.

Now, the following theorem is presented on the capacity gap of AF.

Theorem 5.3 *The gap between R_{AF}^c and R_{UB}^c is less than $\frac{1}{2(N-1)}$ if $P_r \leq (N-1)P$ and $P_r^2 - (N-2)PP_r < NP$ or $(N-1)P < P_r$ and $N(N-1)P^2 - P - 1 < P_r + (N-1)PP_r$.*

Proof: Please see Appendix.

Depending on the SNR and N, the achievable rate of AF may fall under the $\frac{1}{2(N-1)}$-bit gap from the capacity upper bound (figures 5.1, 5.2 and 5.3).

5.3 Rate Analysis for OWR

In this section, we study the achievable rate of OWR. In a MWRC with OWR, transmission time in both uplink and downlink phases is divided into N slots. In each slot, one user
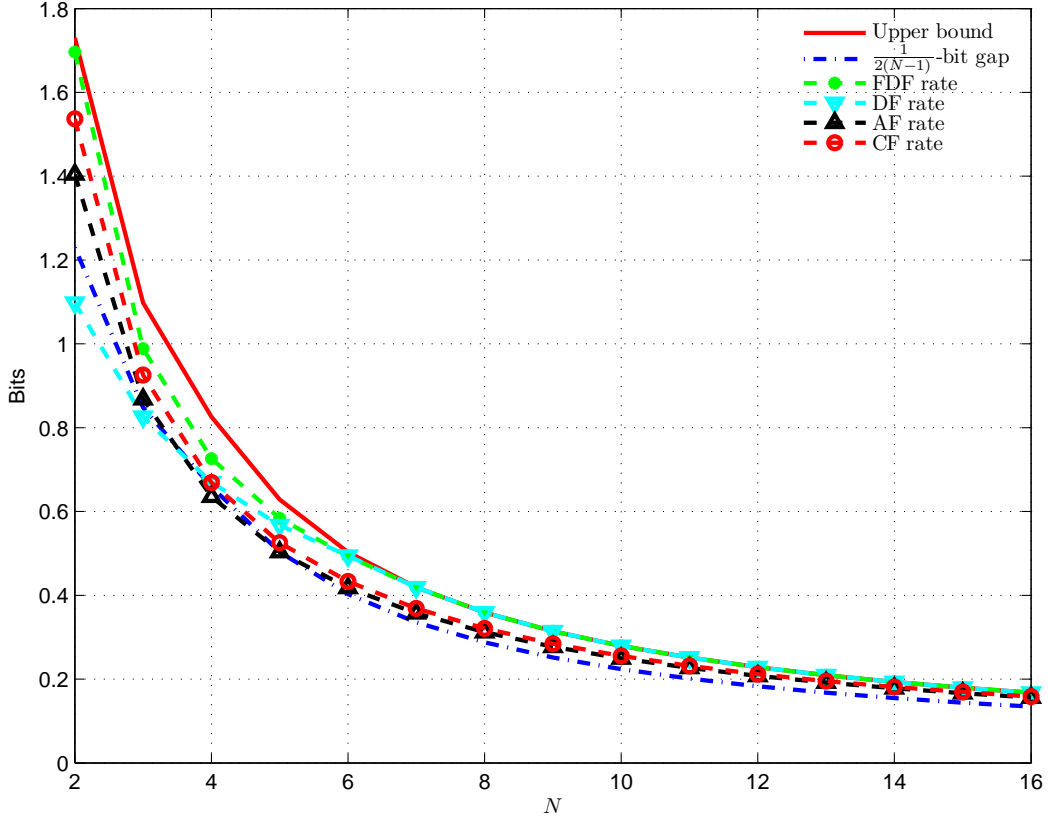
Figure 5.3: Achievable rates of relaying schemes when $P = 10$ dB and $P_r = 15$ dB.

serves as the source and the rest are the data destinations. First, the source user transmits in the uplink slot and then $\mathcal{R}$ broadcasts the data back to the users in the downlink slot. Since each user transmits in only one uplink slot and stays silent in the rest, it can upscale its power to NP during its transmission turn without violating the power constraint.

When DF is employed for OWR, $\mathcal{R}$ first decodes the received data from the source in the uplink and then broadcasts it to the users. Then, destination users decode the received signal from the relay. It is easy to show that the achievable rate of DF OWR is

$$R_{\mathrm{DF_O}} = \min\left\{\frac{\log\left(1 + NP\right)}{2N}, \frac{\log\left(1 + P_r\right)}{2N}\right\} \tag{5.2}$$

For AF, $\mathcal{R}$ amplifies and forwards the received signal in the uplink without further processing. The decoding is done at the destination users. The achievable rate of this scheme is

$$R_{\mathrm{AF_O}} = \frac{1}{2N}\log\left(1 + \frac{NPP_r}{1 + NP + P_r}\right) \tag{5.3}$$

It can be shown that OW (with DF or AF) does not guarantee a $\frac{1}{2(N-1)}$-bit gap.

Now, we like to compare the performance of AF and DF for OW. Using the achievable rates in (5.2) and (5.3), we can derive the following theorem.

Theorem 5.4 *In a symmetric Gaussian MWRC with OWR, DF always outperforms AF in terms of the achievable rate.*

Proof: See Appendix.

5.4   Comparison Between the Rate of OWR and MWR

In this section, we compare the performance of OWR and MWR. For OWR, we consider DF which has the superior performance over AF. Also, FDF and CF are considered for MWR since they provide a guaranteed rate performance (capacity gap).

5.4.1   Comparison of DF OWR and FDF MWR

First, assume $P_r < \frac{NP}{2}$. Thus,

$$R_{\mathrm{FDF}} = \frac{\log(1 + P_r)}{2(N-1)}, \quad R_{\mathrm{DF_O}} = \frac{\log(1 + P_r)}{2N}. \tag{5.4}$$

In this region, it is clear that MWR outperforms OWR due to its smaller pre-log factor. However, increasing N decreases the gap between MWR and OWR. Consider the second SNR region where $\frac{NP}{2} \leq P_r < NP$ and

$$R_{\mathrm{FDF}} = \frac{\log(1 + \frac{NP}{2})}{2(N-1)}, \quad R_{\mathrm{DF_O}} = \frac{\log(1 + P_r)}{2N}. \tag{5.5}$$

In this SNR region, FDF MWR surpasses DF OWR if

$$P_r < (1 + \frac{NP}{2})^{\frac{N}{N-1}} - 1 \tag{5.6}$$

Since the right hand side of (5.6) is an increasing function of P, it can be concluded that for a fixed P_r, decreasing P reduces the chance of holding the inequality (5.6). It means that when the relay's received SNR decreases, OWR may start performing better than MWR.

Now, we consider a third region where $NP \leq P_r$. Here,

$$R_{\mathrm{FDF}} = \frac{\log(1 + \frac{NP}{2})}{2(N-1)}, \quad R_{\mathrm{DF_O}} = \frac{\log(1 + NP)}{2N}. \tag{5.7}$$

Thus, MWR performs better if

$$(1 + NP)^{\frac{1}{N}} < (1 + \frac{NP}{2})^{\frac{1}{N-1}}. \tag{5.8}$$

48

From (5.8) and noticing that $(1+x)^{\frac{1}{x}}$ is a decreasing function and $\lim_{x \to 0}(1+x)^{\frac{1}{x}} = e^x$, it can be concluded that decreasing P or increasing N (without violating $KP \le P_r$) is in favor of OWR. Numerical results for the comparison between the achievable rate of DF OWR and FDF MWR are presented in Figure 5.4 and Figure 5.5. As seen, when $N = 2$, for small P (low receive SNR at the relay), OWR performs close to MWR and even outperforms FDF. Increasing SNR causes the gap between OWR and MWR to largen. By setting $N = 8$, we see that for a significant SNR region OWR surpasses FDF.
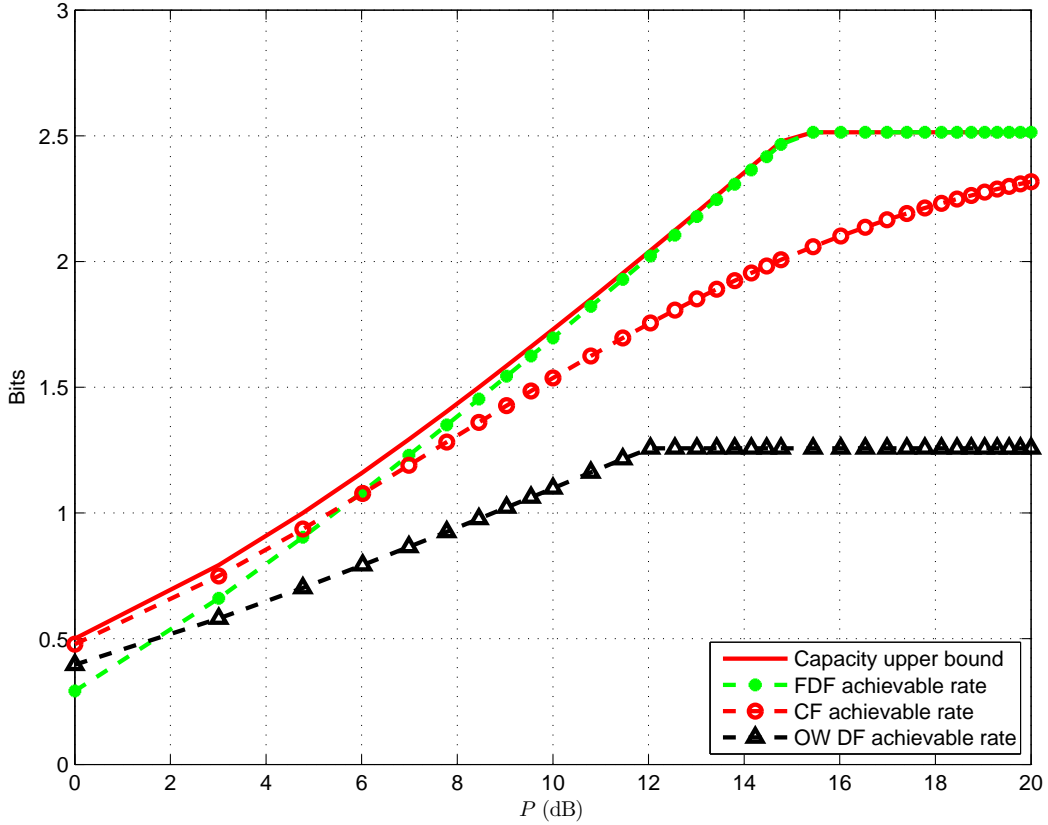
Figure 5.4: Comparison between the achievable rates of OWR and MWR when $P_r = 15$ dB and $N = 2$.

5.4.2   Comparison of DF OWR and CF MWR

To compare the performance of DF OWR and CF MWR, we use two SNR regions. First, assume $P_r < NP$. Thus,

$$R_{\mathrm{CF}} = \frac{1}{2(N-1)} \log\left(1 + \frac{(N-1)PP_r}{1 + (N-1)P + P_r}\right), \quad R_{\mathrm{DF_O}} = \frac{\log(1+P_r)}{2N}. \quad (5.9)$$
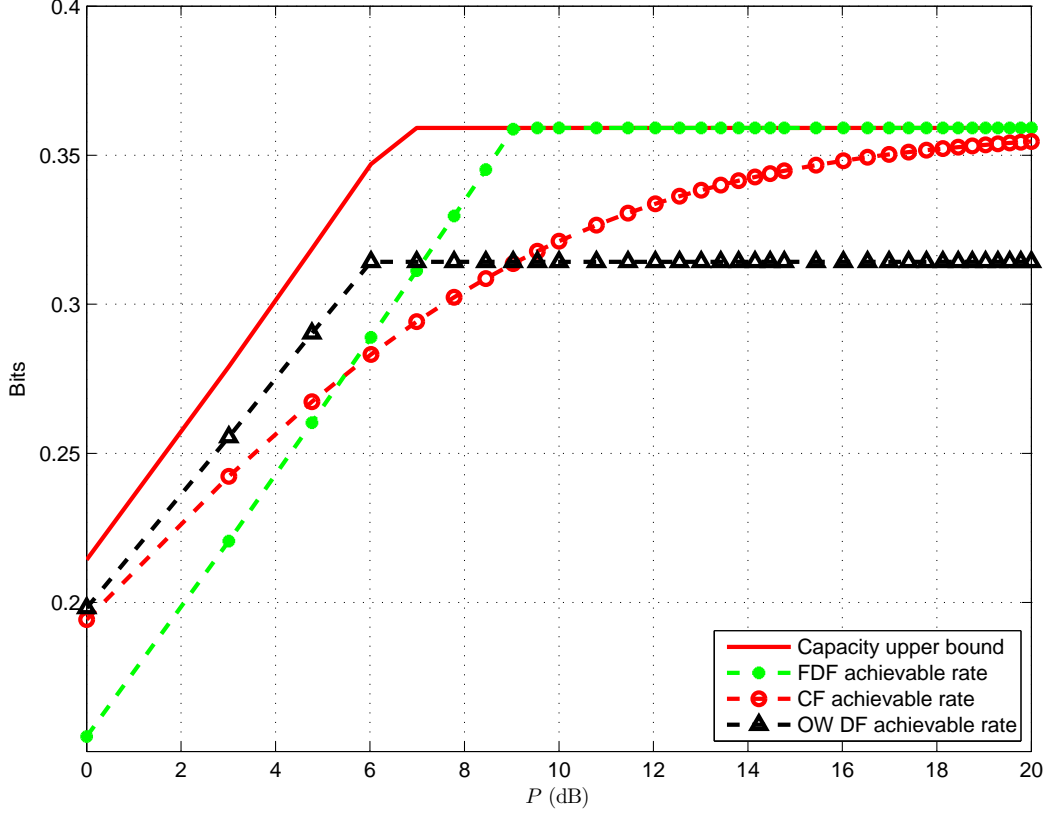
Figure 5.5: Comparison between the achievable rates of OWR and MWR when $P_r = 15$ dB and $N = 8$.

From (5.9), we can conclude that MWR outperforms OWR in this SNR region when

$$P_r < \left(1 + \frac{(N-1)PP_r}{1 + (N-1)P + P_r}\right)^{\frac{N}{N-1}} - 1. \tag{5.10}$$

In (5.10), if $P_r \geq 1$, using the derivative of the right hand side of (5.10), it can be shown that when P decreases, MWR may lose its advantage over OWR.

Now, we consider the second SNR region where $NP \leq P_r$. Thus

$$R_{\text{CF}} = \frac{1}{2(N-1)} \log\left(1 + \frac{(N-1)PP_r}{1 + (N-1)P + P_r}\right), \quad R_{\text{DF}_{\text{O}}} = \frac{\log(1 + NP)}{2N}. \tag{5.11}$$

MWR with CF performs better than DF OWR if

$$\frac{(1 + (N-1)P)((1 + NP)^{\frac{N-1}{N}} - 1)}{(N-1)P + 1 - (1 + NP)^{\frac{N-1}{N}}} < P_r. \tag{5.12}$$

It can be concluded that for low SNRs, (5.12) does not hold and OWR outperforms MWR. Further, the left side of (5.12) is an increasing function of N. Thus, by increasing N, we may start seeing higher rates from OWR than MWR. Figures 5.4 and 5.5 depict the

comparison between the achievable rate of DF OWR and CF MWR. As seen, when the number of users increase from $N = 2$ to $N = 8$, the superiority of OWR over MWR extends to a wider range of SNRs.

5.5   Conclusion

In this chapter, we compared the performance of OWR and MWR in a symmetric Gaussian MWRC where several users share their data through a relay. To this end, we first proved that FDF always have a capacity gap less than $\frac{1}{2(N-1)}$ bit while depending on the users' and relay SNR, AF and DF may have a capacity gap larger than $\frac{1}{2(N-1)}$. Furthermore, for OWR, we showed that DF is always superior to AF. By comparing the achievable rate of DF OWR with CF and FDF MWR, we concluded that MWR is likely to outperform OWR in high SNR regions or for small N. Conducting a similar study for fading AWGN channels is considered as a direction for future research.

Chapter 6

Optimal User Pairing to Maximize the Achievable Rate in Asymmetric MWRCs with AWGN

We study an asymmetric multi-way relay channel where users have different channel conditions. For both FDF and pairwise DF, we first show that due to unequal channel conditions, the achievable common rate of the pairwise strategy depends on the order in which the users are paired. This motivates us to find the pairing strategy maximizing the achievable rate. This rate is then compared with the capacity upper bound and the achievable rate of a random user pairing.

6.1 Introduction

An efficient approach to enable data communication in an MWRC is pairwise users' transmission which is adopted in FDF. In [25], the authors argue that when there is no direct user-to-user link, pairwise network coding is the optimal strategy for the considered network setup. Furthermore, it is shown in [57] that for a class of multi-way relay channels, which can be converted to deterministic broadcast channels, pairwise network coding is the optimal approach. Pairwise transmission also has a reasonable decoding complexity since the relay needs to simultaneously decode only two users at a time. Further, due to its simple transmission scheduling, pairwise transmission can handle a situation where the number of users dynamically changes or significantly increases.

Here, we study the performance of pairwise relaying for MWRCs over asymmetric channels with AWGN. We consider two different scenarios for pairwise relaying: FDF [29, 34] and pairwise decode-and-forward (PDF). In both schemes, at each uplink transmission, only two users communicate with the relay. The difference between these two

approaches lay in the way that the relay treat the users' transmitted messages. While in FDF the relay directly decodes the sum of the users' messages, in PDF, it decodes the users' data separately and then forms the sum of them. Note that our considered pairwise DF is different from full DF where all users simultaneously transmit their data to the relay.

For these two schemes, we first show that the achievable rate of the system depends on how users are paired for transmission. Furthermore, to find the ultimate performance of pairwise relaying, we find the optimal user pairings for FDF and PDF maximizing the achievable common rate. We also derive an upper bound on the common rate of the considered asymmetric MWRC and compare the performance of FDF and PDF (with their optimal pairings) with this bound. Furthermore, the achievable rates of FDF and PDF with their optimal pairings are compared with the rates of FDF and PDF when random pairings are used to investigate the performance improvement made by our proposed pairings. Our study shows that the optimal pairing improvement is more significant in low SNR region for FDF while it is more pronounced in high SNRs when PDF is applied.

The organization of this chapter is as follows: The preliminaries and system model are presented in Section 6.1. Common rate analysis for FDF and PDF and their proposed optimal pairings are brought in Section 6.3 and Section 6.4 respectively. Numerical examples are presented in Section 6.5. Finally, Section 6.6 concludes this chapter.

6.2 Preliminaries

Here, it is assumed that $N \geq 2$ users, called $u_1, u_2, \ldots, u_N$, want to communicate through a relay, $\mathcal{R}$, such that each user sends and receives data from all other users. We refer to the users' data by $x_1, x_2, \ldots, x_N$ and to the relays transmitted data by x_r. Each user has a limited average transmit power P while relay's average transmit power is P_r. Further, users' channel gains to the relay are $h_1, h_2, \ldots, h_N$ respectively. Without loss of generality, it is assumed that $|h_1| \leq |h_2| \leq \ldots \leq |h_N|$. The received signals at the users and the relay are contaminated by Gaussian noise with variance σ^2.

For an MWRC with FDF or PDF, the uplink and downlink phases are divided into $N-1$ MAC and broadcast (BC) slots (phases) [29, 34]. In a MAC slot, a pair of users transmits their data to the relay. With FDF, relay directly decodes the sum of the users' data using nested lattice coding [42] while relay decodes the message of each user separately [35] (similar to conventional full DF relaying) when PDF is used and then forms the sum of the messages. In the BC phase, $\mathcal{R}$ broadcasts the sum message to all users. One round of users'

communication is accomplished after $N-1$ MAC and BC phases. Now, since each user has received $N-1$ independent linear combinations of the other users' data, it can decode the data of all of them. Please notice that in FDF and PDF schemes, users do not transmit in all MAC slots. Thus, to have an average user power of P, u_i's can upscale their power to $\frac{NP}{2}$ in their transmitting slot without exceeding the average power P [34].

We denote the transmission sequence by $u_{o1}, u_{o2}, \ldots, u_{oN}$, meaning that the consecutive users in the sequence are paired for transmission (i.e $\{u_{o1}, u_{o2}\}$, $\{u_{o2}, u_{o3}\}$, ...). Here, the channel gains for $u_{o1}, u_{o2}, \ldots, u_{oN}$ are denoted by $h_{o1}, h_{o2}, \ldots, h_{oN}$. Notice that u_{oi} is not necessarily the same as u_i. Figure 6.1(a) demonstrates the MAC phase for pair $(u_{oi}, u_{o(i+1)})$ and the BC phase is shown in Figure 6.1(b).

(a) ith MAC phase

(b) ith BC phase
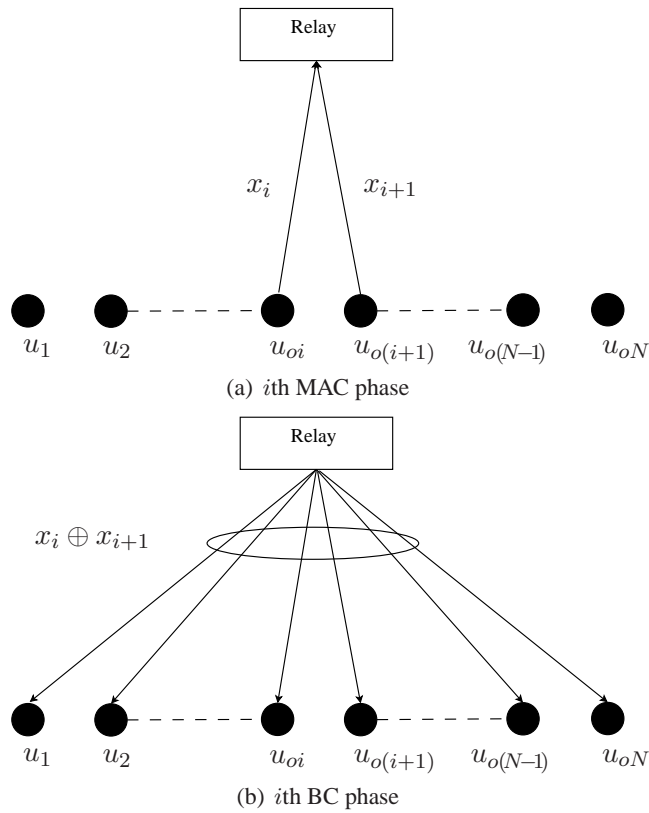
Figure 6.1: Demonstration of the ith MAC and BC phases

In this chapter, we are interested in the common rate capacity of pairwise MWRCs. The common rate capacity is the data rate that all users can reliably transmit and receive data. According to this definition, if we denote the maximum achievable data rate during the ith MAC phase by R_i^{M} and the maximum achievable rate in the ith BC phase by R_i^{B}, then, the rate during the ith MAC and BC phases is $R_i^c = \min\{R_i^{\mathrm{M}}, R_i^{\mathrm{B}}\}$. Now, one round of data communications happens over $N-1$ MAC and BC phases and the users' common-rate

capacity of pairwise relaying, R^c, is defined as $R^c = \frac{1}{N-1} \min_i \{R_i^c\}$.

For the described MWRC, we derive the following bound on the common data rate. This bound is later used to evaluate the performance of the proposed optimal pairings.

Theorem 6.1 *Defining $\mathcal{C}(x) = \frac{1}{2}\log(1+x)$, the common rate of the aforementioned fading MWRC with AWGN is bounded by*

$$R_{\mathrm{UB}}^c = \frac{1}{N-1} \min \left\{ \mathcal{C}(\frac{P\sum_{i=1}^{N-1}|h_i|^2}{\sigma^2}), \mathcal{C}(\frac{P_r|h_1|^2}{\sigma^2}) \right\}. \tag{6.1}$$

Proof: See Appendix. ∎

Corollary 6.1 *Since $\mathcal{C}(\frac{(N-1)P|h_1|^2}{\sigma^2}) < \mathcal{C}(\frac{P\sum_{i=1}^{N-1}|h_i|^2}{\sigma^2})$, when $P_r \leq (N-1)P$, we have $R_{\mathrm{UB}}^c = \frac{1}{N-1}\mathcal{C}(\frac{P_r|h_1|^2}{\sigma^2})$. In this case, the bound is forced by downlink.*

6.3 Common Rate Analysis for an MWRC with FDF

In this section, we first study the achievable rate of FDF and then discuss how the order of users' transmissions affects the achievable rate. As the main result of this section, an optimal user pairing to maximize the common rate is found.

6.3.1 Common Rate of FDF

In the ith MAC phase, u_{oi} and $u_{o(i+1)}$ transmit. According to [58], R_i^{M} satisfies the following conditions

$$R_i^{\mathrm{M}} \leq \frac{1}{2}\log^+\left(\frac{|h_{oi}|^2}{|h_{oi}|^2+|h_{o(i+1)}|^2} + \frac{NP|h_{oi}|^2}{2\sigma^2}\right), \tag{6.2}$$

$$R_i^{\mathrm{M}} \leq \frac{1}{2}\log^+\left(\frac{|h_{o(i+1)}|^2}{|h_{oi}|^2+|h_{o(i+1)}|^2} + \frac{NP|h_{o(i+1)}|^2}{2\sigma^2}\right) \tag{6.3}$$

where $\log^+(x) = \max\{\log(x), 0\}$.

Transmission in the ith BC phase is a broadcast channel with no private message for users. Thus, $\mathcal{R}$ transmits with the rate of the user with the worst channel condition. Hence

$$R_i^{\mathrm{B}} \leq \min_{j=1,2,\ldots,N} \mathcal{C}(\frac{P_r|h_j|^2}{\sigma^2}) = \mathcal{C}(\frac{P_r|h_1|^2}{\sigma^2}). \tag{6.4}$$

Now, common rate of FDF, R_{FDF}^c, is derived using the rate definition in Section 4.2.

Theorem 6.2 *If $0 < P_r \leq \frac{NP}{2} - \frac{\sigma^2}{|h_1|^2}$, FDF achieves the capacity upper bound.*

Proof: From Corollary 6.1, $R^{UB} = \frac{1}{N-1}\mathcal{C}(\frac{P_r|h_1|^2}{\sigma^2})$ is the rate upper bound. Also, for all i, we have

$$\log\left(\frac{NP|h_1|^2}{2\sigma^2}\right) < \log\left(\frac{|h_{oi}|^2}{|h_{oi}|^2 + |h_{o(i+1)}|^2} + \frac{NP|h_{oi}|^2}{2\sigma^2}\right) \tag{6.5}$$

Now, if $0 < P_r \leq \frac{NP}{2} - \frac{\sigma^2}{|h_1|^2}$, then

$$\log\left(1 + \frac{P_r|h_1|^2}{\sigma^2}\right) \leq \log\left(\frac{NP|h_1|^2}{2\sigma^2}\right) \tag{6.6}$$

and $R_{\text{FDF}}^c = \frac{1}{N-1}\mathcal{C}(\frac{P_r|h_1|^2}{\sigma^2})$. Thus, $R_{\text{FDF}}^c = R^{UB}$. ■

Remark 6.1 *When $\sigma \to 0$ and $P_r < NP/2$, pairwise FDF achieves the upper bound.*

6.3.2 Optimal User Ordering

The order of users pairing affects the bound on R_i^{M}'s in (6.2) when $N > 2$. This in turn can influence the achievable common rate, R_{FDF}^c. As a consequence, by carefully choosing the users' pairing, one can maximize the achievable rate.

Theorem 6.3 *The optimal user transmission sequence for FDF, called S_1, is*

$$(u_{o1}, \ldots, u_{oN}) = (u_1, u_2, \ldots, u_N). \tag{6.7}$$

Proof: See Appendix. ■

Remark 6.2 *For FDF, the effect of the optimal pairing is more significant when $1/\sigma^2$ is small. In this situation, $P|h_{oi}|^2/\sigma^2$ and $P|h_{o(i+1)}|^2/\sigma^2$ are small. Thus, the terms within the logarithm in (6.2) heavily depends on $|h_{oi}|^2/(|h_{oi}|^2 + |h_{o(i+1)}|^2)$ and $|h_{o(i+1)}|^2/(|h_{oi}|^2 + |h_{o(i+1)}|^2)$ and consequently user pairing.*

6.4 Rate Analysis for an MWRC with PDF

Here, we find the optimal user pairing maximizing the rate of DF. For this purpose, we first find the achievable rate of DF over an asymmetric MWRC with AWGN.

6.4.1 Common rate of PDF

When PDF is used, the transmission in the ith MAC phase is a conventional multiple access transmission. Thus [35],

$$R_i^{\mathrm{M}} \leq \mathcal{C}\left(\frac{NP|h_{oi}|^2}{2\sigma^2}\right), \tag{6.8}$$

$$R_i^{\mathrm{M}} \leq \mathcal{C}\left(\frac{NP|h_{o(i+1)}|^2}{2\sigma^2}\right), \tag{6.9}$$

$$R_i^{\mathrm{M}} \leq \frac{1}{2}\mathcal{C}\left(\frac{NP(|h_{oi}|^2 + |h_{o(i+1)}|^2)}{2\sigma^2}\right). \tag{6.10}$$

The BC rate constraint is $R_i^{\mathrm{B}} \leq \mathcal{C}\left(\frac{P_r|h_1|^2}{\sigma^2}\right)$, similar to FDF. Now, the achievable rate region of FDF is derived using the common rate definition in Section 4.2.

Theorem 6.4 *If* $P_r \leq \left(\sqrt{1 + \frac{PN|h_1|^2}{\sigma^2}} - 1\right) \frac{\sigma^2}{|h_1|^2}$, *then PDF achieves the upper bound.*

Proof: Note that from (6.10)

$$\forall i : \mathcal{C}\left(\frac{NP|h_1|^2}{\sigma^2}\right) \leq \mathcal{C}\left(\frac{NP(|h_{oi}|^2 + |h_{o(i+1)}|^2)}{2\sigma^2}\right). \tag{6.11}$$

Also,

$$\forall i : \frac{1}{2}\mathcal{C}\left(\frac{NP|h_1|^2}{\sigma^2}\right) \leq \mathcal{C}\left(\frac{NP|h_{oi}|^2}{2\sigma^2}\right) \tag{6.12}$$

Meaning that $\frac{1}{2(N-1)}\mathcal{C}\left(\frac{NP|h_1|^2}{\sigma^2}\right)$ is a lower bound for the rate in the MAC phase. Now, if the condition in the theorem holds, we have $\mathcal{C}\left(\frac{P_r|h_1|^2}{\sigma^2}\right) \leq \frac{1}{2}\mathcal{C}\left(\frac{NP|h_1|^2}{\sigma^2}\right)$. As a consequence $R_{\mathrm{DF}}^c = \frac{1}{N-1}\mathcal{C}\left(\frac{P_r|h_1|^2}{\sigma^2}\right)$ and Corollary 6.1 completes the proof. ∎

Remark 6.3 *The above theorem shows the optimal region for PDF in terms of the achievable rate. Unlike FDF, for a fixed P_r, when σ increases (lower SNRs), the condition in Theorem 6.4 is more likely to hold, decreasing the gap between PDF and the upper bound.*

6.4.2 Optimal User Ordering

The achievable rate of PDF in (6.10) is affected by the order of users' pairing. Thus, by choosing a proper user pairing, the achievable common rate enhances.

Theorem 6.5 *The optimal transmission sequence for maximizing the common rate of PDF, called S_2, is*

$$(u_{o1}, \ldots, u_{oN}) = (u_1, u_N, u_2, u_{N-1}, \ldots, u_{\lfloor \frac{N}{2} \rfloor + 1}). \tag{6.13}$$

Proof: See Appendix. ∎

Remark 6.4 *For small σ, the term inside the logarithm in (6.10) can be well approximated by $P(|h_{oi}|^2 + |h_{o(i+1)}|^2)/\sigma^2$. As a consequence, the improvement of the achievable rate made by the optimal pairing is more significant.*

6.5   Simulation Results

To evaluate the performance of the proposed optimal orderings, we now present some examples. In our simulations, it is assumed that the channels between the users and relay are Rayleigh fading with average power gain equal to 1. More specifically, in each round of communication, users' channel gains are assigned based on N realization of a Rayleigh random variable. Notice that the fading is slow and users' channel gains stay unchanged during one complete round of data exchange between the users ($N - 1$ MAC and BC phases). We use Monte Carlo simulation to average the achievable rate over the channel gains.

Figure 6.2 presents the plots for the normalized gap between the achievable rate of the optimal pairing and a random paring when $P = P_r = 1$. Denoting the achievable rate of optimal pairing and random paring by R_o^c and R_r^c respectively, the normalized gap, G, is defined as $G = (R_o^c - R_r^c)/R_o^c$. The normalized gap is a measure of improvement by optimal pairing over a random pairing. As mentioned in Remark 6.2, for lower SNRs, the improvement over by the optimal pairing is more significant for FDF. As we expect from Remark 6.4, in high SNR region, optimal pairing results in a more visible improvement over random pairing when PDF is used.

Figure 6.3 depicts the comparison between the achievable rate of pairwise relaying, achievable rate of full DF and the rate upper bound. As expected from Remark 6.1 and 6.3, FDF has a better performance over high SNR region and provides rates close to the upper bound, while PDF is more efficient in low SNRs. By increasing the number of users while keeping the SNR fixed, downlink will more likely limit the rate (Corollary 6.1). As a consequence, the gap between FDF and the upper bound decreases. As seen, with a higher complexity cost, full DF provides higher data rates.

In Figure 6.4, we consider the situation where $P_r = N$. In other words, relay linearly increases its power based on the number of users. As seen in this figure, by increasing $1/\sigma^2$, the gap between pairwise relaying and upper bound increases. In this case, the condition in Corollary 6.1 does not hold and uplink is the bottleneck. Notice that the uplink achievable rate is always less than its associated upper bound.

The achievable common rate based on the number of users is depicted in Figure 6.5.
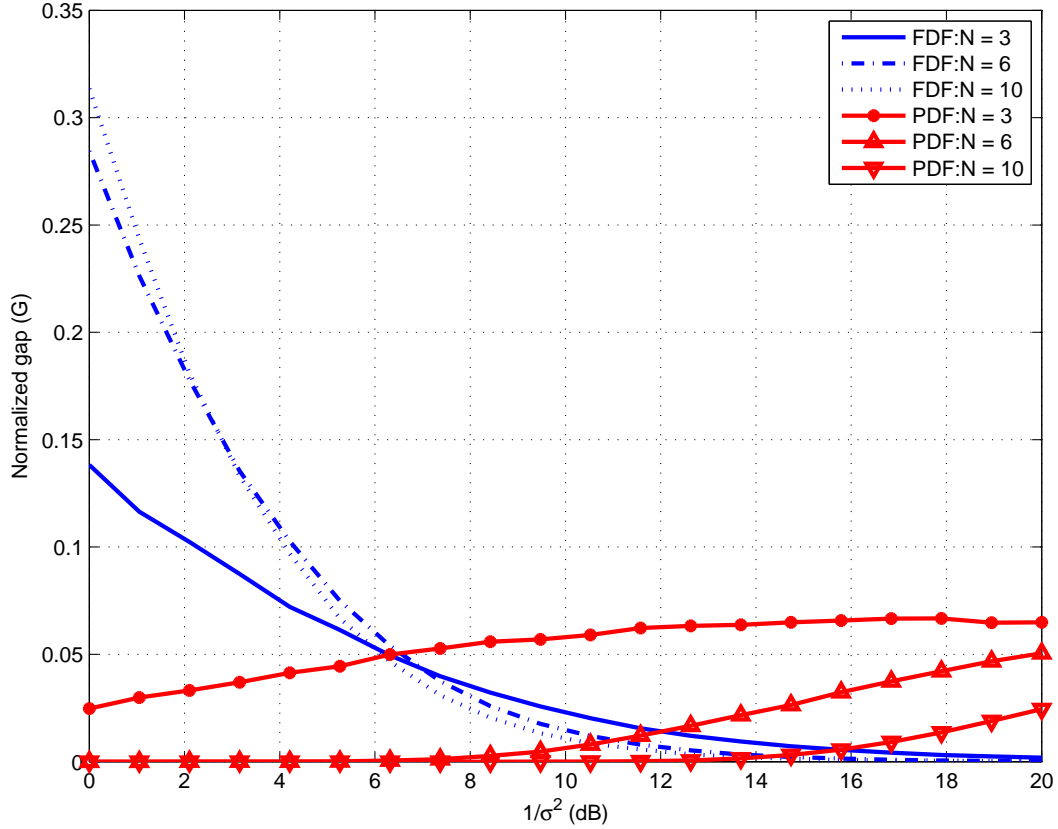
Figure 6.2: Normalized gap for optimal and random pairing when $P_r = P = 1$.

Since we are in the low SNR regions, $1/\sigma^2 = 5$ dB, as we expect, PDF outperforms FDF. Similarly, for larger SNRs, say $1/\sigma^2 = 20$ dB, simulation results show the superiority of FDF over PDF. These results are omitted here in the favor of space.

6.6   Conclusion

Here, we proposed optimal user pairings to maximize the common rate of FDF and PDF over asymmetric fading MWRCs with AWGN. Their achievable rate with optimal pairing were then compared with the rate upper bound as well as the achievable rate of random pairing. The performance improvement by optimal pairing is more significant in low (high) SNRs for FDF (PDF). Also, we concluded that PDF (FDF) is a better pairwise strategy in low (high) SNRs. Finding optimal user pairing in order to maximize the sum-rate in an asymmetric MWRC with AWGN is possible for future work.
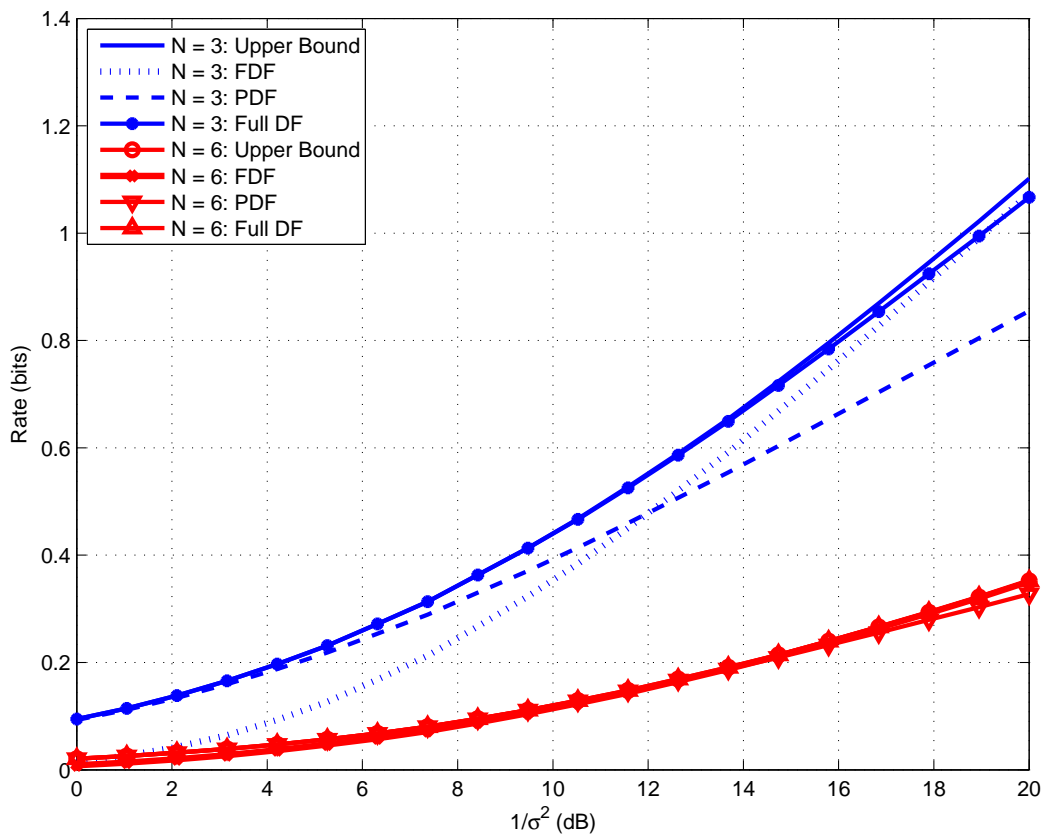
Figure 6.3: Achievable rates when $P_r = P = 1$.
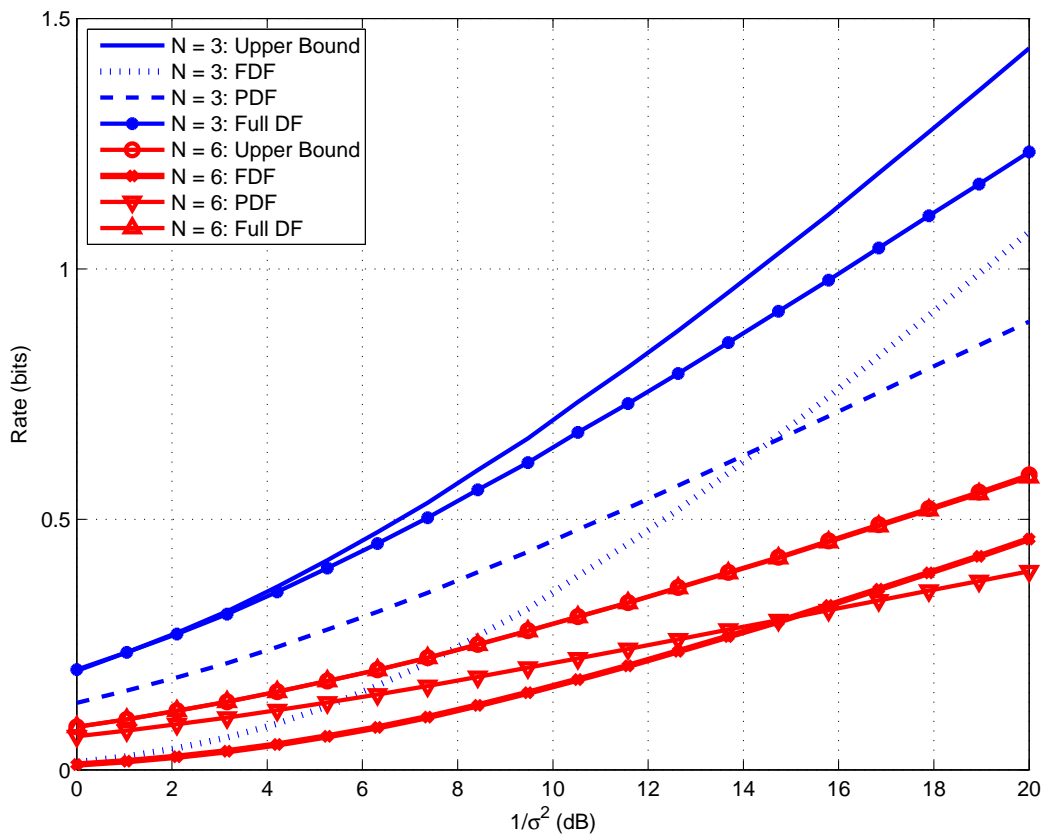
Figure 6.4: Achievable rates when $P_r = N$ and $P = 1$.
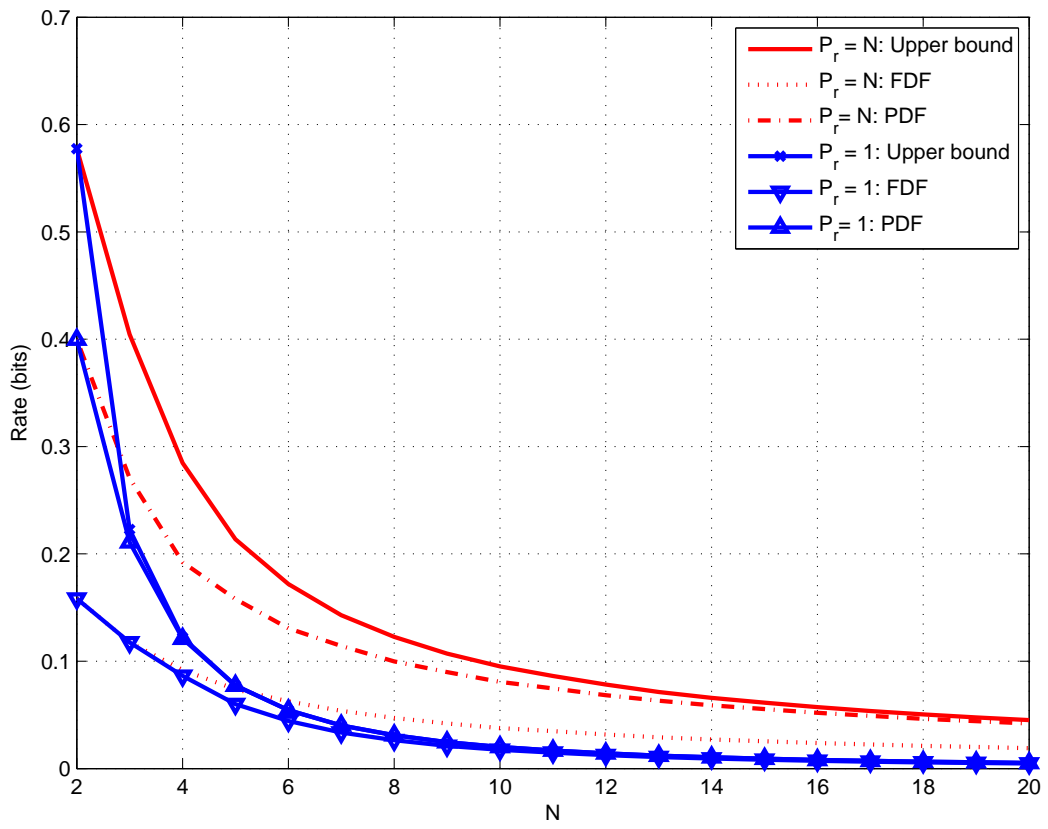
Figure 6.5: Achievable rates when $1/\sigma^2 = 5$ dB.

Chapter 7

Low-Latency Relaying Schemes for Erasure MWRCs

In this chapter, we consider an erasure MWRC (EMWRC). Assuming no feedback channel between the users and the relay, we first identify the challenges for designing a data sharing scheme over an EMWRC. Then, to overcome these challenges, we propose practical low-latency and low-complexity data sharing schemes based on fountain coding. Later, we introduce the notion of end-to-end erasure rate (EEER) and analytically derive it for the proposed schemes. EEER is then used to calculate the achievable rate and transmission overhead of the proposed schemes. We further find an upper bound on the achievable rates of EMWRC and observe that depending on the number of users and channel erasure rates, our proposed solutions can perform very close to this bound.

7.1 Introduction

MWRCs have been initially proposed and studied for Gaussian [22,34] and binary symmetric [29] channels when the channel state information is known at the relay as well as users. Hence, they can use this information to apply appropriate channel coding. However, the channel state information may not be always known, e.g. when the links between the users and relay are time-varying. Under this situation, channel coding fails to provide error-free communication. From the viewpoint of higher network layers, this is seen as an erasure channel where the data (packet) is received either perfectly or completely erased. Another possible situation where the erasure channel fits is a fading environment when one or more users experience a deep fade resulting in the signal loss at the relay. Thus, recently erasure models for multi-user relay communication has been considered [59–61]. In this work, we focus on erasure MWRCs (EMWRCs) and seek effective data sharing schemes for them.

Packet retransmission protocols are a simple solution to combat erasure. However, these protocols are wasteful in EMWRCs especially in the broadcast phase. To be more specific, if any user misses a broadcast message, a retransmission protocol forces the relay to broadcast its message to all users again. Further, implementing packet retransmission schemes or fixed-rate codes to combat erasure requires having feedback channels between the users and the relay [62]. Having such feedback channels is not always feasible. Fountain coding (e.g LT codes [63] or Raptor codes [64]) is another well-known solution which is shown to be near-optimal for erasure channels without the need for feedback [62]. Considering the benefits of fountain coding in broadcast scenarios, in this work, we assume that data sharing is done with the help of fountain codes. As we discuss later, implementing fountain coding for EMWRCs has many challenges. These challenges are identified and considered in the design of our strategies.

The notion of fountain coding for wireless relay networks has been originally proposed in [65] where one source sends its data through one or more relays to a destination. It is shown that the presented fountain coding scheme is simultaneously efficient in rate and robust against erasure. In [66], a distributed fountain coding approach is suggested where two (four) users communicate to a destination via a relay over erasure channels. Also, fountain coding can be exploited to relay data across multiple nodes in a network [67].

In addition, [68–70] consider fountain coding scenarios for different setups of relay networks over fading channels. Molisch *et al.* consider a cooperative setup in [68] where one source sends its data to a destination through multiple relays and argue that using fountain coding reduces the energy consumption for data transmission from the source to the destination. Also, in a fading environment, [69] and [70] apply fountain coding to improve the performance in a four-node (two sources, one relay, and one destination) and a three-node (one source, one relay, and one destination) setup respectively.

Applying fountain coding to EMWRCs, however, has its own challenges. First, it is undesirable to perform fountain decoding and re-encoding at the relay as it requires waiting for all data packets of all users. To avoid this latency, we are interested in data sharing solutions that can work with fountain coding/decoding only at the users. Second, if users' fountain codes are not synchronized, each user needs to track the combinations of packets formed at all other users. This means either extra transmission overhead or extra hardware complexity. Third, since data of all users are mixed during the transmission, fountain decoding will almost surely fail at some users as the received degree distribution will differ from that of the transmitted one. In particular, the weight of degree-one equations will be

very small (due to mixing at the relay), causing the decoder to stop at early stages. Thus, the users' data sharing strategies must be designed to combat this problem. Finally, we like to have data sharing strategies that are readily scalable with the number of users.

It is important to notice that the existence of the side information in each user (i.e. each user knows its own data) makes EMWRCs different from on-way relay networks in which a set of users, called sources, send their data to another set, called destinations. An efficient data-sharing strategy for EMWRCs should make use of this side information effectively.

The focus of this chapter is on devising efficient data transmission strategies based on fountain codes for EMWRCs. Considering the design challenges pointed above, we devise two data-sharing scheme that (i) need fountain coding/decoding only at the users' side (thus they have low latency) (ii) can decode each user's data separately (thus fountain decoding will not fail) and (iii) are easily scalable with the number of users. We also show that the system's performance can be further improved by performing simple matrix operations at the relay as well as shuffling the users' transmission order.

To evaluate the performance of the proposed schemes, we introduce the concept of *end-to-end erasure rate* (EEER). Using EEER, we compare the achievable rate of our schemes with the existing conventional one-way relaying (OWR). Furthermore, we derive an upper bound on the achievable data rate of the considered EMWRC. The achievable rate of our schemes are then compared with this bound to determine their performance gap. This comparison reveals that depending on the uplink and downlink erasure probabilities and number of users, our proposed data sharing strategies can get very close to the rate upper bound and outperform OWR. The proposed schemes are also compared with OWR in terms of their transmission overhead. The implication of this comparison is that for small erasure probabilities or small number of users, the proposed schemes accomplish data sharing between users with a smaller overhead.

7.2 System Model

In this chapter, we study an EMWRC with N users, namely $u_1, u_2, \ldots, u_N$. The users want to fully exchange their information packets with the help of a (low-complexity) relay. Each user has K information packets and we assume that the information packets are seen as data bits. It means that for the kth packet at u_i, denoted by $m_{i,k}$, we have $m_{i,k} \in \{0, 1\}$. Also, at a given transmission turn, the transmit message of u_i, derived from its information messages $m_{i,1}, \ldots, m_{i,K}$, is denoted by $x_i \in \{0, 1\}$. Although the channel inputs are

binary, the channel outputs are from a ternary alphabet $\{0, 1, E\}$. Here, E denotes the erasure output.

To share their data, users first send their transmit messages in the uplink phase. In each uplink phase, some (or all) users send their data to the relay. The transmitted packet of u_i experiences erasure with probability ϵ_{u_i} in the uplink phase. Thus, the relay receives

$$y_{\mathrm{r}} = \sum_{i=1}^{N} a_i\, b_i\, x_i \qquad (7.1)$$

where the summation is a modulo-2 sum. In (7.1), a_i is a binary variable showing whether x_i is transmitted in the uplink or not. For u_i, $a_i = 1$ indicates that x_i is transmitted and $a_i = 0$ otherwise. Also, the Bernoulli variable b_i represents the erasure status of x_i. Here, $b_i = 1$ (with probability $1 - \epsilon_{u_i}$) means that x_i has not been erased in the uplink. In (7.1), if all transmitting users experience erasure, $y_{\mathrm{r}} = E$.

Please note that a similar transmission model has been considered in [59–61] to model erasure two-way relay and multiple-access channels. The erasure multiple access channel in (7.1) models a wireless multiple-access channel where users transmit their data over a fading environment [60]. When some users go into the deep fade, the relay loses their signal and their transmitted data are erased. In the case of deep fade over all users, the relay does not receive a meaningful signal and declares erasure.

After receiving the users' data in the uplink phase, the relay forms its message x_{r} based on y_{r}. In the downlink, relay broadcasts its message to all users. u_i misses relay's broadcast message with erasure probability ϵ_{d_i} and receives it with probability $1 - \epsilon_{d_i}$.

After receiving the relay's broadcast message, each user first tries to separate different users' data from each other and then decodes them. The uplink and downlink transmissions should continue until each user is able to retrieve the information packets of any other user (full data exchange).

7.3   Data Sharing Schemes

In this section, we propose our data sharing schemes for the discussed EMWRCs. Our proposed data sharing schemes consist of four principal parts: i) Fountain coding at the users, ii) Users' transmission strategy, iii) Relay's transmission strategy, and iv) Data separation at the users. In the rest of this section, we discuss each of these parts in detail. The performance of these schemes is later evaluated by comparing their achievable rates with a rate upper bound derived in Section 7.5.

7.3.1 Fountain Coding

To sustain reliable communications in an EMWRC, an appropriate scheme should be employed to combat erasure. Retransmission protocols are a simple approach for this purpose, however, they are wasteful for EMWRCs due to the significantly large number of transmissions that is needed to ensure receiving data by all users in the BC phase [62]. Furthermore, implementing retransmission protocols as well as conventional erasure correcting codes (e.g. Reed-Solomon codes) requires a feedback channel between the users and the relay. Another approach for combating data erasure is fountain coding which provides reliable data communication without the need for a feedback channel. In the following, we describe how fountain coding is employed in our proposed data sharing schemes.

If relay wants to perform fountain decoding and re-encoding before forwarding the data to the users, it should wait to receive all data packets from all users and then decode them. This causes a significant delay in the data sharing process. Thus, in our proposed solution, the fountain encoding and decoding are performed only at the users. More specifically, u_i encodes its information packets, $m_{i,k}$ where $k = 1, 2, \ldots, K$, with a fountain (e.g. a Raptor [64]) code and forms its transmit message x_i. As mentioned previously, we denote the packets by binary symbols for the sake of simplicity.

In addition, the fountain encoders at the users are considered to be synchronized. With synchronized encoders, each user can easily keep track of the combinations of the packets formed at the other users without exposing extra hardware complexity or overhead to the system. Knowing the combination of the formed packets is important to proceed with the fountain decoding at the users. To implement synchronized fountain encoders, users have identical random number generators with equal initial seeds [1].

After encoding their packets, users send them in the uplink phase. They continue transmitting fountain-coded packets until the data sharing is finished and all users have the full data of any other user. Assuming K information packets at each user, if data sharing is accomplished after sending the K'th encoded packet, the overhead is defined as $O = \frac{K'-K}{K}$ [62]. Please note that here, we consider the transmission overhead to evaluate the performance of the data sharing strategies. As we see later, by reducing EEER, our proposed strategies can effectively decrease the transmission overhead. Another commonly-used measure for fountain codes is the reception overhead which depends on the character-

---

[1]An alternative to our synchronized scheme could be *distributed* fountain codes, where the data of multiple sources are independently encoded in a way that the resulting bit stream would have a degree distribution approximating that of the fountain code [66]. The scheme is not easily scalable and its performance suffers from uplink erasures.

istics of the underlying fountain code. Since we do not deal with the fountain code design, reception overhead is irrelevant to our discussions.

7.3.2 Users' Transmission Strategies

In our proposed data sharing schemes, we define a *round of communication* consisting of L uplink and L downlink transmissions (time slots). During one round of communication, users want to exchange one of their fountain coded packets. Depending on the users' transmission strategy, a set of users simultaneously send their fountain coded packets to the relay in each of these L time slots. A users' transmission strategy is determined by the transmission matrix $\mathbf{A} = [a_{l,i}]_{L \times N}$. According to $\mathbf{A}$, u_i transmits in lth uplink slot if $a_{l,i} = 1$. Otherwise, u_i stays silent and does not transmit.

In the lth uplink slot, the relay's received signal is

$$y_{\mathrm{r},l} = \sum_{i=1}^{N} a_{l,i} \, b_{l,i} \, x_i. \tag{7.2}$$

In (7.2), $b_{l,i}$ is a Bernoulli random variable representing the erasure status of x_i in the lth uplink slot. Here, $b_{l,i} = 0$ with probability ϵ_{u_i} and $b_{l,i} = 1$ with probability $1 - \epsilon_{u_i}$. Defining $\mathbf{x} = [x_i]_{N \times 1}$ and $\mathbf{y}_{\mathrm{r}} = [y_{\mathrm{r},l}]_{L \times 1}$, (7.2) can be rewritten in the following matrix form

$$\mathbf{y}_{\mathrm{r}} = (\mathbf{A} \odot \mathbf{B})\mathbf{x} = \mathbf{A}_{\mathrm{r}}\mathbf{x}. \tag{7.3}$$

In (7.3), $\mathbf{B} = [b_{l,i}]_{L \times N}$ and $\odot$ represents the Hadamard product. Also, $\mathbf{A}_{\mathrm{r}}$ is the relay's received matrix.

In this work, we consider three different users' transmission strategies: conventional one-way relaying and our proposed pairwise transmission strategies.

One-Way Relaying (OWR)

In this scheme, $L = N$, and the data of each user is solely sent to the relay in one of the uplink slots. For OWR, the uplink transmission matrix $\mathbf{A}$ is an $N \times N$ identity matrix, i.e. $\mathbf{A} = \mathrm{I}(N)$.

Minimal Pairwise Relaying (MPWR)

The scheme divides the uplink and downlink into $L = N - 1$ transmissions. A sequential pairwise data communication to the relay is used in MPWR. In particular, in time slot l of the uplink, u_l and u_{l+1} transmit to the relay. The scheme is shown to be capacity achieving

when the links are binary symmetric [29]. The MPWR's uplink transmission matrix is

$$
\mathbf{A} = \begin{pmatrix}
1 & 1 & 0 & 0 & \ldots & 0 & 0 \\
0 & 1 & 1 & 0 & \ldots & 0 & 0 \\
\vdots & & & & & & \\
0 & \ldots & & & & 1 & 1
\end{pmatrix}_{(N-1)\times N} . \tag{7.4}
$$

One-Level Protected Pairwise Relaying (OPPWR)

By using one extra uplink time slot compared to MPWR and sending a pairwise combination of the first and the last users, OPPWR has an extra protection against erasure compared to MPWR. More specifically, it can tolerate at least one erasure either in uplink or in downlink transmissions, which does not hold for the MPWR scheme. For this scheme,

$$
\mathbf{A} = \begin{pmatrix}
1 & 1 & 0 & 0 & \ldots & 0 & 0 \\
0 & 1 & 1 & 0 & \ldots & 0 & 0 \\
\vdots & & & & & & \\
0 & \ldots & & & & 1 & 1 \\
1 & 0 & \ldots & & & 0 & 1
\end{pmatrix}_{N\times N} . \tag{7.5}
$$

7.3.3 Relay's Transmission Strategy

After receiving $\mathbf{y}_{\mathrm{r}}$ in the uplink phase, relay forms its message $\mathbf{x}_{\mathrm{r}} = [x_{\mathrm{r},l}]_{L\times 1}$ based on $\mathbf{y}_r$. Then, $\mathbf{x}_{\mathrm{r}}$ is sent to the users in L downlink transmissions. As mentioned before, we like to sustain a low-latency and simple relaying. To this end, we consider two different scenarios for the relay to form its message, $\mathbf{x}_{\mathrm{r}}$.

In the first scenario, relay simply forwards its received signal, i.e. $x_{\mathrm{r},l} = y_{\mathrm{r},l}$, in each time slot. In this case, relay does not need to buffer the received signals in the uplink slots and has the minimum relaying latency.

In the second case, relay has a buffer with length L for its received signal and is capable of performing simple elementary matrix operations. By buffering the received signals in the uplink slots and knowing which packets have been erased, the relay forms $\mathbf{A}_{\mathrm{r}}$. Now, if any erasure has happened in the uplink, relay performs elementary matrix operations on $\mathbf{A}_{\mathrm{r}}$ and tries to retrieve the original transmitted matrix $\mathbf{A}$ or at least some of its erased elements. The result of the matrix operations on $\mathbf{A}_{\mathrm{r}}$ is called $\tilde{\mathbf{A}}$. Relay then performs the same matrix operations on $\mathbf{y}_{\mathrm{r}}$ to form $\mathbf{x}_{\mathrm{r}}$. In other words, $\mathbf{x}_{\mathrm{r}} = \tilde{\mathbf{A}}\mathbf{x}$. We call this method *matrix reconstruction*. Since relay may be able to retrieve some of the erased elements of $\mathbf{A}$, doing matrix reconstruction can lower the effective uplink erasure rate. Note that no fountain decoding is needed at the relay and the low-latency requirements are still met.

Example 7.1 *Consider an EMWRC with $N = 3$ users and OPPWR is used as the users' transmission strategy. In this case,*

$$A = \begin{pmatrix} 1 & 1 & 0 \\ 0 & 1 & 1 \\ 1 & 0 & 1 \end{pmatrix}. \tag{7.6}$$

Now, assume that in the third uplink transmission, u_3's data has been erased. Thus

$$A_r = \begin{pmatrix} 1 & 1 & 0 \\ 0 & 1 & 1 \\ 1 & 0 & 0 \end{pmatrix}. \tag{7.7}$$

If the relay does the modulo-2 sum of the first and second rows of A_r, it can retrieve A. Thus, in this case $\tilde{A} = A$. Note that if the relay does not perform reconstruction and $x_{r,2}$ is erased in the downlink, x_3 will be lost, but with reconstruction, it can be retrieved.

7.3.4 Data Separation

After receiving the downlink signal from the relay and knowing its own transmitted packet, each user first separates the data of users before proceeding with the fountain decoding. If the data separation is not done, the user should treat all data from all other users as a large stream of fountain coded packets. This can result in the failure of fountain decoding due to not receiving enough degree-one packets. After separating data packets, the user stores them to proceed with the fountain decoding.

Here, it is assumed that the users know matrix $\tilde{\mathbf{A}}$. This can be achieved in practice by adding an overhead of size $2N$ to each packet. For practical cases, this extra overhead is negligible compared to the size of the packets.

Let $\mathbf{y}_i = [y_{l,i}]_{L \times 1}$ be the received vector at u_i after one round of communication. Here, either $y_{l,i} = x_{r,l}$ or $y_{l,i} = E$. The received downlink signal at u_i can be written in the following matrix form

$$\mathbf{y}_i = \mathbf{A}_{r_i} \mathbf{x} \tag{7.8}$$

where $\mathbf{A}_{r_i}$ is the received matrix at u_i. Here, the rows of $\mathbf{A}_{r_i}$ are equal to the rows of $\tilde{\mathbf{A}}$ except that some rows are erased.

Without loss of generality, we consider the data separation at u_1. Knowing its own data packet, u_1 tries to find other users' transmitted data by solving the following system of linear equations

$$\mathbf{A}_1 \mathbf{x} = [x_1 \ \mathbf{y}_1]^T \tag{7.9}$$

where

$$\mathbf{A}_1 = \begin{pmatrix} 1 & 0 & \cdots & 0 & 0 \\ & & \mathbf{A}_{\mathrm{r}_1} & & \end{pmatrix}.$$ (7.10)

The transmitted packet of user j, x_j, is erased at u_1 when it cannot be retrieved by solving (7.9). From (7.10), it is seen that L should be at least $N-1$ to make data separation feasible. After separating the data packets of each user, u_1 waits until receiving enough packets to proceed with the fountain decoding.

Example 7.2 *Consider an EMWRC with $N = 4$ users. In this EMWRC, MPWR is used and the relay simply forwards its received messages without doing reconstruction. In this case,*

$$A = \begin{pmatrix} 1 & 1 & 0 & 0 \\ 0 & 1 & 1 & 0 \\ 0 & 0 & 1 & 1 \end{pmatrix}.$$ (7.11)

Now, assume that x_2 is erased in the second uplink transmission. Also, $x_{\mathrm{r},3}$ has been erased in the downlink and the received signal at u_1 is $\mathbf{y}_1 = [0\,1\,E]^T$. Assuming $x_1 = 1$, u_1 forms the following system of linear equations to find x_2, x_3 and x_4:

$$\begin{pmatrix} 1 & 0 & 0 & 0 \\ 1 & 1 & 0 & 0 \\ 0 & 0 & 1 & 0 \\ 0 & 0 & 0 & 0 \end{pmatrix} \begin{pmatrix} x_1 \\ x_2 \\ x_3 \\ x_4 \end{pmatrix} = \begin{pmatrix} 1 \\ 0 \\ 1 \\ E \end{pmatrix}.$$ (7.12)

From (7.12), u_1 finds that $x_2 = x_3 = 1$ while x_4 is declared as erasure.

7.4 End-to-end Erasure Rate

To study the performance of the three aforementioned schemes, we introduce a useful concept called end-to-end erasure rate (EEER). This concept is helpful in: i) finding the achievable rates of the schemes, and ii) calculating their transmission overhead. Consider an arbitrary user, u_i. For any $j \neq i$, if we are able to identify the erasure rate of u_j's packets at u_i, denoted by $\epsilon_{i,j}$, we can simply model the communication between this pair of users with an erasure channel with the erasure probability of $\epsilon_{i,j}$. The achievable data rate over this channel is then $1 - \epsilon_{i,j}$. Also, the transmission overhead of an ideal fountain code for data transmission from u_j to u_i over this channel is

$$O_{i,j} = \frac{\epsilon_{i,j}}{1 - \epsilon_{i,j}}.$$ (7.13)

Based on the above discussion, we define pairwise EEER which is the erasure rate between a pair of users where one of them serves as the data source and the other one as destination. Having N users in the systems results in $\frac{N(N-1)}{2}$ pairwise EEERs. Now, we define

71

maximum EEER, which we simply call EEER and denote it by ϵ_f, as the maximum erasure rate over all pairs of users. In other words, $\epsilon_f = \max_{i,j} \epsilon_{i,j}$. Since the achievable common data rate, R, is determined by the data transmission rate between the users experiencing the worst erasure, we have $R = 1 - \epsilon_f$. With a similar argument, the overall transmission overhead is

$$O = \frac{\epsilon_f}{1 - \epsilon_f}. \tag{7.14}$$

Please note that in practice, the transmission overhead is larger than (7.14) due to using non-ideal fountain codes.

7.4.1 EEER Calculation for OWR

Using OWR, a packet sent from user i is received by user j if it is not erased neither in the uplink nor in the downlink. Thus, defining $\overline{\epsilon}_{u_i} = 1 - \epsilon_{u_i}$ and $\overline{\epsilon}_{d_j} = 1 - \epsilon_{d_j}$, we have $\epsilon_{i,j} = 1 - \overline{\epsilon}_{u_i}\overline{\epsilon}_{d_j}$. Now, EEER is

$$\epsilon_f^{\text{OWR}} = \max_{i,j} \epsilon_{i,j} = 1 - \min_{i,j} \overline{\epsilon}_{u_i}\overline{\epsilon}_{d_j}. \tag{7.15}$$

Note that the reconstruction process at the relay is not helpful when OWR is used since the relay receives the data of a specific user in only one uplink channel use. Further, for a symmetric EMRWC where for all i, $\epsilon_{u_i} = \epsilon_u$ and $\epsilon_{d_i} = \epsilon_d$, pairwise EEERs are all equal for any pair of users.

7.4.2 EEER Calculation for MPWR

For MPWR, the relay receives the data of each user (except the first and the last ones) in two uplink time slots. Thus, it may be able to employ data reconstruction for u_2 to u_{N-1} in order to retrieve their data if it is erased in only one uplink transmission. In the following, we study EEER for both cases when the relay does not perform data reconstruction and when it does.

MPWR without Reconstruction: First, we study $\epsilon_{i,1}$, the pairwise EEER of u_i, $i = 2, \ldots, N$, at u_1. Then we extend the analysis to other users. For decoding at u_1, let us call the probability of finding x_i at ith or $(i+1)$th rows of $\mathbf{A}_1$ by $P_1^1(i)$ and $P_2^1(i)$ respectively.

First, we calculate $P_1^1(i)$. Notice that $P_1^1(1) = 1$ since x_1 is always known at u_1. For $i > 1$, x_i is found in row i when this row is not erased in the downlink phase and : (i) No erasure has happened in row i during the uplink phase and the value of x_{i-1} has been found from row $i-1$ or (ii) In the ith row, x_{i-1} was erased in the uplink phase, while x_i has been

perfectly received (only x_i exists in this row). Hence,

$$P_1^1(i) = \bar{\epsilon}_{d_1}(\bar{\epsilon}_{u_i}\bar{\epsilon}_{u_{i-1}}P_1(i-1) + \bar{\epsilon}_{u_i}\epsilon_{u_{i-1}}). \tag{7.16}$$

Having $P_1^1(1) = 1$, by solving the above recursive equation for $i = 2, \ldots, N$, all $P_1^1(i)$'s are found.

Now, we calculate $P_2^1(i)$. Since x_N appears just once in (7.9) when MPWR is used, $P_2^1(N) = 0$. Also $P_2^1(1) = 1$. By a logic similar to the one used for the calculation of $P_1^1(i)$, for $i = 2, \ldots, N-1$, we have

$$P_2^1(i) = \bar{\epsilon}_{d_1}(\bar{\epsilon}_{u_i}\bar{\epsilon}_{u_{i+1}}P_2(i+1) + \bar{\epsilon}_{u_i}\epsilon_{u_{i+1}}). \tag{7.17}$$

Now, to complete the pairwise EEER calculation, we just need to find $P_c^1(i)$ representing the probability of finding x_i at u_1 in both i and $(i+1)$th equations. Here, x_i can be retrieved from both ith and $(i+1)$th rows if none of these rows is erased in the downlink and x_i does exist in both rows. Also, one of these situations should happen: (i) x_{i-1} in row i and x_{i+1} in row $i+1$ are both erased in the uplink phase, (ii) Either x_{i-1} or x_{i+1} is erased in the uplink phase and the other one was found before solving the corresponding equation, (iii) Nothing is erased in the uplink phase and x_{i-1} and x_{i+1} have been previously found. Thus, for $i = 2, \ldots, N$, we have

$$\begin{aligned} P_c^1(i) = \bar{\epsilon}_{d_1}^2 \bar{\epsilon}_{u_i}^2 \Big[& \epsilon_{u_{i-1}}\epsilon_{u_{i+1}} + \epsilon_{u_{i+1}}\bar{\epsilon}_{u_{i-1}}P_1^1(i-1) + \epsilon_{u_{i-1}}\bar{\epsilon}_{u_{i+1}}P_2^1(i+1) \\ & + \bar{\epsilon}_{u_{i+1}}\bar{\epsilon}_{u_{i+1}}P_1^1(i-1)P_2^1(i+1) \Big]. \end{aligned} \tag{7.18}$$

Now, the probability of finding x_i at u_1 is

$$P^1(i) = P_1^1(i) + P_2^1(i) - P_c^1(i) \tag{7.19}$$

and $\epsilon_{i,1} = 1 - P^1(i)$.

Let us derive the probability of finding x_i at user j, called $P^j(i)$. Since x_j is known at user j, finding the values of $x_{j-1}, x_{j-2}, \ldots, x_1$ can be seen as finding $x_2, x_3, \ldots, x_j$ at u_1 when there are only j users in the system trying to exchange their data. Thus, for $i = 1, 2, \ldots, j-1$, $P^j(i) = P^1(j-i+1)$ where $P^1(\cdot)$ is calculated when there are j users in the system. Similarly, for $i = j+1, j+2, \ldots, N$, we have $P^j(i) = P^1(i-j+1)$ when only $N - j + 1$ users exchange their data. Hence, $\epsilon_{i,j}$ is derived. Similar to OWR, $\epsilon_f^{\mathrm{MPWR}} = \max_{i,j} \epsilon_{i,j}$. Furthermore, the average erasure rate that each user experiences is

$$\epsilon_{\mathrm{ave}}^{MPWR} = 1 - \frac{\displaystyle\sum_{j=1}^{N}\sum_{i=1, i \neq j}^{N} P^j(i)}{N(N-1)}. \tag{7.20}$$

73

The importance of $\epsilon_{\text{ave}}^{MPWR}$ is later discussed in Subsection 7.4.4.

Remark 7.1 *Assume a symmetric EMWRC where $\epsilon_{u_i} = \epsilon_u$ and $\epsilon_{d_i} = \epsilon_d$ for all i. In this case, unlike OWR, pairwise EEERs are not necessarily equal when MPWR is used. Further, it can be shown that*

$$\min_{j,i} P^j(i) = P^1(N) = P^N(1). \tag{7.21}$$

Thus, $\epsilon_f^{\text{MPWR}} = \max_{i,j} \epsilon_{i,j} = 1 - P^1(N)$.

MPWR with Reconstruction: Reconstruction at the relay is performed on $\mathbf{A}_\text{r}$ and gives $\tilde{\mathbf{A}}$. Its purpose is to reduce the uplink erasure rate without affecting the downlink. In the following, we find the equivalent uplink erasure rate when MPWR along with relay reconstruction is used. The equivalent uplink erasure probability of x_i in jth pairwise transmission is the probability of not being able to retrieve it at jth equation even after reconstruction at the relay. Notice that x_i appears in $(i-1)$th and ith equations of $\mathbf{A}$. Thus, $j \in \{i-1, i\}$.

First of all, if x_1 or x_N is erased in its associated transmission, it never can be retrieved since these data packets appear in only one row of $\mathbf{A}$. Now, assume that x_i, $2 \le i \le N-1$, is erased in $(i-1)$th equation. To find x_i from the rest of equations, one of these cases should happen: i) x_{i+1} is erased in ith equation while x_i exists there, ii) Both x_i and x_{i+1} exist in ith equation, and only x_{i+1} is received by the relay in $(i+1)$th equation, and so on. This continues until the case where all x_i's in the ith to $(N-2)$th equations exist and x_N is erased from the $(N-1)$th row of $\mathbf{A}$ while x_{N-1} exists. Thus, the probability of retrieving x_i in the $(i-1)$th row of $\mathbf{A}_\text{r}$ when it has been originally erased in the uplink transmission is

$$P_c^{i,i-1} = \bar{\epsilon}_{u_i}\epsilon_{u_{i+1}} + \bar{\epsilon}_{u_i}\bar{\epsilon}_{u_{i+1}}^2\epsilon_{u_{i+2}} + \ldots + \bar{\epsilon}_{u_i}\bar{\epsilon}_{u_{i+1}}^2 \cdots \bar{\epsilon}_{u_{N-1}}^2\epsilon_{u_N} = \bar{\epsilon}_{u_i}\sum_{j=i+1}^{N}\{\epsilon_{u_j}\prod_{k=i+1}^{j-1}\bar{\epsilon}_{u_k}^2\}. \tag{7.22}$$

Having $P_c^{i,i-1}$, the equivalent uplink erasure rate of x_i in $(i-1)$th equation is

$$\epsilon_u^{i,i-1} = \epsilon_{u_i}(1 - P_c^{i,i-1}). \tag{7.23}$$

Now, assume that x_i is erased in ith equation. It can be found if: i) x_i appears in $(i-1)$th equation while x_{i-1} is erased, ii) Both x_i and x_{i-1} appear in $(i-1)$th equation and only x_{i-1} is received by relay in $(i-2)$th equation, and so on. The last possible situation is when x_1 is erased in the first equation while x_2 exists and none of x_j's in the second to $(i-1)$th

equations is erased. Thus, the probability of erasure correction for x_i at equation i is

$$P_c^{i,i} = \overline{\epsilon}_{u_i}\epsilon_{u_{i-1}} + \overline{\epsilon}_{u_i}\overline{\epsilon}_{u_{i-1}}^2\epsilon_{u_{i-2}} + \ldots + \overline{\epsilon}_{u_i}\overline{\epsilon}_{u_{i-1}}^2 \cdots \overline{\epsilon}_{u_2}^2\epsilon_{u_1} = \overline{\epsilon}_{u_i}\sum_{j=1}^{i-1}\{\epsilon_{u_j}\prod_{k=j+1}^{i-1}\overline{\epsilon}_{u_k}^2\}. \tag{7.24}$$

Similarly, the equivalent uplink erasure rate of u_i when it experiences erasure in ith uplink transmission is

$$\epsilon_u^{i,i} = \epsilon_{u_i}(1 - P_c^{i,i}). \tag{7.25}$$

Notice that $P_c^{1,1} = P_c^{N,N-1} = 0$. To apply the effect of reconstruction on EEER calculation, we should properly replace ϵ_{u_i} with either $\epsilon_u^{i,i-1}$ or $\epsilon_u^{i,i}$. In other words, x_i experiences erasure in the ith row of $\mathbf{A}_1$ with $\epsilon_u^{i,i-1}$ and with $\epsilon_u^{i,i}$ in the $(i+1)$th row.

Remark 7.2 *For a symmetric EMWRC with MPWR, it can be shown that in the limit of $N \to \infty$, we have*

$$E(P_c^{i,i-1}) = \frac{\overline{\epsilon}_u}{1 + \overline{\epsilon}_u}, \tag{7.26}$$

$$E(P_c^{i,i}) = \frac{\overline{\epsilon}_u}{1 + \overline{\epsilon}_u}, \tag{7.27}$$

where $\overline{\epsilon}_u = 1 - \epsilon_u$ and $E(\cdot)$ is the expected value. As a consequence, both $\epsilon_u^{i,i-1}$ and $\epsilon_u^{i,i}$ approach $\frac{\epsilon_u}{2-\epsilon_u}$.

7.4.3 EEER Calculation for OPPWR

OPPWR without Reconstruction: Consider one round of communication for OPPWR which consists of N pairwise user transmissions. Since for OPPWR, $\mathbf{A}$ is a circulant matrix, without loss of generality, we find $\epsilon_{i,1}$ for $i = 2, 3, \ldots, N$. Other pairwise EEERs are similarly found by proper circulation of $\epsilon_{i,1}$.

Having x_1 (the first row of $\mathbf{A}_1$ in (7.10)), u_1 can find x_i either in row i or $i+1$ of (7.9) for $i = 2, 3, \ldots, N$. Let us denote the probability of finding x_i in row i and $i+1$ by $P_1(i)$ and $P_2(i)$ respectively. Thus, the probability of retrieving x_i in u_1, $P(i)$, is

$$P(i) = P_1(i) + P_2(i) - P_c(i) \tag{7.28}$$

where $P_c(i)$ is the probability of being able to retrieve x_i in both ith and $(i+1)$th rows of $\mathbf{A}_1$.

$P_1(i)$ is found similar to (7.16). Further, due to the cyclic structure of $\mathbf{A}$, it can be shown that $P_2(i) = P_1(N - i + 2)$ for $i = 2, 3, \ldots, N$. Derivation of $P_c(i)$ is also similar

to (7.18). To calculate $P_c(i)$ in (7.18), we should substitute $P_2(i+1)$ by $P_2(1) = 1$ when $i = N$. This is because x_1 appears with x_N for the second time and is always known at u_1. Having all terms in (7.28), $\epsilon_{i,1} = 1 - P(i)$. Further, using the circulant structure of $\mathbf{A}$, it can be shown that $\epsilon_{i,j} = \epsilon_{i-j+1,1}$. Having the pairwise EEERs, $\epsilon_f^{\text{OPPWR}} = \max\limits_{i,j} \epsilon_{i,j}$ and users' average erasure rate, $\epsilon_{\text{ave}}^{\text{OPPWR}}$, is simply calculated similar to (7.20).

Remark 7.3 *For a symmetric EMWRC, pairwise EEERs are not equal when OPPWR is used. In this case, it can be shown that $\epsilon_f^{\text{OPPWR}} = \epsilon_{\lfloor N/2 \rfloor + 1,1}$.*

OPPWR with Reconstruction: Similar to MPWR, we calculate $\epsilon_u^{i,i-1}$ and $\epsilon_u^{i,i}$ to derive the uplink equivalent erasure rate. With a similar logic, it can be shown that for OPW

$$P_c^{i,i-1} = \bar{\epsilon}_{u_i}\epsilon_{u_{i+1}} + \bar{\epsilon}_{u_i}\bar{\epsilon}_{u_{i+1}}^2\epsilon_{u_{i+2}} + \ldots + \bar{\epsilon}_{u_i}\bar{\epsilon}_{u_{i+1}}^2 \cdots \bar{\epsilon}_{u_N}^2\bar{\epsilon}_{u_1}^2 \cdots \bar{\epsilon}_{u_{i-2}}^2\epsilon_{u_{i-1}} \tag{7.29}$$

$$= \bar{\epsilon}_{u_i}\sum_{j=i}^{N+i-2}\left\{\epsilon_{u_{m(j)+1}}\prod_{k=i}^{j-1}\bar{\epsilon}_{u_{m(k)+1}}^2\right\}. \tag{7.30}$$

and

$$P_c^{i,i} = \bar{\epsilon}_{u_i}\epsilon_{u_{i-1}} + \bar{\epsilon}_{u_i}\bar{\epsilon}_{u_{i-1}}^2\epsilon_{u_{i-2}} + \ldots + \bar{\epsilon}_{u_i}\bar{\epsilon}_{u_{i-1}}^2 \cdots \bar{\epsilon}_{u_1}^2\bar{\epsilon}_{u_N}^2 \cdots \bar{\epsilon}_{u_{i+2}}^2\epsilon_{u_{i+1}} \tag{7.31}$$

$$= \bar{\epsilon}_{u_i}\sum_{j=1}^{N-1}\left\{\epsilon_{u_{m(i-j)}}\prod_{k=1}^{j-1}\bar{\epsilon}_{u_{m(i-k)}}^2\right\} \tag{7.32}$$

where $m(\cdot)$ represents modulo-N operation. Other stages of EEER calculation are similar to what described for MPWR.

Remark 7.4 *In a symmetric EMWRC with OPPWR, it can be shown that for all i, $P_c^{i,i-1} = P_c^{i,i} = P_c$. Further, in the limit of $N \to \infty$,*

$$P_c = \frac{\overline{\epsilon_u}}{1 + \overline{\epsilon_u}}. \tag{7.33}$$

As a consequence, similar to MPWR, $\epsilon_u^{i-1,i} = \epsilon_u^{i,i} = \frac{\epsilon_u}{2 - \epsilon_u}$.

7.4.4 Numerical Examples

Here, we present some numerical examples for EEER of proposed schemes. Further, we discuss how EEER can be decreased by modifying the users' transmission scheduling and employing a shuffled transmission schedule for users. The following cases are for a symmetric EMWRC with uplink and downlink erasure probabilities ϵ_u and ϵ_d respectively.

Figure 7.1 depicts EEER (maximum pairwise EEER), average pairwise EEER and the minimum pairwise EEER among the users when MPWR is used. As seen, there is a significantly large gap between EEER and average pairwise EEER. Similar results are presented

in Figure 7.2 when OPPWR is used. Having such a large variance between pairwise EEERs noticeably limits the achievable rate of the system. Please note that for OWR, all pairwise EEERs are equal, thus, numerical results are omitted here.
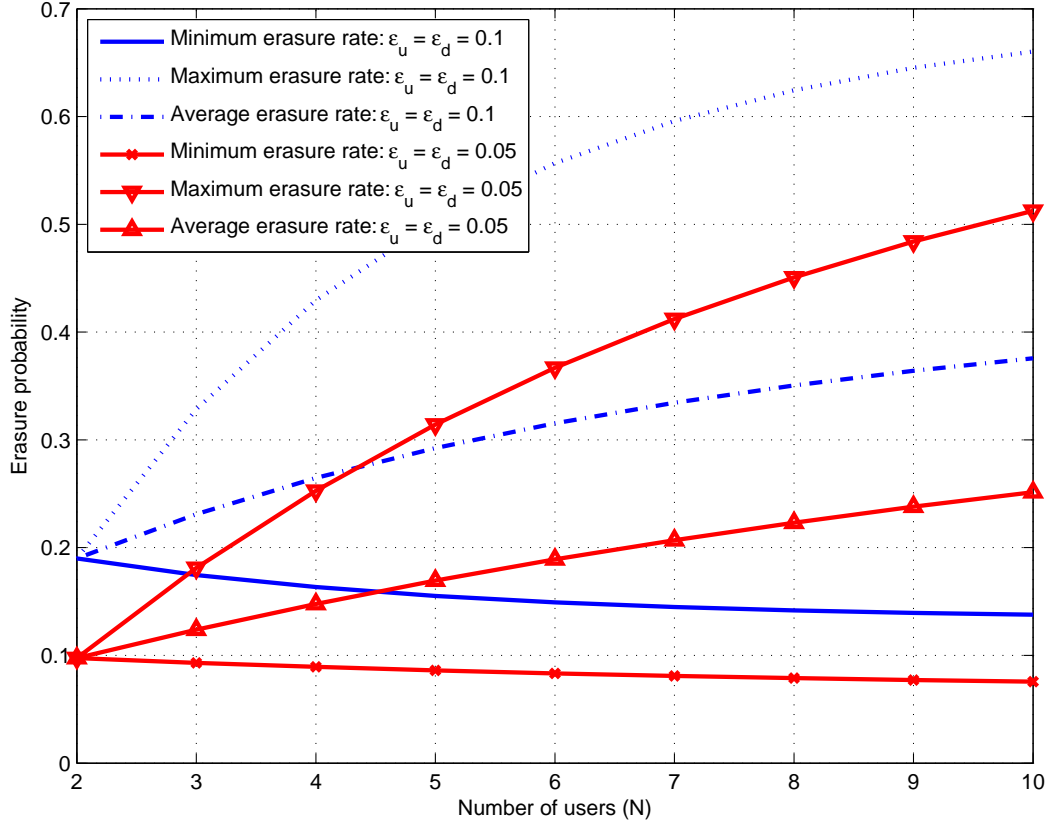
Figure 7.1: EEER, average pairwise EEER and minimum EEER for MPWR.

To improve the system's achievable rate, it is desired to decrease EEER. For this purpose, we suggest using a shuffled (random) transmission scheduling to narrow the gap between the EEER and the average pairwise EEER. In this approach, all users have psuedorandom number generators with the same initial seeds. Thus, the output of number generators are equal at all users. For each round of communication, psuedorandom number generators give a random permutation of numbers from 1 to N. We denote this psuedorandom sequence by $\{S_1, S_2, \ldots, S_N\}$. This random sequence specifies the order of transmission by users. For our proposed pairwise schemes, in the first uplink transmission, user S_1 and user S_2 transmit, in the second uplink transmission, user S_2 and user S_3 transmit and so on. For OPPWR, user S_N and user S_1 also transmit together in the last uplink slot.

In the abovementioned shuffled scheduling, ith row of $\mathbf{A}$ is assigned to the pairwise transmission of u_{S_i} and $u_{S_{i+1}}$ for each round of communication. Note that u_{S_i} and $u_{S_{i+1}}$
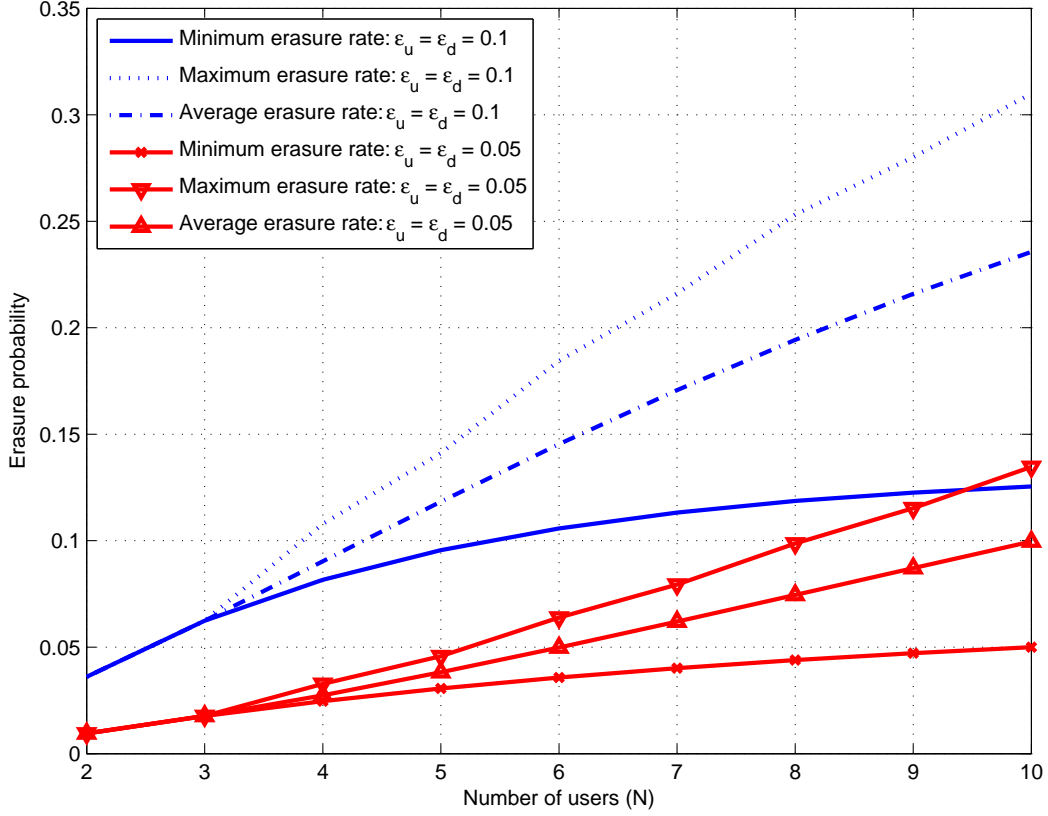
Figure 7.2: EEER, average pairwise EEER and minimum EEER for OPPWR.

can be any arbitrary two users from u_1 to u_N in each round. Thus, by doing shuffled scheduling over large number of communication rounds, we expect EEER and minimum pairwise EEER to converge to the average pairwise EEER. As a consequence, shuffled transmission scheduling significantly evens out the pairwise erasure rates resulting in a lower overall EEER.

Effect of the reconstruction on the equivalent uplink erasure probability is presented in Figure 7.3 and Figure 7.4 for MPWR and OPPWR, respectively. In these figures, the average equivalent uplink erasure probability over all users is depicted versus the uplink erasure probability and the number of users. As seen, for small N, reconstruction is not much helpful when MPWR is used. For instance, if $N = 2$, reconstruction does not improve the performance at all since the data of each user (here, two users) exist in only one uplink transmission. Hence, there is no redundancy for retrieving the users' data from other uplink transmissions if it is erased. On the other hand, reconstruction causes the best improvement in terms of erasure rate for OPPWR when $N = 2$. This is due to the repetitive transmission of users' data (each user's data packet is sent twice). As number of users increases,

performance improvement by reconstruction increases for MPWR while it decreases for OPPWR. However, generally speaking, reconstruction at the relay has a more significant improvement for OPPWR.
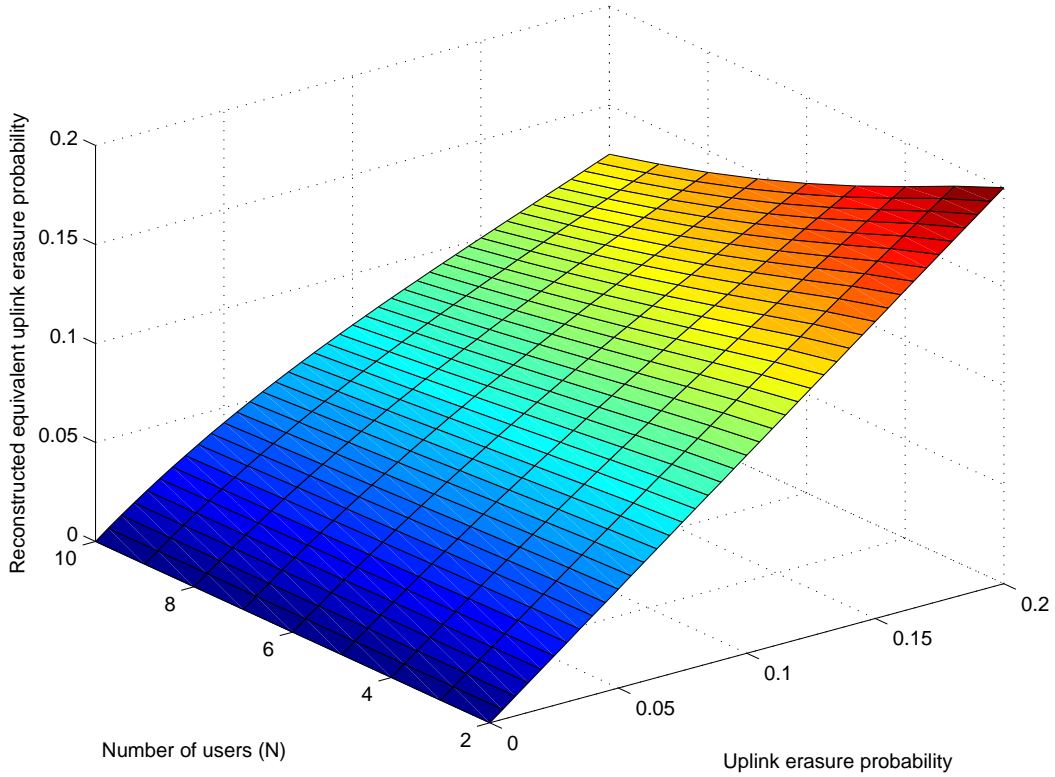
Figure 7.3: Equivalent Uplink erasure probability for MPWR.

7.5 Rate Upper bound

In this section, we derive an upper bound on the achievable common data rate, R, for the described EMWRC. This bound is later used to evaluate the performance of the proposed data-sharing schemes. To find the rate bound, we apply cut-set theorem [37].

To start, we first consider data transmission from other users to u_i and derive the rate upper bound in this case. For this user, two cuts are considered (Figure C.1): the cut considering the relay and u_i as receivers of a multiple-access channel interested in decoding the data of other $N-1$ users, and the cut considering the relay as the transmitter to u_i. For the first cut, the data rate is limited by the user with the worst uplink erasure rate as well as the sum-rate condition. Using similar arguments as [61], it is easy to show that the sum-rate for the first cut is bounded by $1 - \prod_{j=1, j \neq i}^{N} \epsilon_{u_j}$. Thus, by denoting the transmitted common
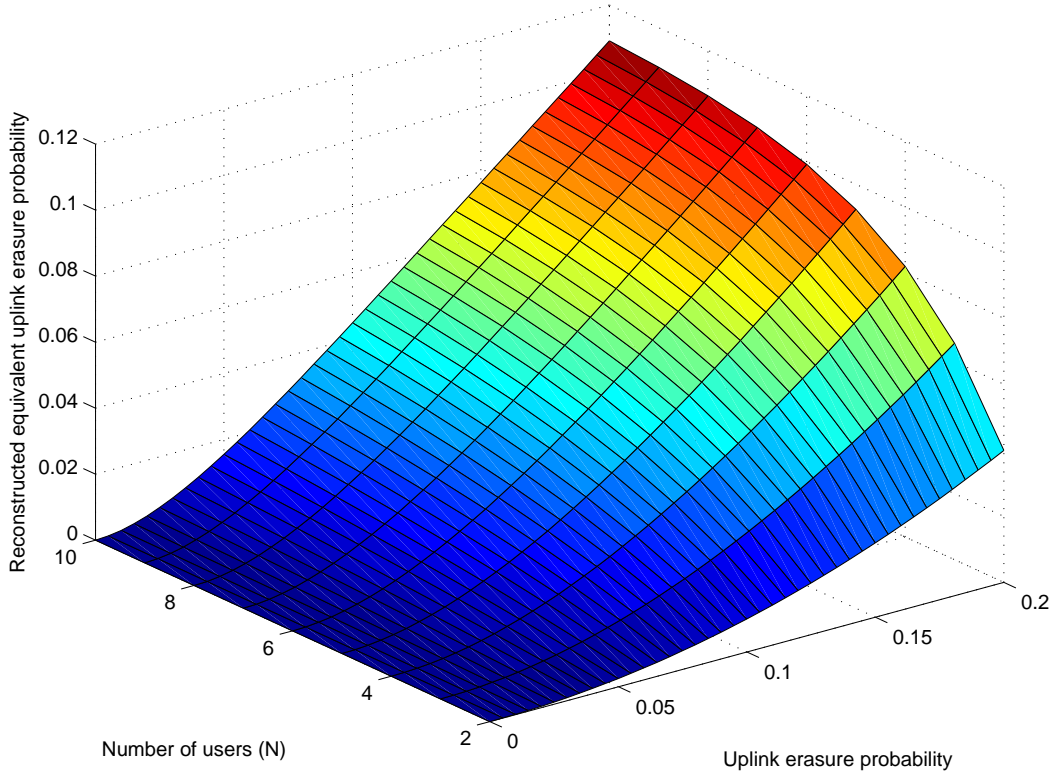
Figure 7.4: Equivalent Uplink erasure for probability OPPWR.

data rate from other users to u_i by R_i, we have

$$R_i \leq \min\{\min_{j=1, j\neq i}\{1 - \epsilon_{u_i}\}, \frac{1}{(N-1)}(1 - \prod_{j=1, j\neq i}^{N} \epsilon_{u_j})\}. \qquad (7.34)$$

The second cut is a simple single user erasure channel. Thus,

$$R_i \leq \frac{1}{N-1}(1 - \epsilon_{d_i}). \qquad (7.35)$$

Now, if we repeat the cut-set discussion for all u_i's, the achievable common rate is $R = \min_i R_i$.

7.6 Performance Analysis

In this section, we study the performance of the three aforementioned schemes (i.e. OWR, MPWR and OPPWR) in terms of their achievable rate and the transmission overhead for the data exchange between the users. Here, we assume a symmetric EMWRC with uplink and downlink erasure probabilities ϵ_u and ϵ_d.

The achievable rate of the schemes is determined by the worst erasure rate between a pair of users which is reflected in EEER. In addition to EEER, the number of consumed

Figure 7.5: Cut-sets used to find the rate upper bound

uplink and downlink slots (number of channel uses) for data exchange between users is also important for to make a fair comparison between the schemes. To this end, we consider the normalized achievable rate which is the carried data over one uplink and downlink time slots. According to this definition, the normalized achievable rate for OWR, MPWR and OPPWR are $R^c_{\text{OWR}} = (1 - \epsilon^{\text{OWR}}_f)/N$, $R^c_{\text{MPWR}} = (1 - \epsilon^{\text{MPWR}}_f)/(N - 1)$ and $R^c_{\text{OPPWR}} = (1 - \epsilon^{\text{OPPWR}}_f)/N$ respectively.

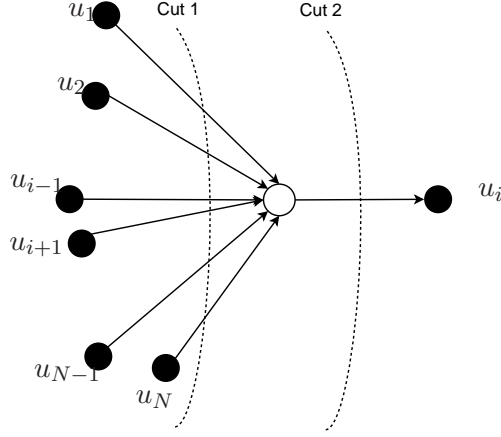Figure 7.6 depicts the comparison between the normalized achievable rates of OWR, MPWR, OPPWR, and the rate upper bound (derived in Section 4.2) for an ideal channel with no erasure, i.e $\epsilon_d = \epsilon_u = 0$. As seen, MPWR can actually achieve the upper bound for such an ideal channel since its division factor, $N - 1$, is equal to the division factor of the upper bound. Also, OPPWR and OWR provide equal rates which always fall under the upper bound and the achievable rates of MPWR.

By increasing the erasure rate of channels, MPWR is no longer the best approach. The results are shown for a more realistic channel with $\epsilon_u = 0.1$ and $\epsilon_d = 0.1$ in Figure 7.7. As seen, for $N \leq 4$, $5 \leq N \leq 8$, and $9 \leq N$, MPWR, OPPWR, and OWR achieve the highest normalized rate. To investigate the effect of reconstruction at the relay as well as the shuffled transmission scheduling, numerical results for symmetric channels with $\epsilon_u = \epsilon_d = 0.1$ are presented in Figure 7.8. Using reconstruction and shuffled scheduling improves the achievable rates of proposed pairwise scheme, specially MPWR.

To better illustrate the performance improvement of random shuffling and relay reconstruction, a comparison between EEER for MPWR, OPPWR and OWR is presented in Figure 7.9 when $N = 6$. Without reconstruction or shuffled transmission, EEER of OWR resides under the EEER of MPWR. However, using these two techniques significantly re-
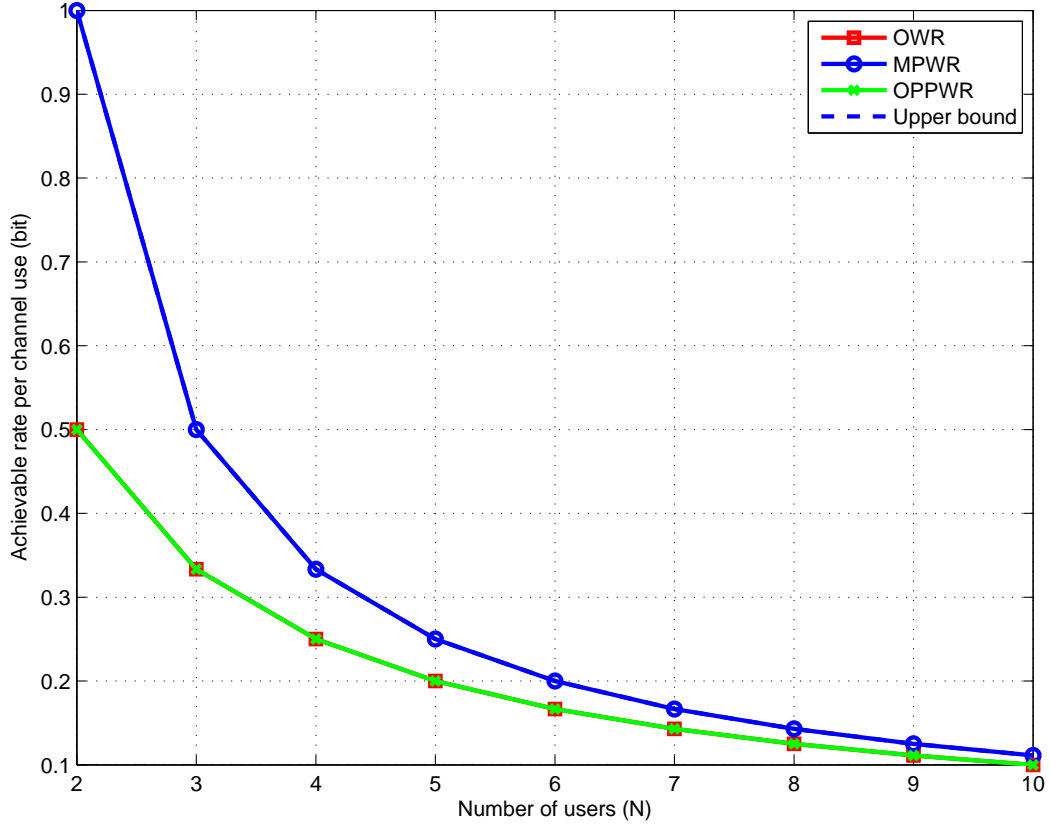
Figure 7.6: Achievable rates when $\epsilon_u = \epsilon_d = 0$.

duces MPWR's EEER and for some erasure probabilities, MPWR's EEER is less than OWR's EEER. Similar behavior is observed for OPPWR where using reconstruction and shuffled scheduling results in outperforming OWR by OPPWR over all erasure probabilities.

Figure 7.10 depicts the simulation and analytical results for the transmission overhead of different schemes when $\epsilon_u = \epsilon_d = 0.1$. Transmission overhead can be considered as a notion of delay in EMWRC. Similar to the achievable rates, here, the transmission overhead for different schemes are normalized due to the difference in the number of uplink transmissions for different schemes. It means that to fairly compare the overhead of MPWR with OPPWR and OWR, the MPWR's transmission overhead is scaled by $\frac{N-1}{N}$. For simulation, a Raptor code with information length 14000 and an outer code (LDPC) of rate 0.9872 has been used for fountain coding. Also, in the simulation setup, a shuffled transmission schedule is used and the relay performs reconstruction to reduce the effective uplink erasure rate. The analytical results are calculated using EEER as explained in Section 7.4. Note that there is a gap between the analytical and simulation results due to assuming ideal fountain code

82
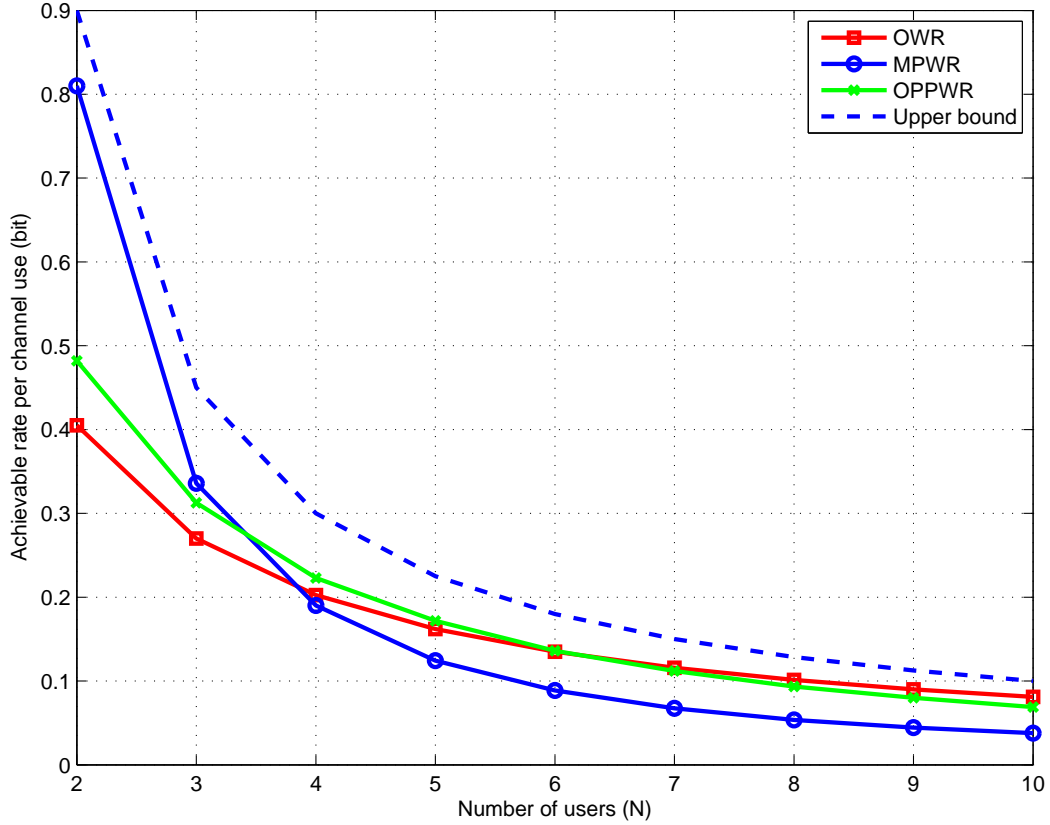
Figure 7.7: Achievable rates when $\epsilon_u = \epsilon_d = 0.1$.

in the analytical overhead calculation. However, using EEER, the transmission overhead of the schemes can be evaluated well without the need for tedious computer simulations.

7.7 Conclusion

In this chapter, we studied low-latency data sharing schemes for EMWRCs. To this end, we first mentioned the challenges confronting the use of fountain coding for EMWRCs. Then, we proposed two simple and low-latency data sharing schemes, namely MPWR and OPPWR, based on fountain coding. We also showed that by performing simple matrix operations at the relay and shuffling the order of users' transmissions, the performance of MPWR and OPPWR can be further enhanced. To find the achievable rate and transmission overhead of our solutions, we introduced EEER and calculated it analytically for our strategies. In addition, an upper bound on the achievable rate of EMWRCs was derived. The achievable rates of MPWR and OPPWR were then compared with this bound as well as the achievable rates of OWR. This comparison along with comparing the transmission overhead of MPWR, OPPWR and OWR revealed that for small N, MPWR has the best performance.
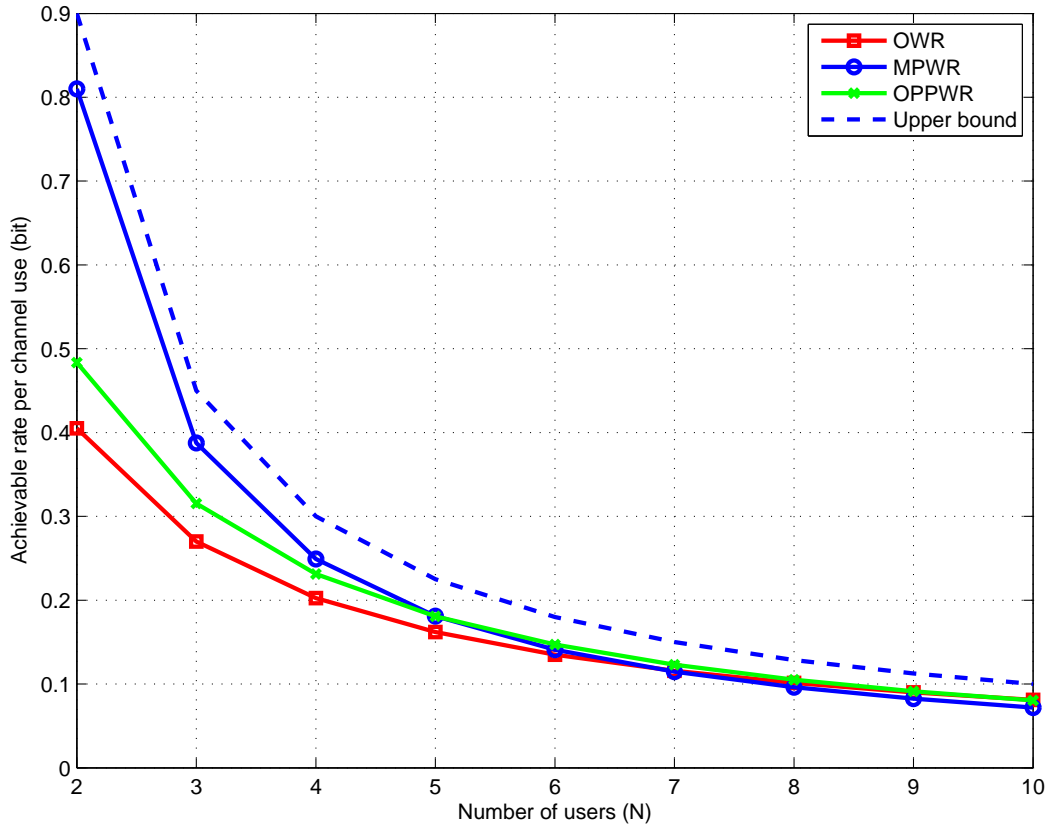
Figure 7.8: Achievable rates when $\epsilon_u = \epsilon_d = 0.1$ and reconstruction and shuffled scheduling are applied.

By increasing N, first OPPWR and then OWR outperform the other two schemes. Seeking methods to improve the performance of data sharing schemes over EMWRCs, for instance through smarter users' and relay transmission strategy, is considered to future research directions.
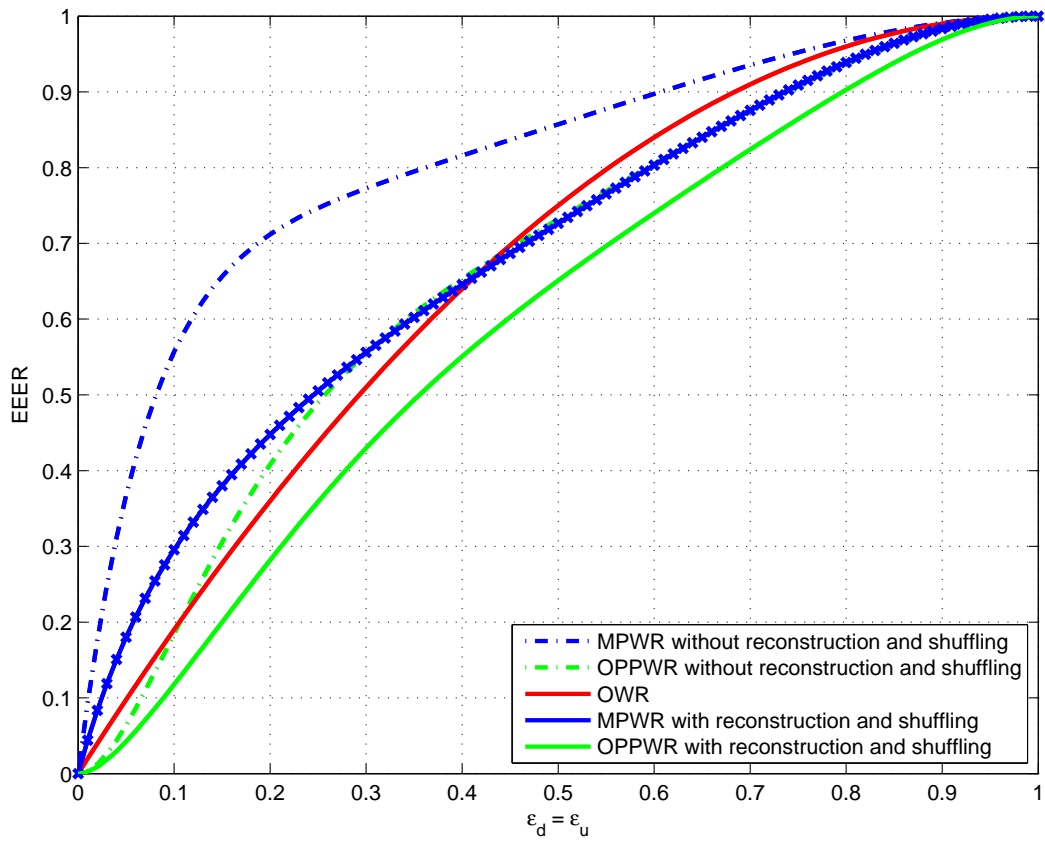
Figure 7.9: EEER comparison when $N = 6$.
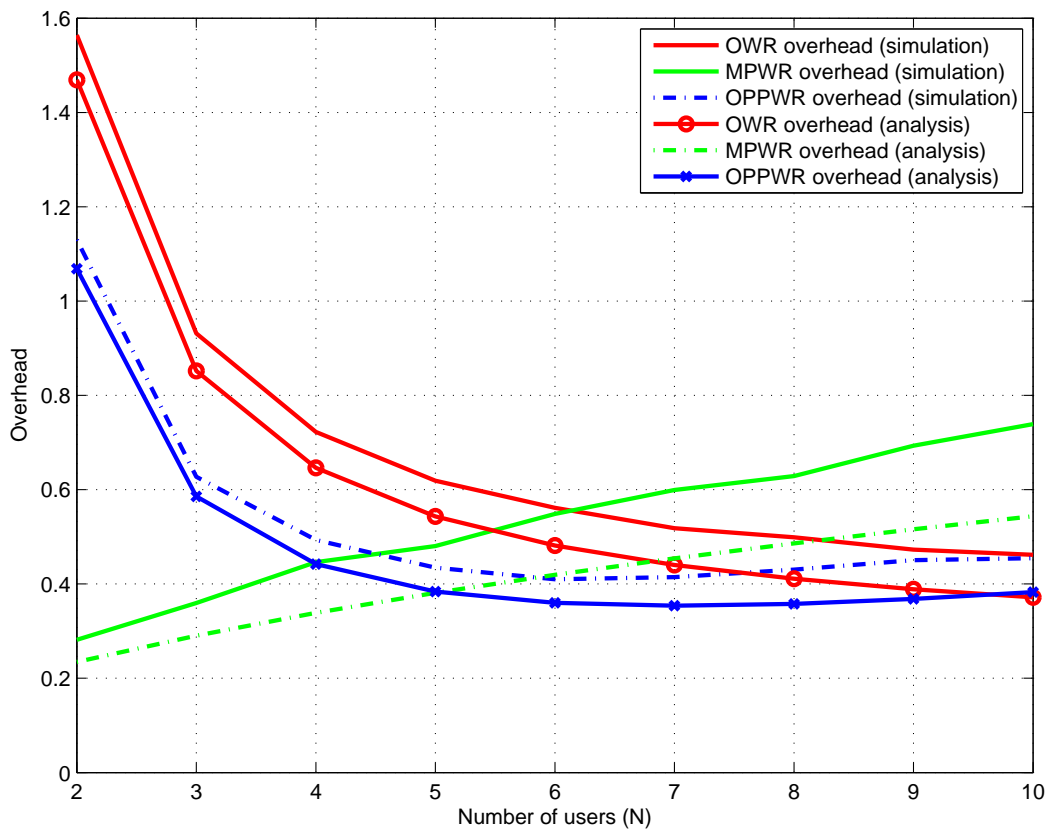
Figure 7.10: Overhead comparison for $\epsilon_u = 0.1, \epsilon_d = 0.1$.

Chapter 8

Conclusion and Future Work

In this chapter, we first summarize the contributions of this dissertation and conclude our work. Then, new problems are described for future research directions.

8.1 Conclusion and Summary of the Contributions

The main focus of this thesis was studying the achievable rates of MWRCs for different channel types including symmetric channels with AWGN, asymmetric channels with AWGN, and erasure channels. We compared the performance of different relaying schemes and also tried to improve the system's achievable rate.

Designing a new constellation mapping for PSK modulation in TWRCs and pairwise MWRCs was the focus of Chapter 3. First, we addressed the issue regarding possible ambiguity points in the received constellation. For this purpose, we found the necessary and sufficient condition on a user bit mapping which removes this ambiguity. Further, we introduced the concept of semi-Gray mapping which improves the system BER performance and achievable rate. The necessary and sufficient condition of having a semi-Gray mapping was also found. Interestingly, the widely used binary reflected Gray mapping does not satisfy the semi-Gray mapping condition resulting in a poorer performance compared to our proposed semi-Gray scheme.

In Chapter 4, we studied the achievable rates of memoryless TWRCs. More specifically, we studied AF and DMF in terms of their achievable data exchange rates and showed that unlike memoryless one-way relaying, increasing users' SNR benefits AF more than DMF. Another interesting observation was that while with DMF a higher data rate is provided for the user whose channel condition is better, with AF the situation is the reverse. That is, the user with a worse channel condition can receive at a higher data rate. Further, we found that for a TWRC with asymmetric users' channels, AF can take advantage of power back-off

at the users, without degrading the data rate, to save energy while power back-off is not beneficial for DMF.

Assuming an MWRC with N users, OWR and MWR were compared in Chapter 5 in terms of their achievable rates. First, we proved that for MWR, FDF ensures a gap less than $\frac{1}{2(N-1)}$ bit from the capacity upper bound while MWR based on DF or AF is unable to guarantee this rate gap. For DF and AF, we identified situations where they also have a rate gap less than $\frac{1}{2(N-1)}$ bit. Later, we showed that although MWR has higher relaying complexity, surprisingly, it can be outperformed by OWR depending on N and the system SNR. Summarily speaking, for large N and small users' transmit power, OWR usually provides higher rates than MWR.

In Chapter 6, we studied an asymmetric MWRCs with AWGN where users have different channel conditions. To enable data communication in this scenario, we considered two different strategies: FDF and PDF. For both FDF and PDF, we first showed that due to unequal channel conditions, the achievable common rate of the pairwise strategy depends on the order in which the users are paired. This motivated us to find the pairing strategy maximizing the achievable rate. The maximum achievable rate of each scheme was then compared with the capacity upper bound and the achievable rate of a random user pairing.

We proposed practical low-latency data sharing strategies, called MPWR and OPPWR, for EMWRCs based on fountain coding in Chapter 7. To evaluate the performance of our proposed schemes, we introduced the notion of end-to-end erasure rate (EEER) which is the probability of missing the transmitted data of a user in another one. EEER was analytically derived for MPWR and OPPWR and was later used to derive their achievable rate and transmission overhead. We further showed that by performing simple matrix operations at the relay and implementing a shuffled users' transmission scheduling, EEER can be decreased. We also found an upper bound on the achievable rates of EMWRC and observed that when the number of users is not large or the channel erasure probability is small, our proposed schemes operate close to this bound. The results of the comparison between our proposed schemes and OWR suggested that MPWR and OPPWR can outperform OWR when the number of users and the links' erasure rates are not large.

A general conclusion of our work in this thesis is that MWR outperforms OWR when the error rate as well as the number of users are not large. Note that large error rate is associated with small SNRs in AWGN channels while it is indicated by large erasure rate in the erasure channels. To get the best of both worlds, for a practical relayed data sharing system, users can take a hybrid approach and switch between MWR and OWR depending

on the systems circumstances.

8.2 Future Research Directions

Since MWRCs are a new field in wireless communications, different aspect of them are still unexplored. In the following, we define several research problems which can be studied to extend the scope of our presented work.

8.2.1 Optimal Symbol Mapping for MWRCs with PSK Modulation

Different legitimate mappings have different performance in terms of BER and achievable rate. Thus, it is desired to find the users' symbol mapping providing the lowest BER and highest achievable rate. As we discussed in Chapter 3, depending on the systems SNR, the effect of second closest points in the constellation becomes important. Thus, depending on the system SNR, finding a unique optimal mapping for all SNRs may not be possible. However, one can think of designing an adaptive symbol mapping at the user side. In this adaptive scheme, the mapping is chosen based on the current system's SNR such that the performance is improved.

8.2.2 Generalized FDF for Pairwise MWRCs

In Chapter 6, the focus of the study was on pairwise strategies where the users have (almost) equal number of transmissions in the uplink phase. It means that almost all users transmit in two uplink time slots. We are interested to see whether using unbalanced pairwise strategy improves the performance or not. To this end, a generalized FDF (GFDF) can be considered. In a GFDF scheme, users still communicate with the relay in pairs and one round of communication consists of $N - 1$ MAC and BC transmissions. The difference between GFDF and FDF is the number of transmissions that each user makes. While in FDF each user has at most two MAC transmissions, it can transmit up to $M \geq 2$ times in a GFDF. However, the total number of users' uplink transmission is still $2(N - 1)$, i.e two transmissions in each MAC slot. When $M = 2$, GFDF and FDF are equivalent. Please note that in GFDF, different users may have different number of uplink transmissions which leads to unbalanced power expenditure at users. Thus, GFDF can be an approach for heterogeneous networks where users in the network have different (power) resources and requirements. Studying the achievable rates of GFDF and finding its optimal transmission strategy to maximize the achievable rate over asymmetric channels is considered for future work.

8.2.3 Optimal User Pairing to Maximize the Sum-Rate

Another measure to evaluate the data rate performance in a communication system is the sum-rate. It is usually considered a measure for the overall network data transfer capacity. First of all, we need to conduct a sum-rate analysis for MWRCs, especially for the asymmetric case. Then, we are interested to find the optimal transmission strategy to maximize the network sum-rate over asymmetric channels. The optimal pairing strategy for sum-rate is expected to be different from the one for common rate.

8.2.4 Improving the Proposed Data Sharing Schemes for EMWRC

In Chapter 7, we improved the performance of our proposed data sharing schemes through shuffling the users' transmission order as well as the reconstruction at the relay. However, the achievable rate of our proposed data sharing schemes still has a gap with the rate upper bound. Another solution which we did not explore is to design a more effective transmission matrix, $\mathbf{A}$, in the first place. To design a better transmission matrix $\mathbf{A}$, EEER can be effectively used. To this end, an optimization problem can be formulated whose goal is to minimize EEER of a transmission matrix $\mathbf{A}$ such that the data separation at the users is accomplished without difficulty.

Bibliography

[1] "ICTs as a clean technology." [Online]. Available: http://www.itu.int/themes/climate/docs/report/05-ICTCleanTechnology.html

[2] "Frequency allocation." [Online]. Available: http://en.wikipedia.org/wiki/Frequency-allocation

[3] "Gartner estimates ICT industry accounts for 2 percent of global CO_2 emissions." [Online]. Available: http://www.gartner.com/it/page.jsp?id=503867

[4] "Canadian table of frequency allocations." [Online]. Available: http://www.ic.gc.ca/eic/site/smt-gst.nsf/eng/h-sf01678.html

[5] "United States 2008 wireless spectrum auction." [Online]. Available: http://wireless.fcc.gov/auctions/default.htm?job=auction-summary&id=73

[6] "F.C.C. moving forward on a UHF spectrum auction." [Online]. Available: http://www.nytimes.com/2012/09/08/business/media/fcc-to-consider-uhf-spectrum-auction.html?-r=0

[7] V. Chandrasekhar, J. Andrews, and A. Gatherer, "Femtocell networks: a survey," *IEEE Commun. Mag.*, vol. 46, no. 9, pp. 59 –67, September 2008.

[8] "Spectrum occupancy measurements location 4 of 6." [Online]. Available: http://www.sharedspectrum.com/wp-content/uploads/4-NSF-NYC-Report.pdf

[9] O. lleri and N. Mandayam, "Dynamic spectrum access models: toward an engineering perspective in the spectrum debate," *IEEE Commun. Mag.*, vol. 46, no. 1, pp. 153 –160, January 2008.

[10] D. Cox and D. Reudnik, "Dynamic channel assignment in high capacity mobile communications systems," *The Bell System Technical Jounral*, vol. 50, pp. 1833–1857, July/August 1971.

[11] D. Everitt and D. Manfield, "Performance analysis of cellular mobile communication systems with dynamic channel assignment," *IEEE J. Select. Areas Commun.*, vol. 7, no. 8, pp. 1172 –1180, October 1989.

[12] C. Raman, R. Yates, and N. Mandayam, "Scheduling variable rate links via a spectrum server," in *IEEE Intl. Symp. on New Frontiers in Dynamic Spectrum Access Networks (DySPAN)*, November 2005, pp. 110 –118.

[13] M. Buddhikot and K. Ryan, "Spectrum management in coordinated dynamic spectrum access based cellular networks," in *IEEE Intl. Symp. on New Frontiers in Dynamic Spectrum Access Networks (DySPAN)*, November 2005, pp. 299 –307.

[14] I. Mitola, J. and J. Maguire, G.Q., "Cognitive radio: making software radios more personal," *IEEE Personal Commun. Mag.*, vol. 6, no. 4, pp. 13 –18, August 1999.

[15] S. Haykin, "Cognitive radio: brain-empowered wireless communications," *IEEE J. Select. Areas Commun.*, vol. 23, no. 2, pp. 201–220, February 2005.

[16] A. Ghasemi and E. Sousa, "Spectrum sensing in cognitive radio networks: requirements, challenges and design trade-offs," *IEEE Commun. Mag.*, vol. 46, no. 4, pp. 32 –39, April 2008.

[17] R. Ahlswede, N. Cai, S.-Y. Li, and R. Yeung, "Network information flow," *IEEE Trans. Inform. Theory*, vol. 46, no. 4, pp. 1204 –1216, July 2000.

[18] R. Appuswamy, M. Franceschetti, N. Karamchandani, and K. Zeger, "Network coding for computing: Cut-set bounds," *IEEE Trans. Inform. Theory*, vol. 57, no. 2, pp. 1015 –1030, February 2011.

[19] Y. Wu, P. A. Chou, and S. Kung, "Information exchange in wireless networks with network coding and physical-layer broadcast," Microsoft Research, Tech. Rep., August 2004.

[20] Y. Wu, P. Chou, and S.-Y. Kung, "Minimum-energy multicast in mobile ad hoc networks using network coding," *IEEE Trans. Commun.*, vol. 53, no. 11, pp. 1906 – 1918, November 2005.

[21] B. Rankov and A. Wittneben, "Spectral efficient signaling for half-duplex relay channels," in *Asilomar Conference on Signals, Systems, and Computers*, November 2005, pp. 1066 – 1071.

[22] D. Gunduz, A. Yener, A. Goldsmith, and H. Poor, "The multi-way relay channel," in *IEEE Intl. Symp. on Information Theory (ISIT)*, July 2009, pp. 339 –343.

[23] P. Popovski and H. Yomo, "The anti-packets can increase the achievable throughput of a wireless multi-hop network," in *IEEE Intl. Conf. on Communications (ICC)*, vol. 9, June 2006, pp. 3885 –3890.

[24] S. Zhang, S. C. Liew, and P. P. Lam, "Hot topic: physical-layer network coding," in *ACM Intl. Conf. on Mobile Computing and Networking (MobiCom)*, September 2006, pp. 358–365.

[25] S. Katti, H. Rahul, W. Hu, D. Katabi, M. Médard, and J. Crowcroft, "XORs in the air: practical wireless network coding," in *ACM Conf. on Applications, technologies, architectures, and protocols for computer communications*, ser. SIGCOMM '06, October 2006, pp. 243–254.

[26] S. Katti, S. Gollakota, and D. Katabi, "Embracing wireless interference: analog network coding," in *ACM Conf. on Applications, technologies, architectures, and protocols for computer communications*, ser. SIGCOMM '07, October 2007, pp. 397–408.

[27] W. Nam, S.-Y. Chung, and Y. Lee, "Capacity bounds for two-way relay channels," in *IEEE Intl. Zurich Seminar on Communications*, March 2008, pp. 144 –147.

[28] S. J. Kim, B. Smida, and N. Devroye, "Capacity bounds on multi-pair two-way communication with a base-station aided by a relay," in *IEEE Intl. Symp. on Information Theory (ISIT)*, June 2010, pp. 425 –429.

[29] L. Ong, S. Johnson, and C. Kellett, "An optimal coding strategy for the binary multi-way relay channel," *IEEE Commun. Lett.*, vol. 14, no. 4, pp. 330 –332, April 2010.

[30] L. Ong, C. M. Kellett, and S. J. Johnson, "On the equal-rate capacity of the awgn multiway relay channel," *IEEE Trans. Inform. Theory*, vol. 58, no. 9, pp. 5761 –5769, September 2012.

[31] L. Ong, S. Johnson, and C. Kellett, "The capacity region of multiway relay channels over finite fields with full data exchange," *IEEE Trans. Inform. Theory*, vol. 57, no. 5, pp. 3016 –3031, May 2011.

[32] K. Doppler, C. Ribeiro, and J. Kneckt, "Advances in d2d communications: Energy efficient service and device discovery radio," in *Intl. Conf. on Wireless Communication, Vehicular Technology, Information Theory and Aerospace Electronic Systems Technology (Wireless VITAE)*, March 2011, pp. 1 –6.

[33] N. Bambos, "Toward power-sensitive network architectures in wireless communications: concepts, issues, and design aspects," *IEEE Personal Commun. Mag.*, vol. 5, no. 3, pp. 50 –59, June 1998.

[34] L. Ong, C. Kellett, and S. Johnson, "Capacity theorems for the AWGN multi-way relay channel," in *IEEE Intl. Symp. on Information Theory (ISIT)*, June 2010, pp. 664 –668.

[35] T. Cover and J. Thomas, *Elements of Information Theory*. Wiley-Interscience, 2006.

[36] E. Tuncel, "Slepian-wolf coding over broadcast channels," *IEEE Trans. Inform. Theory*, vol. 52, no. 4, pp. 1469 –1482, April 2006.

[37] T. Cover and A. Gamal, "Capacity theorems for the relay channel," *IEEE Trans. Inform. Theory*, vol. 25, no. 5, pp. 572 – 584, September 1979.

[38] D. Gunduz, E. Tuncel, and J. Nayak, "Rate regions for the separated two-way relay channel," in *Allerton Conference on Communication, Control, and Computing*, September 2008, pp. 1333 –1340.

[39] D. Slepian and J. Wolf, "Noiseless coding of correlated information sources," *IEEE Trans. Inform. Theory*, vol. 19, no. 4, pp. 471 – 480, July 1973.

[40] A. Wyner and J. Ziv, "The rate-distortion function for source coding with side information at the decoder," *IEEE Trans. Inform. Theory*, vol. 22, no. 1, pp. 1 – 10, January 1976.

[41] R. B. Serrano, "Coding strategies for compress-and-forward relaying," Ph.D. dissertation, KTH Royal Institute of Technology, 2012.

[42] U. Erez and R. Zamir, "Achieving $\frac{1}{2}$log (1+SNR) on the AWGN channel with lattice encoding and decoding," *IEEE Trans. Inform. Theory*, vol. 50, no. 10, pp. 2293 – 2314, October 2004.

[43] M. Wilson, K. Narayanan, H. Pfister, and A. Sprintson, "Joint physical layer coding and network coding for bidirectional relaying," *IEEE Trans. Inform. Theory*, vol. 56, no. 11, pp. 5641 –5654, November 2010.

[44] B. Nazer and M. Gastpar, "Compute-and-forward: A novel strategy for cooperative networks," in *Asilomar Conference on Signals, Systems, and Computers*, October 2008, pp. 69 –73.

[45] H. J. Yang, Y. Choi, and J. Chun, "Modified high-order pams for binary coded physical-layer network coding," *IEEE Commun. Lett.*, vol. 14, no. 8, pp. 689 –691, August 2010.

[46] J. R. Barry, E. A. Lee, and D. G. Messerschmitt, *Digital Communications*, 3rd ed. Springer, 2003.

[47] E. Agrell, J. Lassing, E. Strom, and T. Ottosson, "Gray coding for multilevel constellations in Gaussian noise," *IEEE Trans. Inform. Theory*, vol. 53, no. 1, pp. 224 –235, January 2007.

[48] T. Cui, T. Ho, and J. Kliewer, "Memoryless relay strategies for two-way relay channels," *IEEE Trans. Commun.*, vol. 57, no. 10, pp. 3132 –3143, October 2009.

[49] G. Ungerboeck, "Channel coding with multilevel/phase signals," *IEEE Trans. Inform. Theory*, vol. 28, no. 1, pp. 55 – 67, January 1982.

[50] E. Agrell, J. Lassing, E. Strom, and T. Ottosson, "On the optimality of the binary reflected gray code," *IEEE Trans. Inform. Theory*, vol. 50, no. 12, pp. 3170 – 3182, December 2004.

[51] G. Caire, G. Taricco, and E. Biglieri, "Bit-interleaved coded modulation," *IEEE Trans. Inform. Theory*, vol. 44, no. 3, pp. 927 –946, May 1998.

[52] N. Jacobsen and U. Madhow, "Coded noncoherent communication with amplitude/phase modulation: from Shannon theory to practical architectures," *IEEE Trans. Commun.*, vol. 56, no. 12, pp. 2040 –2049, December 2008.

[53] K. R. Kumar and G. Caire, "Structured lattice space-time trellis coded modulation," in *IEEE Intl. Symp. on Information Theory (ISIT)*, June 2007, pp. 1931 –1935.

[54] K. S. Gomadam and S. A. Jafar, "Optimal relay functionality for SNR maximization in memoryless relay networks," *IEEE J. Select. Areas Commun.*, vol. 25, no. 2, pp. 390 –401, February 2007.

[55] ——, "On the capacity of memoryless relay networks," in *IEEE Intl. Conf. on Communications (ICC)*, vol. 4, June 2006, pp. 1580 –1585.

[56] W. Nam, S.-Y. Chung, and Y. Lee, "Capacity of the Gaussian two-way relay channel to within 1/2 bit," *IEEE Trans. Inform. Theory*, vol. 56, no. 11, pp. 5488 –5494, November 2010.

[57] V. R. Cadambe, "Multi-way relay based deterministic broadcast with side information: Pair-wise network coding is sum-capacity optimal," in *Annual Conf. Information Sciences and Systems (CISS)*, March 2012.

[58] W. Nam, S.-Y. Chung, and Y. Lee, "Capacity of the Gaussian two-way relay channel to within $\frac{1}{2}$ bit," *IEEE Trans. Inform. Theory*, vol. 56, no. 11, pp. 5488–5494, November 2010.

[59] A. Khisti, B. Hern, and K. Narayanan, "On modulo sum computation over an erasure multiple access channel," in *IEEE Intl. Symp. on Information Theory (ISIT)*, July 2012, pp. 3013 –3017.

[60] B. Hern and K. Narayanan, "Joint compute and forward for the two-way relay channel with spatially coupled LDPC codes," May 2012. [Online]. Available: http://arxiv.org/pdf/1205.5904v1.pdf

[61] B. Smith and S. Vishwanath, "Unicast transmission over multiple access erasure networks: Capacity and duality," in *IEEE Information Theory Workshop (ITW)*, September 2007, pp. 331–336.

[62] D. MacKay, *Information Theory, Inference and Learning Algorithms*. Cambridge University Press, 2003.

[63] M. Luby, "LT codes," in *IEEE Symp. on Foundations of Computer Science*, November 2002, pp. 271 – 280.

[64] A. Shokrollahi, "Raptor codes," *IEEE Trans. Inform. Theory*, vol. 52, no. 6, pp. 2551–2567, June 2006.

[65] J. Castura and Y. Mao, "Rateless coding for wireless relay channels," in *IEEE Intl. Symp. on Information Theory (ISIT)*, September 2005, pp. 810 –814.

[66] S. Puducheri, J. Kliewer, and T. Fuja, "The design and performance of distributed lt codes," *IEEE Trans. Inform. Theory*, vol. 53, no. 10, pp. 3740 –3754, October 2007.

[67] R. Gummadi and R. Sreenivas, "Relaying a fountain code across multiple nodes," in *IEEE Information Theory Workshop (ITW)*, May 2008, pp. 149 –153.

[68] A. Molisch, N. Mehta, J. Yedidia, and J. Zhang, "Cooperative relay networks using fountain codes," in *IEEE Global Communications Conf. (GLOBECOM)*, December 2006, pp. 1 –6.

[69] C. Gong, G. Yue, and X. Wang, "Analysis and optimization of a rateless coded joint relay system," *IEEE Trans. Wireless Commun.*, vol. 9, no. 3, pp. 1175 –1185, March 2010.

[70] M. Uppal, G. Yue, X. Wang, and Z. Xiong, "A rateless coded protocol for half-duplex wireless relay channels," *IEEE Trans. Signal Processing*, vol. 59, no. 1, pp. 209 –222, January 2011.

Appendix A

Proofs for Chapter 3

A.1 Proof of Lemma 3.1

C_0 can be superimposed with M points, including itself. Also, C_1 can be superimposed with $M - 1$ constellation points (all constellation points except C_0) to give new points on $\mathcal{C}_R$. Continuing on the same fashion and noticing that the superimposition of any $\frac{M}{2}$ opposite pairs gives the central point of $\mathcal{C}_R$ at $(0, 0)$, the total number of distinct points on $\mathcal{C}_R$ is

$$\sum_{i=1}^{M} i - \frac{M}{2} + 1 = \frac{M^2}{2} + 1. \tag{A.1}$$

Now, notice that $C_0 + C_{\frac{M}{2}-1}$ and $C_0 + C_0$ give (0,0) and (2,0) in $\mathcal{C}_R$. Also, for any $0 < i < \frac{M}{2} - 1$, $C_0 + C_i$ and $C_0 + C_{M-i-1}$ gives two points in $\mathcal{C}_R$ which are equally distanced from the center. Each different i results in a pair with different distance from the center. Now, one can show that by producing the rest of the points in $\mathcal{C}_R$ through rotation, $\frac{M}{2}$ circles are formed with M points on each of them.

A.2 Proof of Theorem 3.1

First, we claim that the neighbors of a point in g_i are either in the same group, or can be in one or two groups away from it. Assume this claim is not true. Now take an arbitrary point P_1 in $\mathcal{C}_R$ whose neighbor P_2 belongs to g_{i+j} (or g_{i-j} if $i > 2$), such that $j > 2$. From the geometry of $\mathcal{C}_R$, there is a point P_3 on g_{i+j-2} (g_{i-j+2}) which is on the same line passing through P_2 and $(0, 0)$. Clearly, P_3 is closer than P_2 to P_1. This contradicts our assumption that P_2 is a neighbor of P_1.

Now, to find $d_{\min}$, we find three types of minimum distances on $\mathcal{C}_R$: $d_1 =$ minimum distance between two neighboring points on g_i, $d_2 =$ minimum distance between two nearest points on g_i and g_{i+1} and $d_3 =$ minimum distance between two nearest points on g_i and

g_{i+2}.

For d_1, notice that all of the constellation circles in $\mathcal{C}_R$ have M points on them. Thus, the neighboring points on g_1 have the smallest distance equal to

$$d_1 = 2 \left[1 - \cos \left(\frac{2\pi}{M} \right) \right] = 4 \sin^2 \left(\frac{\pi}{M} \right). \tag{A.2}$$

Also, from Lemma 3.2, the distance between two nearest points on g_i and g_{i+1} is

$$d_2 = 2 \sin \left(\frac{\pi}{M} \right). \tag{A.3}$$

For d_3, let us take $P_1 = C_j + C_{M/2+j-i-1}$ in g_i and $P_2 = C_{j+1} + C_{M/2+j-i-2}$ in g_{i+2}. It can be shown that $d(P_1, P_2)$ is decreasing with i. For $i = \frac{M}{2} - 2$, this distance has its smallest value

$$d_3 = 2 \left[1 - \cos \left(\frac{2\pi}{M} \right) \right] = 4 \sin^2 \left(\frac{\pi}{M} \right). \tag{A.4}$$

Now, $d_{\min} = \min\{d_1, d_2, d_3\}$.

A.3 Proof of Theorem 3.2

First, we assume that the mapping is legitimate and for any $i = 0, 1, \ldots, M-1$, S_i and S_{i+2} differ in only one bit. We show that this results in a semi-Gray mapping at the relay. As mentioned in Theorem 3.1, $d_{\min}$ is the distance between two neighboring points in g_1 or a point from $g_{\frac{M}{2}-2}$ and another from $g_{\frac{M}{2}}$. The mapping of a point in g_1 is $S_i \oplus S_{\frac{M}{2}+i-1}$. Now, we show that the mappings of two arbitrary consecutive points in g_1, shown by $S_i \oplus S_{\frac{M}{2}+i-1}$ and $S_{i+1} \oplus S_{\frac{M}{2}+i}$, differ in just one bit. Assume that S denotes the mapping of the central point of $\mathcal{C}_R$. Since the mapping is legitimate, we have

$$S_{i+1} = S \oplus S_{\frac{M}{2}+i+1}, \quad S_{\frac{M}{2}+i} = S \oplus S_i. \tag{A.5}$$

Now, using (A.5),

$$S_{i+1} \oplus S_{\frac{M}{2}+i} = S \oplus S_{\frac{M}{2}+i+1} \oplus S \oplus S_i = S_i \oplus S_{\frac{M}{2}+i+1}. \tag{A.6}$$

Recall that $S_{\frac{M}{2}+i-1}$ and $S_{\frac{M}{2}+i+1}$ differ in just one bit. As a consequence, $S_i \oplus S_{\frac{M}{2}+i-1}$ and $S_i \oplus S_{\frac{M}{2}+i+1}$ differ in only one bit as well.

On the other hand, all the points of $g_{\frac{M}{2}}$ are mapped to the all zero sequence. Also, the mapping of a point in $g_{\frac{M}{2}-2}$ is in the form of $S_i \oplus S_{i+2}$. Since S_i and S_{i+2} differ in just one bit, $S_i \oplus S_{i+2}$ has just one non-zero bit. Hence, the mapping generates a semi-Gray mapping at the relay.

Now, assume that the mapping is semi-Gray. Thus, all points in $g_{\frac{M}{2}-2}$ has only one non-zero bit. Considering that the points in $g_{\frac{M}{2}-2}$ are in the form of $S_i \oplus S_{i+2}$, it turns out that for all i, $S_i \oplus S_{i+2}$ has just one non-zero bit. This concludes that S_i and S_{i+2} differ in just one bit.

Appendix B

Proofs for Chapter 5

Before presenting proofs, we state the following propositions based on Lemma 2.1, 2.4 and 2.2.

Proposition B.1 *If $P_r \le (K-1)P$, i.e. downlink is the rate bottleneck, we have*

$$R_{\text{UB}}^c = \frac{\log\left(1 + P_r\right)}{2(K-1)}. \tag{B.1}$$

Otherwise

$$R_{\text{UB}}^c = \frac{\log\left(1 + (K-1)P\right)}{2(K-1)}. \tag{B.2}$$

Proposition B.2 *In a Gaussian MWRC with FDF MWR, if $P_r \le \frac{K}{2}P - \frac{1}{2}$, then downlink is the bottleneck resulting in*

$$R_{\text{FDF}}^c = \frac{\log\left(1 + P_r\right)}{2(K-1)}. \tag{B.3}$$

If $\frac{K}{2}P - \frac{1}{2} \le P_r$

$$R_{\text{FDF}}^c = \frac{\log\left(\frac{1}{2} + \frac{KP}{2}\right)}{2(K-1)}. \tag{B.4}$$

Proposition B.3 *When $P_r \le (1 + KP)^{\frac{K-1}{K}} - 1$, downlink constrains the rate of DF MWR and*

$$R_{\text{DF}}^c = \frac{\log\left(1 + P_r\right)}{2(K-1)}. \tag{B.5}$$

Further, when $(1 + KP)^{\frac{K-1}{K}} - 1 < P_r$, uplink is the rate bottleneck and

$$R_{\text{DF}}^c = \frac{\log\left(1 + KP\right)}{2K}. \tag{B.6}$$

B.1   Proof of Theorem 5.1

We start the proof by partitioning the range of P_r and P using Proposition B.1 and B.2. Then, the achievable rate of FDF and the rate upper bound are compared in each region in order to complete the proof. The partitions specify which constraints in (2.4) and (2.12) are

active. Since $K \geq 2$, we have $\frac{K}{2}P - \frac{1}{2} < (K-1)P$. To this end, the regions of interest are specified as $P_r \leq \frac{K}{2}P - \frac{1}{2}$, $\frac{K}{2}P - \frac{1}{2} < P_r \leq (K-1)P$, and $(K-1)P < P_r$. These partitions are denoted by A_1^{FDF}, A_2^{FDF} and A_3^{FDF} respectively.

Capacity Gap on A_1^{FDF}: The achievable rate of FDF as well as the upper bound is determined by downlink on this region. Using Proposition B.1 and B.2, we conclude that $R_{\text{FDF}}^c = R_{\text{UB}}^c$. In other words, FDF achieves the capacity upper bound and the gap between R_{UB}^c and R_{FDF}^c, $G_U = R_{\text{UB}}^c - R_{\text{FDF}}^c$, is 0.

Capacity Gap on A_2^{FDF}: For this region, the achievable rate of FDF is bounded by uplink while the rate upper bound is forced by downlink. Thus,

$$G_U = \frac{1}{2(K-1)} \left[\log(1 + P_r) - \log(\frac{1}{2} + \frac{K}{2}P) \right] = \frac{1}{2(K-1)} \log \left(\frac{1 + P_r}{\frac{1}{2} + \frac{K}{2}P} \right). \quad \text{(B.7)}$$

Since $\log(\cdot)$ is an increasing function, the maximum of G_U happens when P_r has its maximum value on A_2. Since $P_r < (K-1)P$, it is easy to show that

$$\frac{1 + P_r}{\frac{1}{2} + \frac{K}{2}P} < 2. \quad \text{(B.8)}$$

As a consequence, $G_U < \frac{1}{2(K-1)}$.

Capacity Gap on A_3^{FDF}: Both R_{FDF}^c and R_{UB}^c are limited by the uplink in this case. Thus, using Proposition B.1 and B.2

$$G_U = \frac{1}{2(K-1)} \log \left(\frac{1 + (K-1)P}{\frac{1}{2} + \frac{K}{2}P} \right). \quad \text{(B.9)}$$

Now, it is inferred from (B.9) that $G < \frac{1}{2(K-1)}$. ∎

B.2 Proof of Theorem 5.2

Similar to FDF, we partition the SNR region and study the capacity gap for DF over different partitions. First, we point out that $(1 + KP)^{\frac{K-1}{K}} < (K-1)P$. To this end, we define three SNR regions namely A_1^{DF}, A_2^{DF}, and A_3^{DF} denoting $P_r \leq (1 + KP)^{\frac{K-1}{K}} - 1$, $(1 + KP)^{\frac{K-1}{K}} - 1 < P_r \leq (K-1)P$, and $(K-1)P < P_r$ respectively.

Capacity gap on A_1^{DF}: R_{UB}^c and R_{DF}^c are limited by downlink. Using propositions B.1 and B.3, it is concluded that $G_U = R_{\text{UB}}^c - R_{\text{DF}}^c = 0$.

Capacity gap on A_2^{DF}: For this partition

$$G_U = \frac{\log(1 + P_r)}{2(K-1)} - \frac{\log(1 + KP)}{2K} = \frac{1}{2(K-1)} \log \left(\frac{1 + P_r}{(1 + KP)^{\frac{K-1}{K}}} \right). \quad \text{(B.10)}$$

Now, the capacity gap is less than $\frac{1}{2(K-1)}$ bit if

$$P_r < 2(1 + KP)^{\frac{K-1}{K}} - 1. \tag{B.11}$$

Considering that $(1 + KP)^{\frac{K-1}{K}} \leq P_r < (K-1)P$, it is easy to show that (B.11) does not necessarily hold for all values of P_r and P in this region.

Capacity gap on A_3^{DF}: Here, uplink is the rate bottleneck for the upper bound as well as DF. Thus,

$$G_U = \frac{1}{2(K-1)} \log \left(\frac{1 + (K-1)P}{(1 + KP)^{\frac{K-1}{K}}} \right) \tag{B.12}$$

and $G_U < \frac{1}{2(K-1)}$ if $(K-1)P < 2(1 + KP)^{\frac{K-1}{K}} - 1$ which does not necessarily hold for all P and P_r values within A_3^{DF}. ∎

B.3 Proof of Theorem 5.3

We again define SNR regions, called A_1^{AF} and A_2^{AF} based on Proposition B.1. The first region is where $P_r \leq (K-1)P$ and the second region includes $(K-1)P < P_r$.

Capacity Gap on A_1^{AF}: In this region, we have

$$G_U^{\mathrm{AF}} = R_{\mathrm{UB}}^c - R_{\mathrm{AF}}^c = \frac{1}{2(K-1)} \log \left(\frac{(1 + P_r)(1 + KP + P_r)}{1 + KP + P_r + (K-1)PP_r} \right) \tag{B.13}$$

Now, from (B.13), one can show that $G_U^{\mathrm{AF}} < \frac{1}{2(K-1)}$ if $P_r^2 - (K-2)PP_r < KP$.

Capacity Gap on A_2^{AF}: On this partition,

$$G_U^{\mathrm{AF}} = \frac{1}{2(K-1)} \log \left(\frac{(1 + (K-1)P)(1 + KP + P_r)}{1 + KP + P_r + (K-1)PP_r} \right) \tag{B.14}$$

Using (B.14), it is easy to conclude that if $K(K-1)P^2 - (K-1)PP_r < 1 + P_r + P$ then AF has a capacity gap smaller than $\frac{1}{2(K-1)}$. ∎

B.4 Proof of Theorem 5.4

First assume $P_r < KP$. Since

$$\frac{KPP_r}{1 + KP + P_r} < P_r \tag{B.15}$$

holds, then $R_{\mathrm{DF_O}} > R_{\mathrm{AF_O}}$. For $KP \leq P_r$,

$$\frac{KPP_r}{1 + KP + P_r} < KP \tag{B.16}$$

is always correct. As a consequence, for this SNR region $R_{\mathrm{DF_O}} > R_{\mathrm{AF_O}}$ still holds. ∎

Appendix C

Proofs for Chapter 6

C.1 Proof of Theorem 6.1

Let us define $U = \{u_1, u_2, \ldots, u_N, \mathcal{R}\}$. Now consider Cut 1 in the network separating $U_i = U - \{u_i, \mathcal{R}\}$ from $\{u_i, \mathcal{R}\}$. Assuming that users send data with a common rate R^c, from the cut-set theorem [35], we have

$$(N - 1)R^c \leq \mathcal{C}(\frac{P \sum_{i \in U_i} |h_i|^2}{\sigma^2}). \tag{C.1}$$

Please notice that to derive (C.1), we use the fact that data flow over Cut 1 is a multiple access channel from U_i to $\mathcal{R}$. Now, consider Cut 2 separating $U - u_i$ and u_i. Applying the cut-set theorem to Cut 2 gives $(N - 1)R^c \leq \mathcal{C}(\frac{P_r |h_i|^2}{\sigma^2})$. Hence, the upper bound for the data rate form U_i to u_i is

$$R^c_{\mathrm{UB}_i} = \frac{1}{N-1} \min \left\{ \mathcal{C}(\frac{P \sum_{i \in U_i} |h_i|^2}{\sigma^2}), \mathcal{C}(\frac{P_r |h_i|^2}{\sigma^2}) \right\}. \tag{C.2}$$

Noticing $R^c_{\mathrm{UB}} = \min_i R^c_{\mathrm{UB}_i}$ and $h_1 < h_i$, for $i > 1$, the proof is complete. ∎
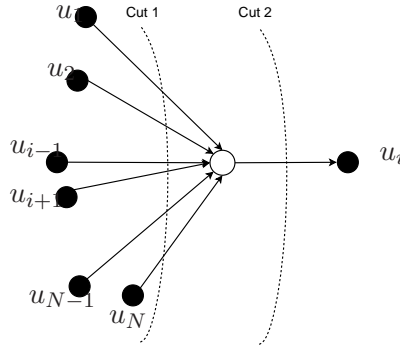

Figure C.1: Network cut-sets

C.2 Proof of Theorem 6.3

If S_1 is limited by (6.4), there is no better pairing than S_1 since all pairings will be limited by the same constraint. If not, from (6.2), the optimal pairing is the one which maximizes $V = \min_i \left\{ \frac{|h_{oi}|^2}{|h_{oi}|^2 + |h_{o(i+1)}|^2} \right\}$ which is equivalent to finding the pairing that minimizes $W = \max_i \left\{ \frac{|h_{o(i+1)}|^2}{|h_{oi}|^2} \right\}$. We claim that S_1 minimizes W. Assume that S_1 results in $\min\{\max_i |h_{o(i+1)}|^2 / |h_{oi}|^2\} = |h_{j+1}|^2 / |h_j|^2$. Recall that in S_1, $h_{oi} = h_i$. Now, consider another pairing S'. To outperform S_1, S' should not have (u_j, u_{j+1}). It also should avoid any other pair resulting in a larger gain ratio. To this end, we make a swap and pair u_{j+1} with u_l where $l > j$. This swap results in $|h_{j+1}|^2 / |h_l|^2 < |h_{j+1}|^2 / |h_j|^2$, but on the other hand forms the (u_j, u_{l+1}) pair which results in having $|h_{l+1}|^2 / |h_j|^2 \geq |h_{j+1}|^2 / |h_j|^2$. This contradicts with the assumption that S' outperforms S_1. If S' wants to minimize W by making more swaps to S_1, the pigeonhole principle guarantees that S' has always a pair (h_k, h_m) such that $k \leq j$ and $m \geq j + 1$. Thus, it cannot do better than S_1.

C.3 Proof of Theorem 6.5

Assume that the rate of S_2 is limited by (6.10), otherwise any other pairing has the same rate limit. With S_2, the transmission pairs are in the form of

$$(u_1, u_N), (u_N, u_2), (u_2, u_{N-1}), \ldots, (u_j, u_{N-j+1}), \ldots \tag{C.3}$$

where (u_j, u_{N-j+1}) is the pair whose MAC phase limits the rate. To have a strategy with a higher common rate, we must connect u_j with a user having a larger channel gain than u_{N-j+1}. This change forms the following transmission pairs

$$(u_1, u_N), (u_N, u_2), \ldots, (u_j, u_{N-l+1}), \ldots, (u_l, u_{N-j+1}), \ldots \tag{C.4}$$

Since the channel gain of u_l is smaller than u_j's channel gain, the common rate in (C.4), due to pair (u_l, u_{N-j+1}), is smaller than the rate of S_2 forced by pair (u_j, u_{N-j+1}). Thus, the common rate is degraded by swapping u_j and u_l. Trying to improve the rate by making more swaps, the pigeonhole principle guarantees that there is always a pair (u_m, u_{N-n+1}) where $m \leq j$ and $n \geq j$. The rate constraint forced by this pair is surely smaller than or equal to the rate constraint of (u_j, u_{N-j+1}). Hence, no other pairing strategy can have a higher rate than S_2, and consequently S_2 is optimal.